SETTLEMENT BEHAVIOR OF A SANDY LOAM DUE TO SUCTION CHANGES ASSOCIATED WITH SIMULATED ARTIFICIAL TREE ROOTS

Joseph Isimenmen AREGHAN, B.Sc

A Thesis Submitted to the Faculty of Graduate and Post Graduate Studies under the Supervision of

Prof. Sai K. Vanapalli, P.Eng. & Dr. Myint Bo, P.Eng.

In partial fulfillment of the requirements for the degree of Masters of Applied Science in Civil Engineering

Department of Civil Engineering

University of Ottawa

Ottawa, Ontario

Canada K1N 6N5

May 2012

The Masters of Applied Science in Civil Engineering is a joint program between Carleton University and University of Ottawa, which is administered by the Ottawa-Carleton Institute for Civil Engineering

ABSTRACT

Shallow foundations rested on Leda clay that are widely distributed in Eastern Canada exhibit shrinkage characteristics and are prone to differential settlements. Due to this reason, significant repairs are necessary to the foundations and basements of residential structures constructed in Leda clay deposits. Differential settlements are commonly attributed to the changes in the natural water content of soils associated with water infiltration, evaporation or plant transpiration (i.e., tree-roots-suction). Various research studies have been undertaken to estimate the possible settlements of shallow foundations associated with the water infiltration or evaporation. Several thumb rules have been proposed through research studies, providing recommendations with respect to the distance at which trees must be planted as a function of their heights at maturity such that differential settlements can be avoided. However, limited studies have been carried out to estimate or model the settlements of shallow foundations taking into account the influence of tree-roots-suction.

In the present research program, a comprehensive experimental study regarding the deformation characteristics of a sandy loam soil from Ottawa due to tree-root-suction is undertaken, using specially designed equipment. The study has been undertaken using a sandy loam soil so that the testing program can be conducted in a shorter period of time. An artificial rooting system (*ARS*) was designed and placed in a specially designed tank at the University of Ottawa to simulate tree-roots-suction and measure soil surface settlements associated with a decrease in natural water content (or increase in soil suction) using particle image velocimetry (*PIV*) technique. The *ARS* consists of an artificial root, suction generator, matric suction and volumetric water content monitoring devices. The variation of matric suction and volumetric water content are monitored at various depths using the instrumentation of the *ARS*. Based on the results of the experimental studies, a methodology is proposed to model the settlement behaviour of sandy loam soils due to suction from *ARS*, using commercial finite element software, *SEEP*/*W* and *SIGMA*/*W* (i.e. software package of GeoStudio 2007). The study offers a reasonably good comparison

between the measured surface settlements and those estimated using the finite element modelling analysis. The modelling methodology presented in this thesis is promising and may be extended for estimating the settlement behaviour associated with the tree roots suction of Leda clay deposits and to other soils.

ACKNOWLEDGMENTS

I am indebted to my supervisor, friend and mentor Prof. Sai K. Vanapalli who provided immense help and encouragement throughout my graduate studies. This research started as a challenge on several fronts with respect to planning and designing the experimental program and gathering the data. His assistance was invaluable in addressing one of the most difficult challenges of my life. I also thank my co-supervisor Dr. Myint Bo for his guidance and input particularly with respect to practical problems associated with the research.

I am grateful to Dr. Oh Won Taek for patiently answering my many questions and constantly encouraging me. PhDs; I appreciate the help and support of Fathi Mohammed for helping me modify the UOBCE that he designed. Thanks go to Hana Adem and Nil Taylan and Othman Nasir for their help and support. I am also indebted to undergrad students A Khan, A. Reza and A Hassan for their help in the laborious preparation of the soil samples needed for the represent project.

Thanks also go to my office colleagues, who constantly bought cheer to the room and the working surroundings. I would also like to appreciate the help and support of technical and administrative staff of the Department of Civil Engineering, that include other members of the Department Civil Engineering; Mark Lapointe, Jean Claude Celestin, Yolande Hogan and Manon Racine. The staff always provided a warm and welcoming environment for conducting the research.

Others without whose encouragement this thesis would have been impossible to complete are my loving and caring parents, Chief and Mrs. Areghan, Chief and Mrs. Otomewo, Mrs. Mojume, Mr. and Mrs. Okohoh, C. Eyiyobo, M. Dada. They provided valuable encouragement for me to pursue higher education. My brother and sisters, Pius, Juliet, Elizabeth and Edith (deceased) provided love and support throughout my life.

I also would like to acknowledge the funding support received from the National Sciences and Engineering Research of Canada (NSERC) for this project.

"*No research can be completed by a single individual even though it is authored by one. It requires the effort, support and encouragement of several individuals*"

....Thank you God above all. I will always be indebted to you for providing me with this opportunity which was a great learning experience of my life!

TABLE OF CONTENTS

LIST OF FIGURES

LIST OF TABLES

CHAPTER 1

INTRODUCTION

1.1 Problem Statement

Trees around residential structures are aesthetically pleasing in residential areas. However, there are also adverse effects associated with their growth which contributes to excessive ground displacements or differential settlements of the foundations in some soils, such as the Leda clay, which is widely present in Eastern Canada. The settlement problems may predominantly be attributed to the tree-roots-suction that contributes to a decrease in natural water content (or increase in soil suction). Property owners depend on the consulting engineer or contractor's services to address these rather expensive to correct problems. Researchers have been investigating solutions for reducing the settlement problems associated with the extra drying around the tree-foundation proximity for several decades. Many rules of thumb and empirical applications have been promoted in practice to control soil deformation associated with tree-roots-suction based on the types of trees by investigators (Cameron et al. 2006). However, the existing methodologies cannot be generalized for all types of soils and practical scenarios, since there are limited field and experimental studies. Also, there is a lack of theoretical background to explain this behaviour from a geotechnical engineering standpoint of view, based on the mechanics of unsaturated soils.

Several settlement problems in Leda clay deposits have been reported in Eastern Canada (Crawford, 1968). A survey of 574 structures in central Ottawa highlighted the nature of movements in relation to soil and vegetation conditions (Bozozuk, 1962). In this study, differential settlements up to 14 inches (35 cm) were reported in buildings of 60-80 years old without vegetation influence. However, significant movements associated with the large elms and other broad-leafed trees were also reported and summarized. The

conclusion was that shrinkage of the subsoil causes serious damages to shallow foundations of residential structures constructed in Leda clay.

As per Statistics Canada (2006), the population of Ottawa has risen by 7.3% between 2001 and 2005 which contributed to a significant rise in residential structures construction activity. Ottawa region is now considered to be the undisputed *town house* capital of Canada with 65% of its total population (1.3 million) living in single family units and town homes. Most of these town homes are constructed in Leda clay deposits, as they are widely spread in Ottawa region and are posing differential settlement problems associated with tree roots action.

There is an urgent need to develop a methodology or approach that can be used to estimate the tree-roots-suction related foundation settlement taking into account the site classification, single or group of trees and seasonal or environmental changes. Such studies can be useful not only for the Ottawa area but also for other regions in the world where similar problems are encountered.

1.2 Objectives of the Thesis

The objectives of this thesis are; i) to design specialized equipment that can be used to investigate the deformation characteristics of soils with respect to tree-roots-suction; ii) to develop a numerical modelling methodology to simulate the surface settlement of a soil due to tree-roots-suction, using commercial finite element software, extending the mechanics of unsaturated soils (Geo Studio 2007).

To achieve these objectives, a comprehensive experimental research program was carried out at the University of Ottawa, using a specially designed artificial rooting system (*ARS*) with sandy loam soil (a local soil collected from Ottawa). This system comprised: a Piezocone (artificial root), a vacuum gauge, a conventional Tensiometer, a direct suction measurement MPS-1 probe (for monitoring the variation of matric suction in the soil) and 5TM Volumetric Water Content and Temperature Probe, monitoring the variation of

volumetric water content in the soils. The system assembly was powered by air pressure that could be converted to vacuum (analogous to tree-roots-suction) by a vacuum generator. Experimental results gathered from the research studies were modelled using Geo Studio (2007), which is a finite element method based commercial software. One of the key parameters required to estimate surface settlement was the suction modulus, *H*. A modelling method to estimate reasonable surface settlements due to tree-roots-suction using the suction modulus, *H* is detailed in the present research program.

1.3 Scope of Thesis

This thesis consists of two parts: experimental program and numerical analysis.

The experimental program, details the *ARS* and the procedures used to conduct the laboratory tests for simulating surface settlement caused by tree-roots-suction. This part also includes the following:

i. Preparation of soil sample and compacting the soil in the tank

ii. Saturation and desaturation of the compacted soil by adjusting the level of water in the tank

iii. Installation of various apparatus to monitor the variation of matric suction (i.e. conventional Tensiometer) and volumetric water content (5TM)

iv. Monitoring surface settlement using a software package by analyzing the images taken from an HD camera

v. Performing various experiments to determine the physical and mechanical properties of the sandy loam soil referred to in this thesis

The numerical analysis part, details the simulation of the experimental results, including:

i. Introduction of the commercial finite element software, Geo Studio 2007, SEEP/W and SLOPE/W.

ii. Details of simulating saturated and unsaturated conditions using the SEEP/W

iii. Details of modelling the artificial root and tree-roots-suction

iv. Comparison between the measured surface settlements and those estimated using the finite element analysis (*FEA*)

v. Comparison between the measured matric suction distribution profile with depth and those estimated using the *FEA.*

1.4 Organization of the Thesis

The research undertaken is organized in seven main chapters as follows:

The *First Chapter* describes the problem statement, the objectives of the research, scope of the thesis and the organization of the thesis.

The *Second Chapter*, "Review of Literature", provides research background related to artificial rooting system along with brief review related to the mechanics of unsaturated soils that are relevant to the estimation of the settlement behaviour of soils due to suction induced by tree roots.

The *Third Chapter*, "Methodology and Equipment Details" presents the design details of Artificial Rooting System (*ARS*) along with (physical and mechanical) soil properties, sample preparation, installation and operation of various apparatus, including monitoring techniques.

The *Fourth Chapter*, "Experimental Testing Program and Results", presents *ARS* test results such as surface settlement and variation of matric suction, volumetric water content in the compacted soils with time for different vacuum pressures (analogous to tree-roots-suction).

The *Fifth Chapter*, "Numerical Modelling Studies', presents a summary of how finite elements method analysis has been used for estimating the surface settlement behaviour of soil associated with the simulated tree-roots-action.

The *Sixth Chapter*, "Analysis of Laboratory and Model Results", provides comparisons between the experimental results and those estimated using the *FEA*.

In the last Chapter, "Conclusions", summary of the experimental program and numerical modelling analysis results is presented. In addition, the various applications of this research work for professional practice are presented.

CHAPTER 2

REVIEW OF LITERATURE

2.1 Introduction

The Champlain Sea, as referred to in the present day literature, was once a vast body of salt water found 12,500 of years ago, extending from the present Pembroke region to Quebec City. As the glaciers retreated, so did the sea, leaving large pockets of sensitive marine clay known as “Leda clay” in its wake (Smiderle, Feet of Clay, Weekly journal, 9th year, no. 44, Friday, October 15, 2004). Leda clay still exists in thick pockets at varying depths beneath Ottawa (one recent study estimated about 30% of Ottawa is resting above a layer of marine clay). Ottawa had at least 377,100 households on this sensitive Leda clay deposit by the end of 2010. Many of these houses have already encountered or will be having foundation problems associated with the soil shrinkage due to tree-roots-suction.

According to the Canada Mortgage and Housing Corporation survey (CMHC-2004), 50% of the 19,381 households reported "wear and tear" requiring renovations and 29 per cent of them have reported issues related to basement problems. The Bank of Montreal (BMO) surveys (see Figure 2.1) conducted by the Leger Marketing Department, identified that 38% of the top 10 Canadian home renovation loans was spent on basement repairs.

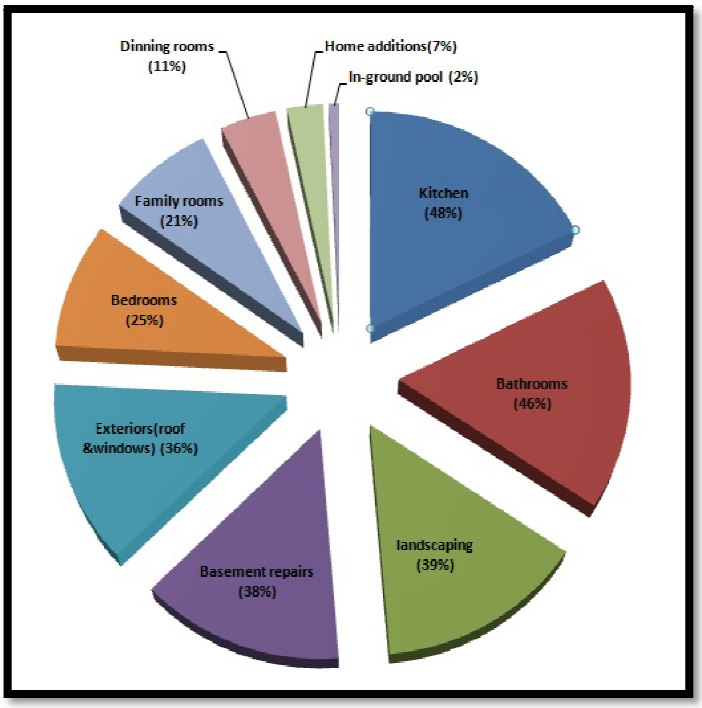

Figure 2.1: Top 10 Canadian Home Renovation Projects for 2011(Source: BMO survey)

Basement and foundation damage necessitating home renovation and repair can be caused by many factors including shrinkage of the clay soil which leads to cracks and contributes to leakage into the basements and subsequently poor fitting doors and windows caused by the differential settlements.

2.2 Potential role of roots in soil shrinkage

In the capital region of Canada, which constitutes the Ottawa-Gatineau region, higher transpiration from trees occurs during the warm dry months of June, July and August each year. In this highly urbanized area, the amount of water transpired by trees is estimated to be larger than that provided by natural rainfall, specifically during the trees' growing season. When the soil experiences water shortage, trees exploit all sources of water at their immediate disposal. The longer the drought conditions exist, the higher will be the risk associated with the trees which contribute to the shrinkage of the surrounding soil.

The key parameters that influence the soil settlement behaviour due to trees transpiration (see Figure 2.2). Transpiration involves the movement of water vapour from the leaves' canopy into the atmosphere. The soil in which trees grow is the reservoir from which the roots replenish the tree. In most tree species, 80 % of roots are found in the upper 0.3 m of the soil. Most of the remaining 20 % of roots are typically found within the top 1.0 to 1.5 m of soil, with some growing up to 2.0 m, and rarely as deep as 3.0 m (CHMC, Understanding and dealing with Interactions between trees, Sensitive Clay and Foundations, 2005). Generally, trees take up water where the soil is in contact with fine or small feeder roots. Once the soil dries out around the root, roots are capable of withdrawing water from surrounding soil areas, but only within an area about 0.3 m from the tips of tree roots.

The zone of influence of the trees demonstrates why shallow-foundations in the range of 1.5 m deep, such as those of town homes and single family units, are at greater risk than deeper foundations in the range of 3.0 m deep (Figure 2.3). The zone of influence of trees is generally related to the extent of their root growth (Figure 2.4). The lateral spread of roots is recorded to be two to four times the height of the tree.

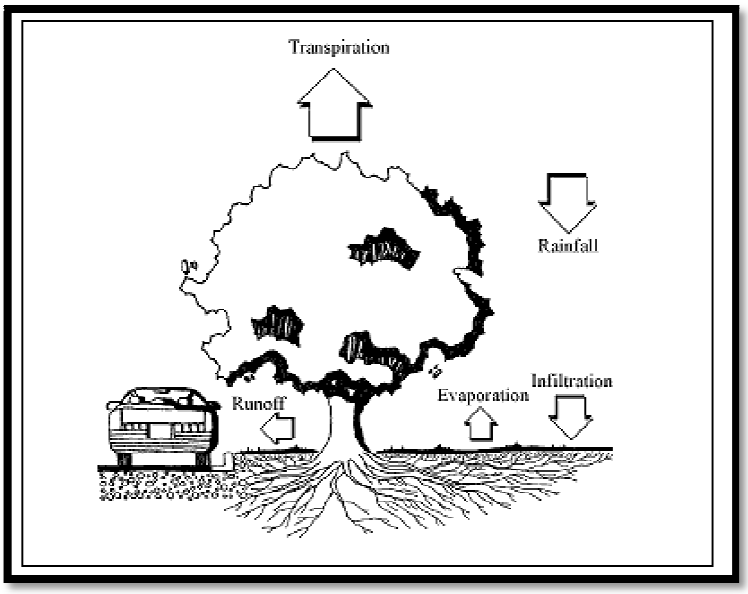

Figure 2.2: Movement of water in an urban area

(Source: Canada Mortgage and Housing Corporation)

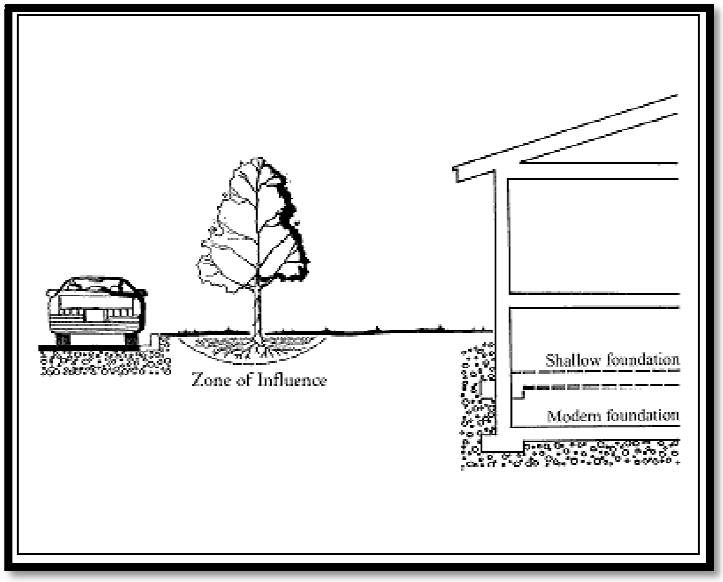

Figure 2.3: The correlation between an immature tree and building foundation

(Source: Canada Mortgage and Housing Corporation)

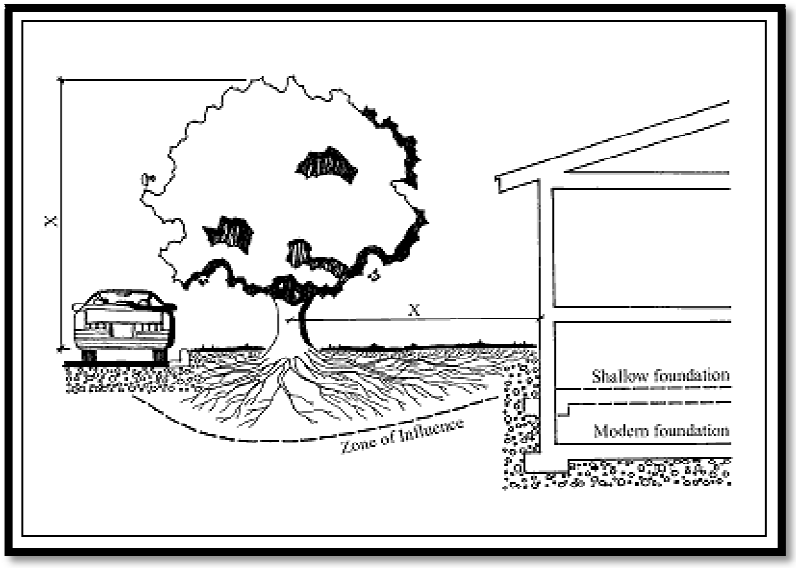

Figure 2.4: The correlation between a mature tree and building foundation

(Source: Canada Mortgage and Housing Corporation)

Soil shrinkage is localized to the zone of influence, where soil water is removed leading to differential settlements. Water can also be removed from the soil by several other mechanisms apart from transpiration, such as construction activities, e.g. excavation.

The conventional housing construction is not designed to handle differential settlements, deformation and cracks on foundation associated with tree roots suction. Due to this reason, in this research work, the *ARS* is used to investigate deformation characteristics of sandy loam soil associated with the capillary action. An artificial root for inducing capillary suction movement of moisture in the soil was first discussed about a century ago by Briggs and Lapham (1900). The concept of artificial root has progressed slowly over the past decades. Research work, in recent years, has revived more interest, particularly in the agricultural science field (Bar-tal et al., 1991 and van Bruggen et al., 2000).

2.3 Capillary Suction

Figure 2.5 details the concept of capillary rise which can be used as a tool to explain the influence of root action. The voids present within the soil can be considered as 'bottle necked' capillaries, which begin to fill as the water present in the particles integrate. Due to gravity, there will be maximum water quantity present in the voids. The soil suction is in the state of reduced pressure compared to the free water surface. As the moisture content of the soil decreases, the water quantity seeps into smaller voids, their radii of curvature also decrease, finally causing increased soil suction.

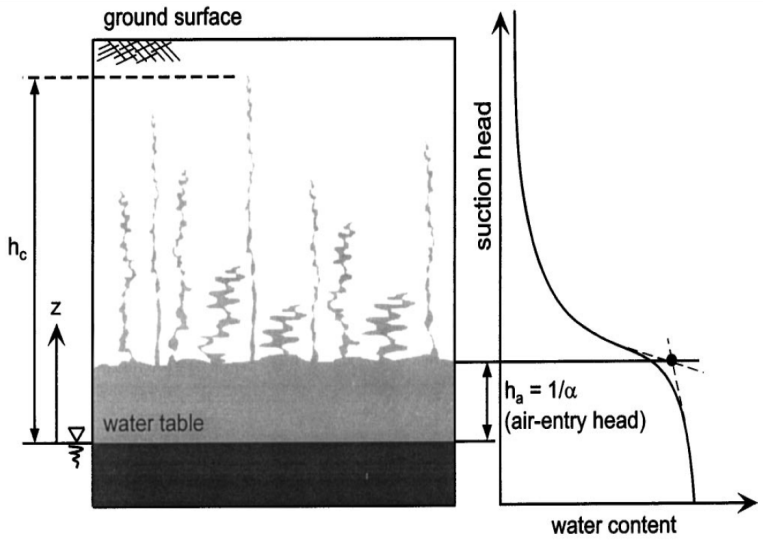

Figure 2.5: Capillary rise in soils of different textures (Source: Lu and Likos 2004)

Water evaporating from the leaves starts the suction pull. The water molecule evaporates from the leaf and pulls on the molecules around it as it departs. This creates a small suction in the water column and pulls water along the leaves-stem-branch-root wall causing capillary action. The chain continues to the surrounding soil acting as a pump, bringing water to the surface from a well. The artificial rooting system (*ARS*) adopts this same concept using a pump and porous material as the interface between the soil and tree root.

2.4 Key Studies Related to Artificial Roots

There are three different types of approaches reported in literature with respect to artificial roots or artificial root systems. The first approach is based on the experimental methods which were adopted by early researchers of agricultural science. The other two approaches are based on using the empirical methods or field studies. Both these approaches are used by geotechnical engineers across the world. The flow chart in Figure 2.6 highlights some key contributions in this research area.

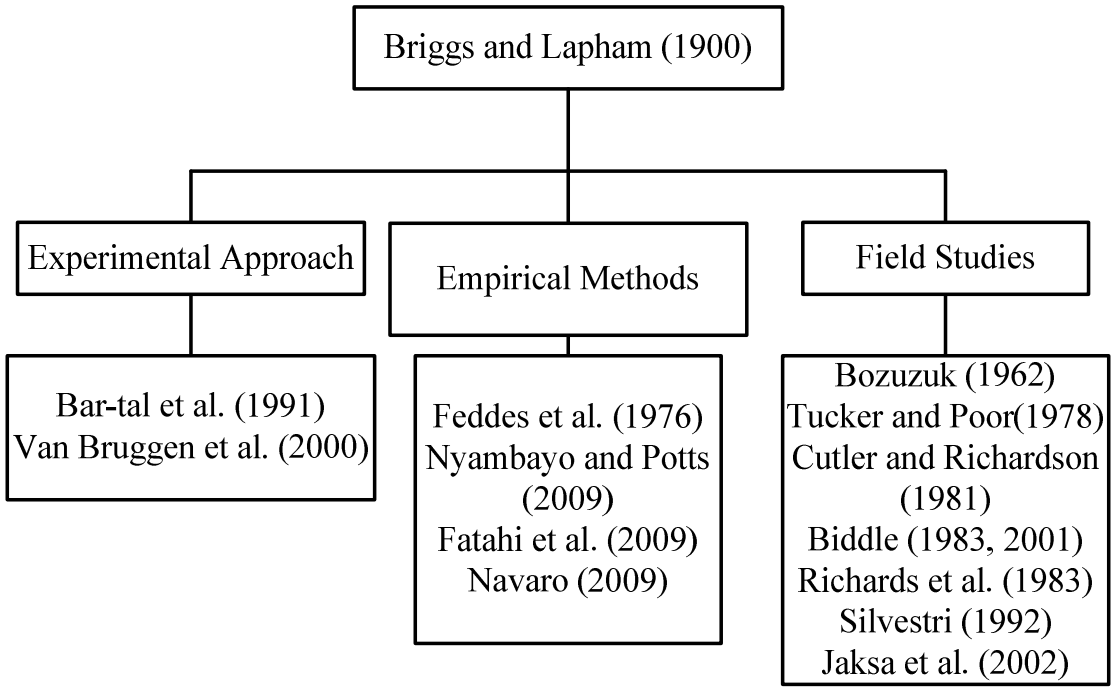

Figure 2.6: Shows development of studies related to artificial roots

2.4.1 Experimental Methods

Briggs and Lapham (1900)

Briggs and Lapham (1900) were the earliest investigators to study the capillary movement of soil moisture using an artificial root. The key parameters required for a

successful artificial root was highlighted by these investigators in the Bulletin 19, Division of Soils of the Department of Agriculture. They proposed different ways to determine the rate at which a soil with certain moisture content is able to supply moisture to the roots of a plant considering an analogous pulling force to the action of the plant root.

Bar-tal *et al*. (1991)

Nearly a century after Briggs et al. (1900 and 1903) and King (1904) pioneering contributions, Bar-tal et al (1991) extended a close to similar concept to study zinc transportation into an artificial root. The objective of this agricultural research was to practically test the transportation of Zinc and validate a model for absorption in plants.

The experimental system adopted consisted of;

(i) A 15-bar bubbling pressure ceramic tube (manufactured by a soil-moisture equipment corporation in Santa-Barbara, CA) with dimensions 0.8 g mass, 100 cm long, 0.2 cm inner diameter, 0.4 cm outer diameter and 12.6cm^2 surface area simulated as the artificial root.

(ii) A solution flowing from a source container towards a fraction collector through connecting Tygon tubes and ceramic tube.

(iii) Tygon tubing

(iv) A peristaltic pump which drove the source solution through the rate of $3.5 \pm 0.5 cm^3 h^{-1}$

(v) Water and Sand: Montmorillonite mixture of known mass ratio.

Bar-tal et al. (1991) suggested from their experimental studies that zinc transportation can be decreased by increasing the fines fraction of clay in the source solution. In other words, zinc present in fertilizers can be prevented to a great extent from contaminating food supply if clay soil is mixed up with the growing soil. The assembly used for conducting this study is shown below (Figure 2.7).

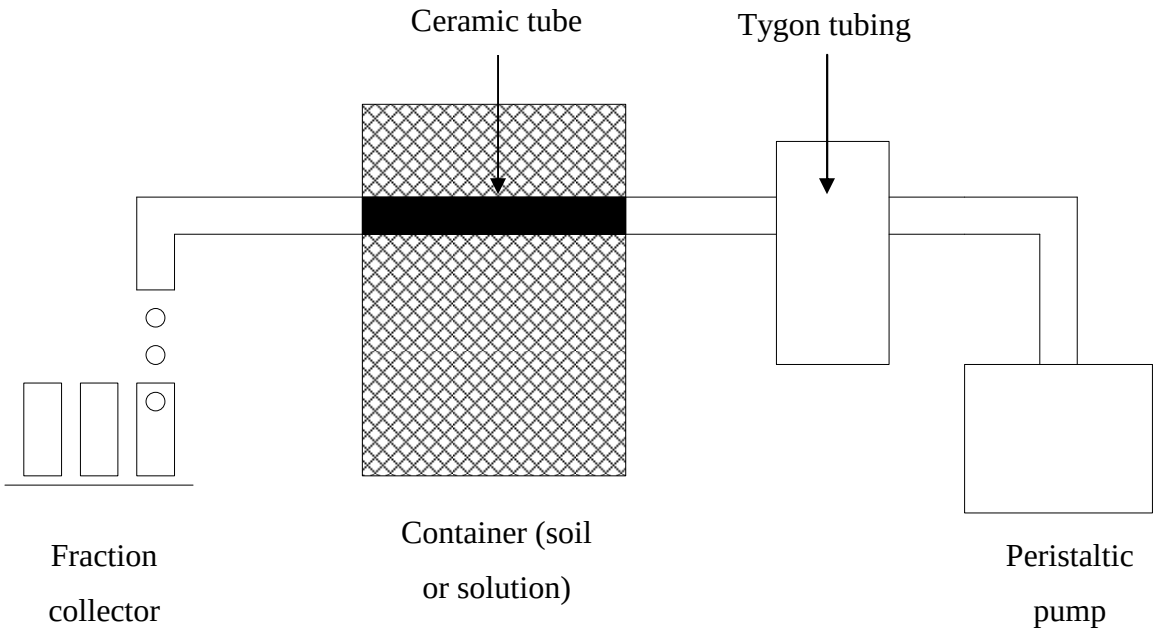

Figure 2.7: Experimental set up by Bar-tal *et al.* (1991)

Van Bruggen *et al.* (2000)

The use of artificial roots cut across disciplines and contributed to the development of several models that are used in practice today. Van Bruggen et al. (2000) proposed a model to study the movement of rhizosphere bacteria populations along wheat roots. Based on their study results, a wave-like distribution (called BACWAVE) is suggested to simulate and model the growth and death of bacteria in relation to their substrate.

2.4.2 Empirical Methods

Several investigators proposed empirical methods which include some models developed to understand the influence of root action on the ground movement. Root water uptake modelling is the process of generating an abstract, conceptual and graphical method, with or without mathematical models to determine pore water pressures and ground

movements considering dynamic factors of the atmosphere, vegetation and soil. Research literature offers a growing collection of methods, techniques and theoretical background including finite element analysis models.

Feddes *et al.* (1976)

Feddes et al. (1976) developed a model for root-water uptake by adding a volumetric sink term to the continuity equation for soil-water flow. Darcy's law was used to describe the flow of water in the unsaturated-saturated soil system. For one-dimensional vertical flow, the origin of z (cm) at soil surface and positive in downward direction, the volumetric flux q $(cm^3\ H_2O.cm^{-2}\ soil.sec^{-1})$ can be written as:

$$q = -K(\theta)\frac{\partial H}{\partial z} \qquad [2.1]$$

where;

$\theta =$ volume water content $(cm^3\ H_2O.cm^{-2}\ soil)$

$K(\theta) =$ hydraulic conductivity$(cm.sec^{-1})$

H = total head (cm) i.e. sum of the pressure $h(\theta)$ and the gravitation head $(-z)$

Applying the principle of continuity and representing the water uptake by the roots as a sink term S $(cm^3\ H_2O.cm^{-3}\ soil.sec^{-1})$ depending on volume water content (θ), the time rate of change of the soil-water content is:

$$\frac{\partial \theta}{\partial t} = \frac{\partial q}{\partial z} - S(\theta) \qquad [2.2]$$

where t is the time (sec).

The basic differential equation for one dimensional vertical flow can be obtained by combining equation (2.3) and (2.4) as given below:

$$\frac{\partial \theta}{\partial t} = \frac{\partial}{\partial z}\left(K(\theta)\frac{\partial H}{\partial z}\right) - S(\theta) \qquad [2.3]$$

Equation (2.4) is a second order, parabolic partial differential equation which is non-linear because of the dependence of K upon θ. Substituting $H = h - z$, assuming a single-valued relationship between h and θ (i.e., hysteresis taken into account) and representing $K\,\partial h/\partial\theta$ by the symbol of diffusivity $D(cm^2.sec^{-1})$

$$\frac{\partial \theta}{\partial t} = \frac{\partial}{\partial z}\left(D(\theta)\frac{\partial \theta}{\partial z}\right) - \frac{\partial K(\theta)}{\partial z} - S(\theta) \qquad [2.4]$$

The sink term can be considered as a function of the soil water content as illustrated in Figure 2.8.

For conditions drier than the wilting point and wetter than a certain anaerobiosis point, it may be assumed that the water uptake by roots is zero. Wilting points vary with the variation in the osmotic pressure of plant-tissues.

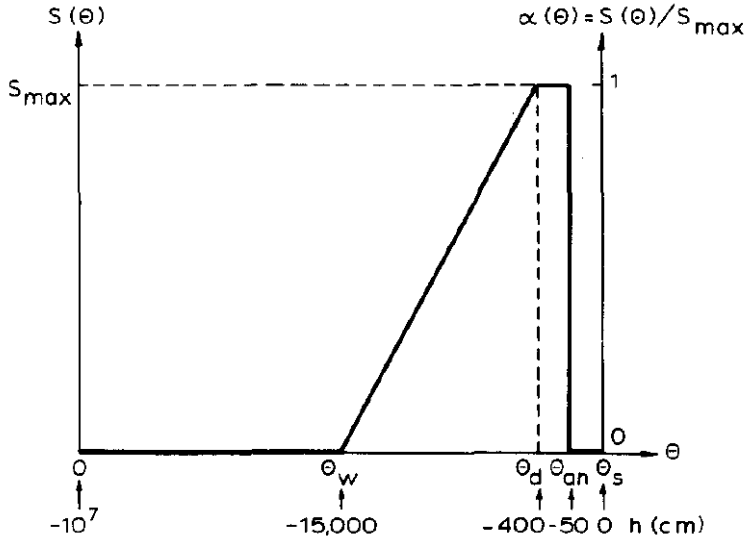

Figure 2.8: General sink term as a function of soil-water content and pressure heads critical for water uptake by roots. (Source: Feddes et al. 1976)

Some differences were observed between the measured experimental results and the computed values due to the adoption of a single moisture retention curve and a single hydraulic conductivity curve for the entire soil profile. More so, boundary conditions at the top of the soil compared to the water uptake by roots in-situ differ due to oversimplified expressions used for sink terms in both in-situ and experimental results.

Nyambayo and Potts (2009)

Nyambayo and Potts (2009) present a root water uptake model in finite element program that can perform mechanical and fluid flow behavior analyses (RWUM) Figure 2.9. The authors consider the soil-plant-atmosphere continuum using rainfall and evapotranspiration as input data in coupled analyses (RWUM). The root water uptake is assumed to be zero at pore water suctions (negative pore water pressure) greater than the wilting point (S_4) and below the life sustained by the tree root in the absence of oxygen (S_1). A linear variation similar to Feddes et al. (1976) was proposed for transpiration (α) to suction.

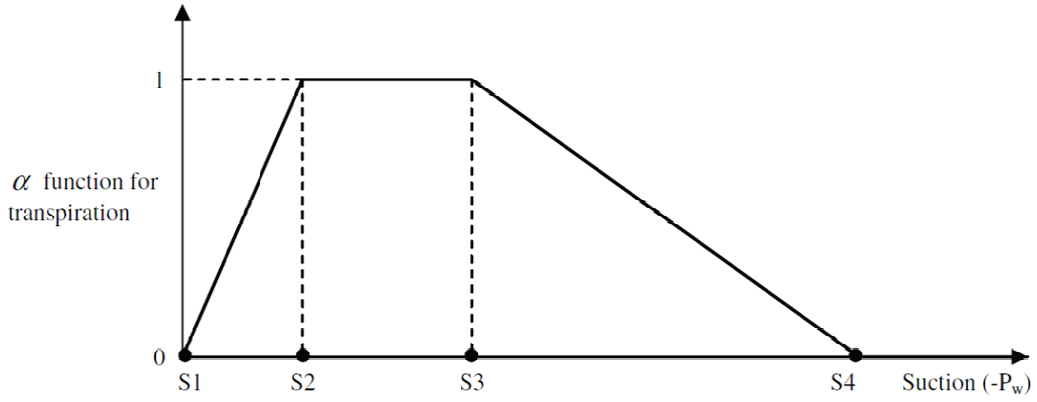

Figure 2.9: Linear variation of transpiration to suction (Source: Nyambayo and Potts 2009)

The results of this model demonstrated that RWUM can be used as a tool to model the ground movement in different seasons. RWUM further showed that in the summer seasons desiccated profile formed cannot return to its initial thickness during winter when

evapotranspiration reduces totally. The results of this study also show that the influence of S_3 is limited to the suction range of 50-200 kPa, which is unlikely to have any significant influence on the ground movements.

Fatahi et al. (2009)

Biddle's (1998) investigated the influence of Poplar trees roots suction on the ground settlement behaviour. Fatahi et al. (2009) have undertaken numerical analysis and parametric studies using the case study results summarized by Biddle (1998). From these studies, they found that the most important factors in root-water uptake are the root density, root distribution, and potential transpiration.

A two-dimensional finite element analysis was used to determine the distribution of soil moisture within radial distance of the tree. In this analysis, it was assumed that rainfall and evaporation compensated each other. The parameters listed below were recommended to be measured or estimated accurately to achieve reliable predictions of the ground settlement using the finite element method (FEM) model.

i. Soil permeability
ii. Suction of wilting point
iii. Soil density
iv. Root length distribution
v. Rate of potential transpiration

This study further stated that the potential transpiration with depth had marginal to no effect on ground movements.

Navarro et al. (2009)

Extending the studies originally presented by Indraratna et al. (2006), Navarro et al. (2009) presented an approach for understanding the influence of root distribution on foundation settlement behaviour in urban areas. The conceptual model used the hydro-mechanical behaviour of unsaturated soils to validate a real stabilization problem. The model investigated makes it possible to point out schematically the functions of the

building-tree system in a large number of cases. It was applied in supporting the identification of damage mechanism in a real case of stabilization, playing a key role in the design of remedial works. Table 2.1 summarizes other key studies based on empirical methods or models.

Table 2.1: Other studies based on empirical methods

Author	Publication
Prasad (1987)	A liner root water uptake model
Gardner (1990)	Modeling water uptake by roots
Green et al. (2006)	Root uptake and transpiration: From measurements and models to sustainable irrigation
Rees and Ali (2006)	Seasonal water uptake near trees: a numerical and experimental study

2.4.3 Field Studies

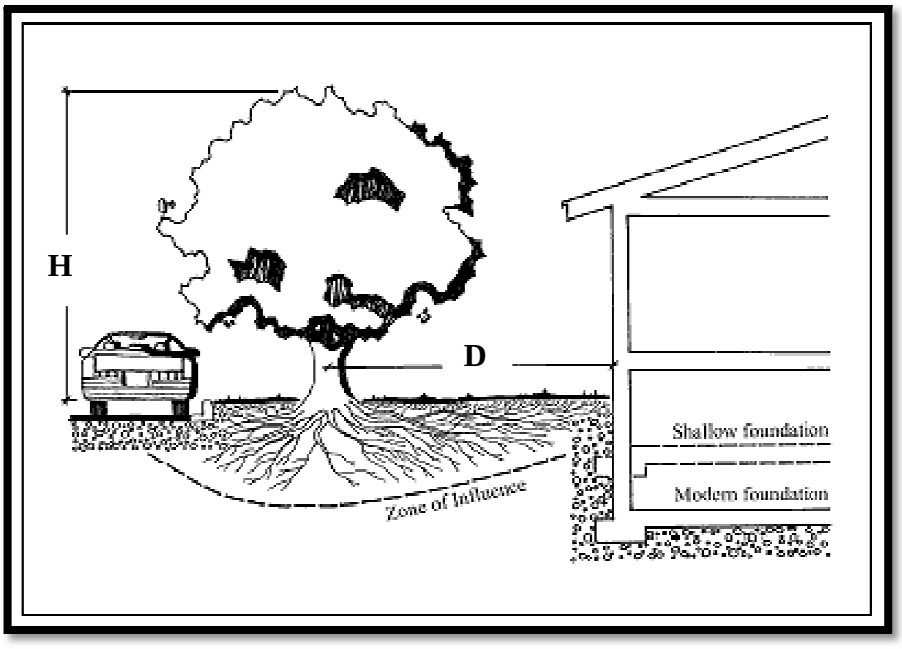

Figure 2.10: Showing Safe distance D/H, (Source: CHMC)

Bozozuk (1962) was one of the earliest pioneers who monitored settlement and shrinkage with depth and distance from an elm tree. Subsequently, several researchers have investigated using a field approach to monitor the validity of safe distance and provided their recommendations (see Table 2.2). Safe distance Figure 2.10 can be expressed as a ratio of minimum horizontal distance, *(D)* to foundation base and the height of tree *(H).*

Table 2.2: History of attempts made using the field approach

Author	Related studies
Bozozuk (1962)	Pioneered and monitored settlement and shrinkage with depth and distance from an elm tree. Recommended: Safe distance of foundation using $(D:H)$.
Ward (1953)	Monitored planting of trees and soil desiccation in United Kingdom. Recommended: Safe distance $(D:H)$ should be equal to one.
Tucker and Poor (1978)	Studied a demolished estate caused by tree roots. The species present were mulberry, elm, cottonwood and willows. Recommended: $(D:H)$ greater than one.
Cutler and Richardson (1981)	Reported cases on 2,600 cases of building damage in UK. Data base of specie findings showed 75% of building damage was influenced by a particular tree species. Recommended: The farther the tree related to the height the more dangerous the tree.
Biddle (1983, 2001)	Conducted soil water changes around specific tree species in open grass land in the UK. Water changes were monitored with neutron moisture meter. Recommended: The depth, radius, horizontal and vertical drying was dependent on the specie of the tree.
Richards et al. (1983)	Conducted tree species within two cities in Australia. The eucalypts and pine tree species. Recommended: Eucalypts had more drying effects than pine on clay soil.
Silvestri et al.	Monitored soil moisture over three years for two damaged

(1992)	buildings in Montreal, Canada. The results show that Lombardy popular and other species match Biddle (1983) efforts. Recommended: Desiccating effects would affect any shallow foundation constructed at distances $1H$ to $1.5H$.
Jaksa et al. (2002)	Used suction profiles to study influence from large gum trees in two cites. Single gum tree and Row of trees. Recommended: The single gum trees influenced suction when $D/H \leq 0.5$, the row of trees influenced suction when $D/H \leq 0.8$, this was in accordance with Richards et al. (1983).

Tree pruning can play an important role in reducing foundation damage. When pruning the mass of trees in terms of branches and roots are reduced, to maintain a balanced system. This role reduces the amount of water needed to meet transpiration. Some researchers in geotechnical engineering Table 2.3 have investigated the effect of tree pruning.

Table 2.3 : Effect of Tree pruning on foundation damage

Author	Publication
Holtz , Forth geotechnique symposium in print (1983-6)	The influence of vegetation on the swelling and shrinking of clays in the United State of America
Driscoll, Forth geotechnique symposium in print (1983-6)	The influence of vegetation on the swelling and shrinking of clays in Britain
Blight (2002)	The vadose zone soil-water balance and transpiration rates of vegetation
Smethurst et al. (2006)	Seasonal changes in pore water pressure in a grass-covered cut slope in London clay

2.5 Other Studies

Some investigators have studied the damage caused by tree roots on buildings foundations from laboratory tests conducted in model tanks.

Satriani *et al.* (2010)

Satriani *et al.* (2010) studied the influence of the direct and indirect root effects on monumental and historical buildings using non-destructive geophysical techniques. A three year old peach tree was planted at the centre of the wooden box of 1.10 m x 1.10 m x 0.60 m and filled with about 60% of sand and 40% of clay to understand the growth rate of roots. The results of this study were useful in extending geophysical techniques to the identification of tree root growth close to buildings.

2.6 Studies related to Leda Clay and roots action

The Table 2.4 summarizes the key contributions by several researchers who studied the shrinkage characteristics of Leda clay due to tree roots suction using different approaches.

Table 2.4: Summary of the key research contributions related to the shrinkage behavior of Leda clay.

Authors	Publication	Summary
Bozozuk (1962)	Soil shrinkage damages shallow foundations at Ottawa, Canada	Drying of undisturbed Leda clay breaks down flocculated structure of the soil. Large trees cause severe settlements in buildings and damage streets and sidewalks. To minimize effects of flocculated break down vegetation should be watered during summer months
Crawford (1968)	Summary of Eastern Canada Quick clays	Large settlements occur due to shrinkage in the upper 10 or 15ft of Leda clay. Shrinkage is caused primarily by withdrawal of soil water by vegetation. Restricting tree growth near shallow foundation unless soil is dried with low

		water content it has little swelling potential.
Burn (1973)	House settlements and trees	Trees cause the most damage under the fast growing species. Damage is caused by lack of rainfall during the growing season Where subsoil is Leda clay, problems can be avoided by judiciously planting slow growing tree species.
Penner and Burn (1978)	Review of engineering behavior of Leda Clay Electron micrographs of Leda Clay	Foundation damage by trees include consumption of water proportional to size of tree Fast-growing trees require large amounts of water During landscaping trees should have distance equivalent to height of tree. Rows of trees are more aggressive and water consumption extends beyond influence zone, compared to individual trees. As soon as damage is observed offending tree should be removed.

The species recommended by the City of Ottawa and the Forestry Service, were selected according to their height and root depth. This classification can serve as a means to mediate the problem statement but it does not stop the moisture demand of trees, especially during prolonged summer seasons or drought.

2.7 Tree species planted in the Ottawa area

The summary shown gives a list of trees recommended species for the Ottawa area, compiled by the forestry services. The species are selected depending on the localization of the tree; also certain species are categorized as sensitive to the marine clay soil. The trees are classified in terms of maximum height. The Table 2 in [Appendix D] shows height and species of trees in terms of: (i) small, (ii) medium and (iii) large.

2.8 Estimation of Settlement Behaviour from the Modulus of Elasticity extending to the Mechanics of Unsaturated Soils

The modulus of elasticity can be used as a tool to better understand the stress and deformation behaviour of unsaturated soils in terms of two stress state variables; namely, net normal stress $(\sigma - u_a)$ and matric suction $(u_a - u_w)$. Several investigators have provided relationships for soil structure, water phase and flow laws for the water phase to determine the deformation behavior of an unsaturated soil (Alonso et al. 1990, Gens and Alonso 1992, Fredlund and Rahardjo 1993, Vu and Fredlund 2004).

The primary interactive processes involved with a volume change analysis of an unsaturated soil are stress deformation and water flow.

There are four different types of modulus of elasticity discussed by Vu and Fredlund (2004).

i. E is an elastic deformation parameter for the re-arrangement of soil structure or soil with respect to net normal stress.
ii. H is an elastic deformation parameter for the re-arrangement of soil structure or soil with respect to a change in matric suction.
iii. E_w is an elastic deformation parameter for the re-arrangement of soil structure or soil with respect to the change in the amount of water in the soil with respect to a change in net normal stress.
iv. H_{w} is an elastic deformation parameter for the re-arrangement of soil structure or soil with respect to the change in the amount of water in the soil with respect to a change in matric suction.

In addition to any these parameters, a successful deformation model would include Poisson ratio μ; slopes of the soil structure and water phase constitutive surface see Figure 2.11.

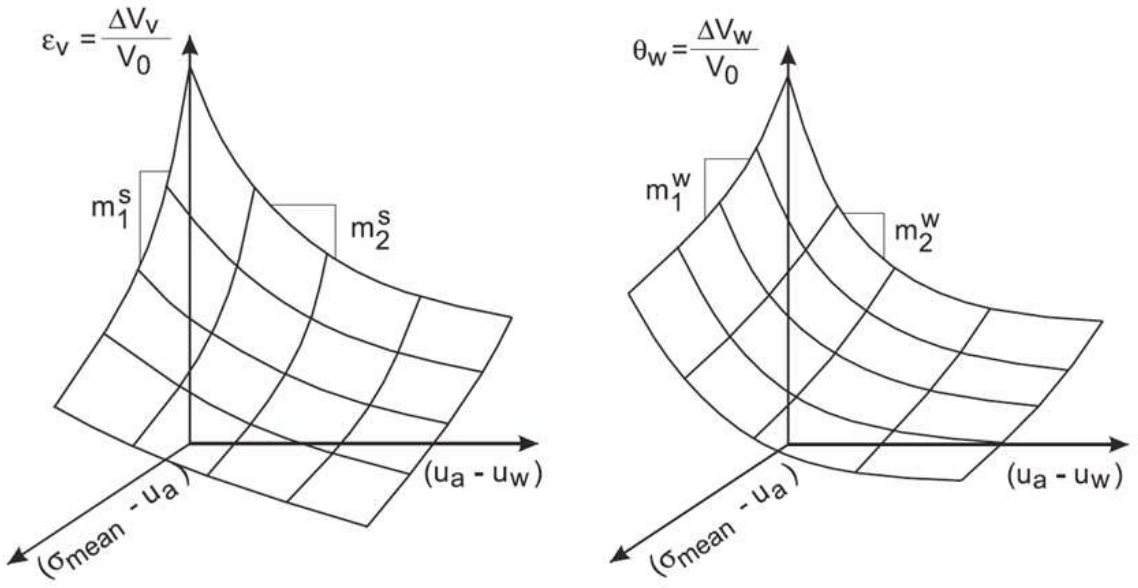

Figure 2.11: Constitutive surfaces for (a) Soil structure (b) water phase of an unsaturated soil (Source: Vu and Fredlund 2006)

where $\varepsilon_v = \Delta e/(1 + e_0)$, e_0 is the initial void ratio of the soil as a reference element σ_{mean} is the mean net total stress.

The above relationships can also be used to understand the volume change characteristics due to root action of the Leda clay using the mechanics of unsaturated soils.

2.9 Summary

The influence of root capillary suction on soil deformation behaviour has been investigated since 1900. Several researchers have adopted different approaches towards understanding the behaviour of ground movements caused by maturity of tree roots as summarized in this Chapter. However there are limited studies using a laboratory artificial rooting system to monitor surface deformation behaviour of soils. In this thesis, surface deformation of soil with respect to matric suction was investigated using an experimental approach from laboratory studies. In addition, a finite element modelling approach is also presented to estimate the settlement behaviour associated with roots

action. The results of both these approaches were interpreted using the mechanics of unsaturated soils. Comparisons between the experimental results and the modelling approach were also provided. The objective of this thesis is to provide a rational basis of not only interpreting the settlement behaviour of ground settlements due to tree roots but also to provide a modelling approach using commercial software Geo-Slope (2007) to estimate the settlements.

CHAPTER 3

EQUIPMENT DETAILS AND METHODOLOGY

3.1 Introduction

A comprehensive experimental program was planned and conducted for investigating the settlement behaviour in a loam soil when subjected to artificial-roots-suction (*ARS*) in the University of Ottawa Bearing Capacity Equipment (UOBCE). The UOBCE was originally designed by Mohamed and Vanapalli (2006) for determining the bearing capacity of unsaturated soils using model plate load tests. Several design modifications were introduced into the UOBCE for conducting the proposed research. This chapter provides key details with respect to the modifications introduced into the UOBCE along with the instrumentation and other accessories used for collecting the necessary data. The data collected from the modified UOBCE include matric suction, volumetric water content and surface deformation changes associated with suction changes due to the *ARS*. The instrumentation used for collecting the data includes conventional Tensiometers and decagon MPS-1 for measuring matric suction and 5TM probes for measuring volumetric water content and temperature. A new and innovative non-contact method is used to measure surface deformation of the soil in the UOBCE using the *PIV* technique. In addition, design details with respect to the *ARS* for simulating tree-roots-suction in the UOBCE are also detailed.

3.2 Experimental program

The experimental program performed for the proposed research is summarized in Figure 3.1 as a flow chart. The details related to the various phases of this research are summarized succinctly in the following sections.

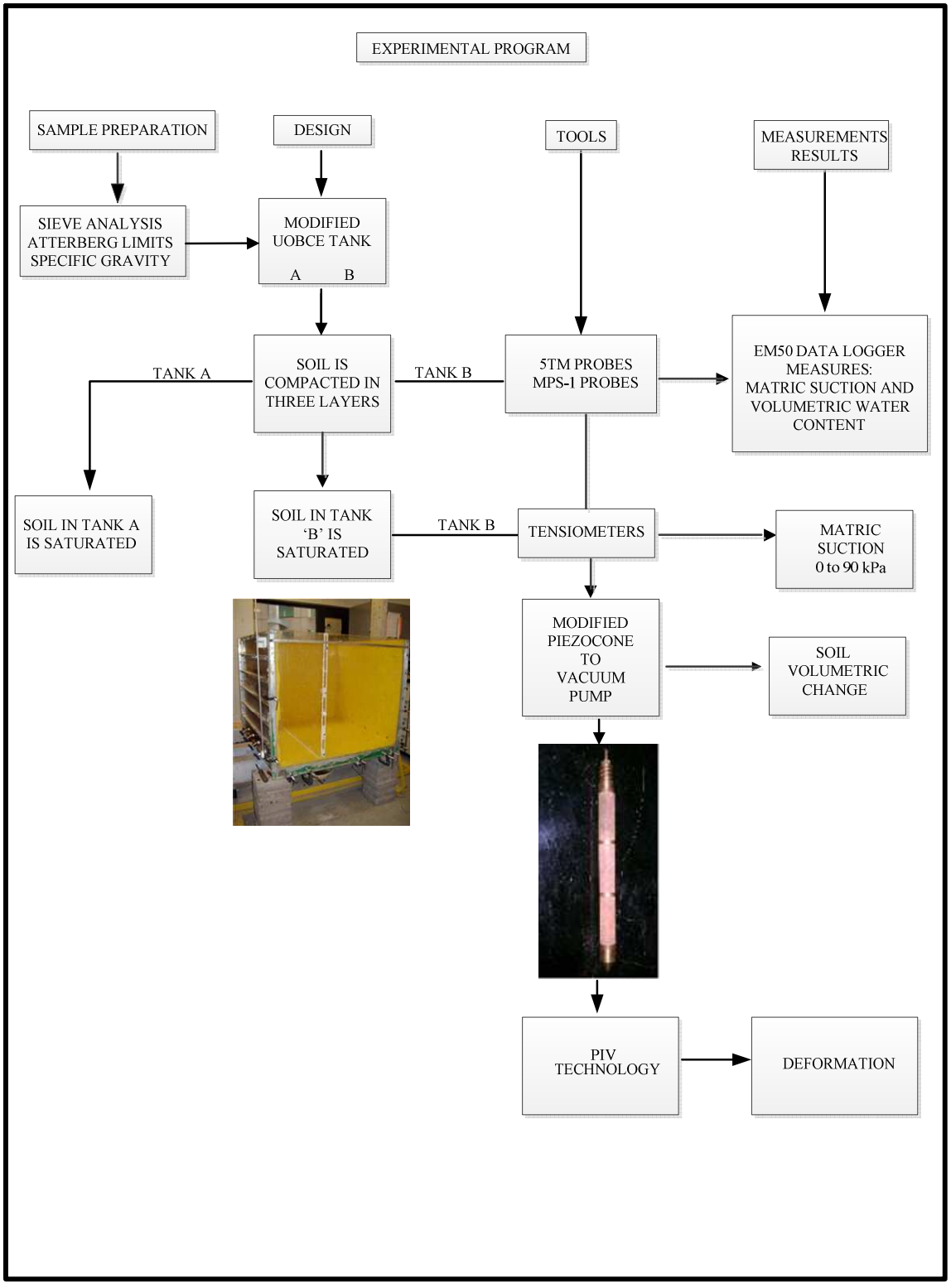

Figure 3.1: Proposed Experimental Program

3.3 Experimental setup

The key experimental setup for collecting the required data include the University of Ottawa Bearing Capacity Equipment tank and the artificial rooting system (*ARS*) which is comprised of a piezocone, a peristaltic pump and a suction probe along with nine volumetric water content probes. In addition, eight conventional Tensiometers, several MPS-1s and two high definition cameras were used in the experimental setup. While Tensiometers and MPS-1 were used for gathering the data of matric suction; the surface settlement information was estimated using *PIV* technology from the high definition cameras.

3.3.1 University of Ottawa Bearing Capacity Equipment (UOBCE-2006)

Mohamed and Vanapalli (2006) designed and constructed special equipment to determine the bearing capacity of sand under saturated and unsaturated conditions. This equipment is referred to as the University of Ottawa Bearing Capacity and is abbreviated throughout this thesis as UOBCE. The aluminum tank was constructed using a 6mm thick aluminum sheet. Metal stiffeners were added along the horizontal direction to prevent any lateral bending or bulging that may occur during the loading of the soil. Several modifications have been introduced into this equipment to conduct the proposed research program. The key features along with the modifications in the UOBCE are shown in Figure 3.2. The major modifications in the UOBCE includes the division of the single tank into two independent tanks A and B with dimensions 375 mm × 900 mm × 750 mm and 500 mm × 900 mm × 750 mm, respectively.

The smaller tank, A with no artificial-root-system (*ARS*) is used as a reference tank. The settlement, suction and volumetric water content changes are measured in the larger tank B with the *ARS* and other accessories. Similar procedures were used for placing the loam in both the tanks A and B with respect to compaction density and initial conditions. More details of the functions of the tanks A and B and the *ARS* are provided in later sections and while discussing results in later chapters.

Two piezometers, one on the left and the other on the right side of the tank were added to monitor the level of water table in tanks A and B respectively (Figure 3.2). The front elevation of the tank was made from transparent acrylic panel. The acrylic panel served the function of a window to allow observation of the water table. The acrylic panel was 25 mm thick fastened with C-clamps and acrylic glue. There were no observed deformations in the acrylic panel or water leakage in the test tank during the soil fill and throughout the duration of the tests carried out in the tank.

The decagon 5TM and MPS-1 probes were buried during the soil fill in three layers. With the aid of the acrylic panel and drainage valves, the amount of water supplied to the tank was controlled to avoid over-flooding in the tank. There were two elevated buckets (on the left side of tank 'A' and right side of tank 'B') at 1.2 m above ground level connected to the modified UOBCE by four supply valves and flexible pipes. The HD cameras are firmly glued; one on the acrylic panel and the other on the rigid aluminium walls avoiding any form of movements.

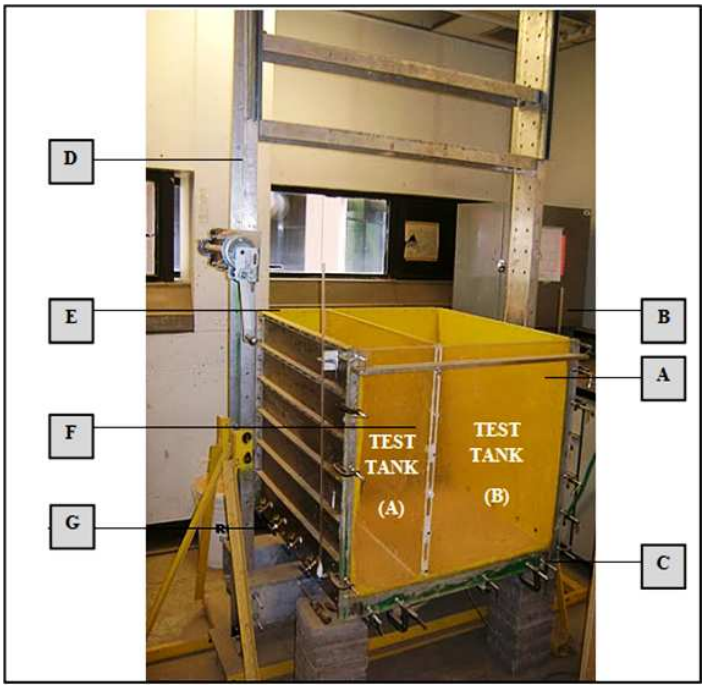

Figure 3.2: Modified UOBCE Special equipment

(A) 25 mm-thick Acrylic panel
(B) Piezometer for the water table level
(C) Clamps used to hold Acrylic panel to aluminum walls
(D) Metal form work and cross bar
(E) Rigid-aluminum walls
(F) 20 mm-thick Acrylic panel separating the test tanks (A and B)
(G) Water supply valves

3.3.2 Test Tank

The modified UOBCE with the tanks (A and B) shares the same frame work as shown in Figure 3.3. A single sheet acrylic partition panel of 19 mm was braced to the walls of the aluminum and the 25 mm acrylic front panel by bolts and waterproofed sealant.

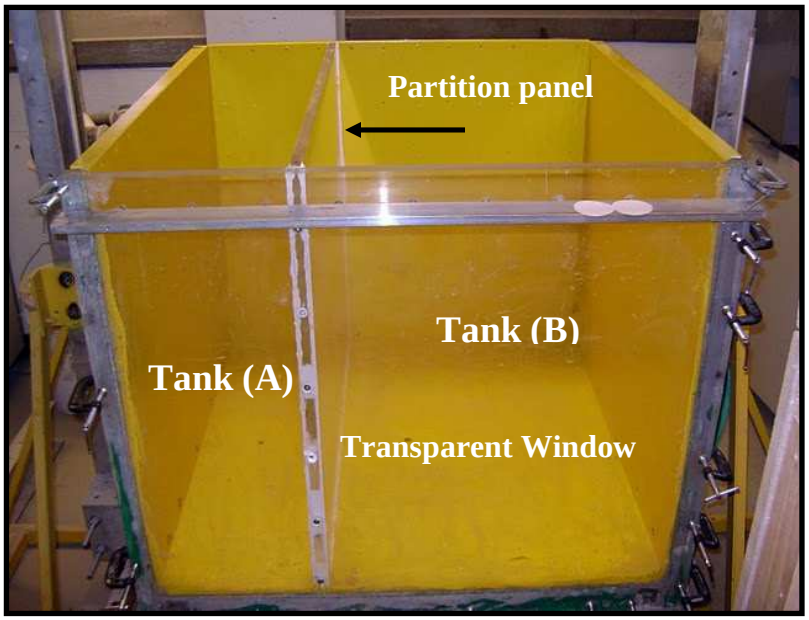

Figure 3.3: Empty test tanks (A and B)

The soil collected from the site was prepared by removing roots and rocks by hand picking. This soil was oven dried at 110^{o}C for a period of 24 hours to remove the natural water content. The soil was allowed to reach room temperature conditions in the laboratory and then poured into a 60 liter rubber drum. The drum with the soil was rolled across the laboratory to achieve homogenous soil conditions.

The prepared soil was compacted in both the tanks in three equal layers. Each layer was compacted using a 5 kg hammer to achieve density of 17.4 kN/m^3. A total of 214 kg and 435 kg of soil were needed respectively in tank A and tank B to achieve this density.

The compacted soil was saturated from the bottom of tanks using valves. This was achieved by allowing the water to seep from elevated bucket to the respective tanks (A and B). The saturation valves were installed at the bottom left and bottom right side of the test tank (see Figure 3.4 (a)). For flood control, drainage flow valves were installed under both test tanks (see Figure 3.4 (b)).

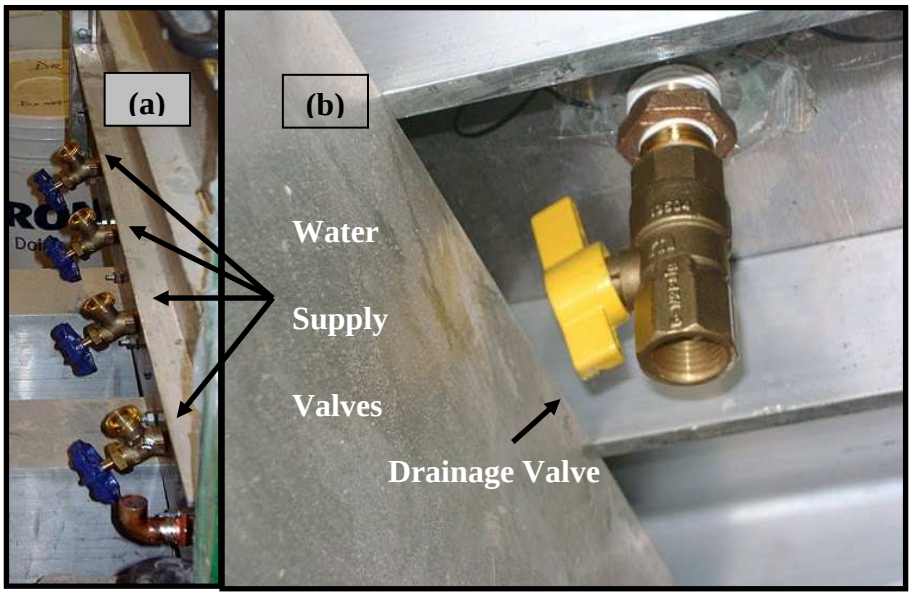

Figure 3.4:(a) Water supply valves on left of the test tank (b) Draining valve

3.3.3 Artificial Root System

A special system was designed to simulate the action of tree roots in the modified UOBCE tank which is referred to as the artificial-root-system (*ARS*). The *ARS* used for of the research consisted of (i) piezocone; (ii) soil moisture suction vacuum gauge; (iii) rubber tube and (iv) peristaltic pump.

Piezocone is essentially a piezotube (i.e., brass tube with fine perforations) that can be easily inserted in the soil. A single piezocone is used in the present research program to

simulate tree roots. A peristaltic pump in the *ARS* facilitates to generate suction by displacing water from the soil surrounding the piezocone through a flexible tube.

Figure 3.5 shows the *ARS* assembly which consists of the piezocone connected to a flexible 9.5 mm rubber tube and the vacuum gauge which is capable of measuring suction from 10 kPa to 100 kPa. The peristaltic pump has a capacity to generate a minimum of 40 kPa at 10 rpm (revolution per minute) and a maximum of 90 kPa at 100 rpm under ideal conditions. The number of revolutions per minute can be controlled to achieve different values suctions. The limitation of the present set up however is that a uniform suction cannot be generated all along the length of the piezocone and its surroundings. More details of the performance of the *ARS* are detailed in later sections.

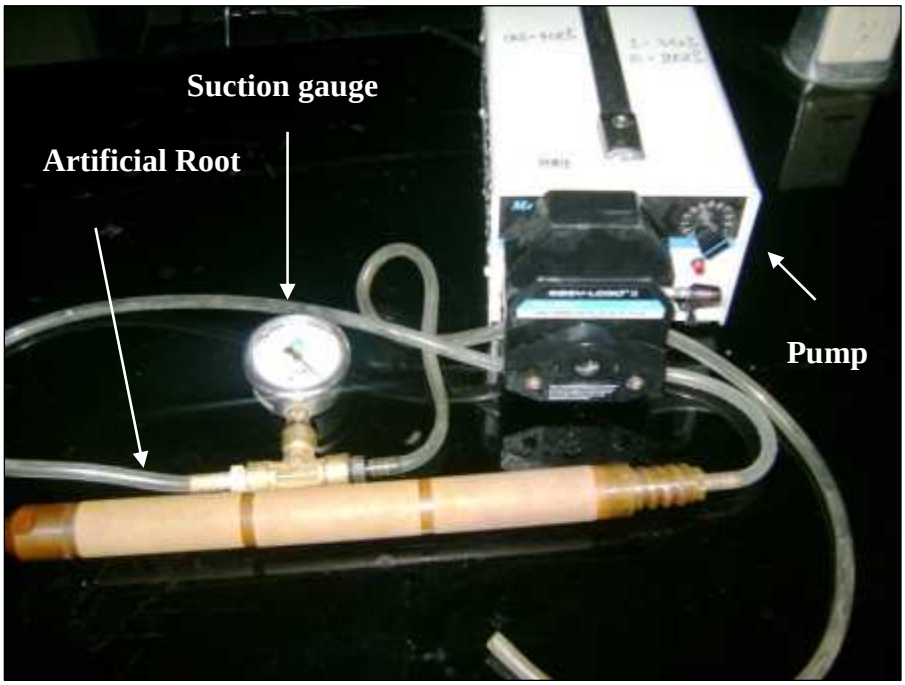

Figure 3.5: Artificial root system assemblies

The peristaltic pump of the *ARS* assembly shown in Figure 3.5 experienced problems during the lengthy periods of testing (e.g. 15 hours). Longer time periods were required to achieve equilibrium conditions with respect to the removal of water using the peristaltic pump (running it at a constant capacity, rpm). Due to this reason, in some cases

irregular suction values were achieved around the piezocone that was buried within the soil. The single stage vacuum generator manufactured by Gast incorporation is used in the *ARS*. This vacuum converts air pressure to suction, using a hydraulic pump system. The vacuum generator does not need any source of electrical power and can work for extended periods of time without laboratory hazards. The Gast-single stage vacuum generator uses a vacuum splitter to regulate the amount of suction transferred to the piezocone which simulates as an artificial root in the UOBCE.

The Artificial Rooting System (*ARS*) used in the present research is shown in Figure 3.6 includes the piezocone, vacuum gauge from Soil Moisture Inc., Gast Inc. single stage vacuum generator all connected by fisher scientific tubing with a diameter of 9.5 mm.

Figure 3.6: Single stage vaccum generator

3.4 Tensiometer

A Tensiometer is a device that can be used to directly measure the negative pore-water pressure in a soil. The measured negative pore-water pressure is numerically equal to the matric suction when the pore-air pressure is atmospheric (i.e., u_a = 0 gauge pressure). Tensiometers are conventionally used both in the laboratory and in the field to measure the matric suction in unsaturated soils reliably in the range of 0 to 90 kPa.

Figure 3.7 : Tensiometer with a vacuum gauge and other accessories

The Tensiometer assembly consists of a high air-entry, porous ceramic cup connected to a pressure-measuring device such as the vacuum gauge through a small bore tube (Figure 3.7). The tube is usually made from plastic due to its low heat conduction and noncorrosive nature.

To measure suction, the tube and the cup are filled with distilled de-aired water and inserted into a pre-cored hole such that there is a good contact with the soil. The water in the Tensiometer will have the same negative pressure as the pore-water in the soil once equilibrium is achieved between the soil and the measuring system.

Tensiometers cannot measure matric suction values higher than 90 kPa due to problems associated with cavitation of the water in the Tensiometer. The osmotic component of soil suction is not measured with Tensiometers since soluble salts are free to move through the porous cup.

3.5 Volumetric Water Content (5TM Hoskin Scientific probes)

Figure 3.7 shows the Decagon 5TM Hoskin Scientific probe used for the present research program. The probe dimensions are 100 mm × 32 mm × 7 mm. This device is capable of measuring the volumetric water content, θ and the temperature. The 5TM is designed to measure the volumetric water content (VWC) and temperature of soil and growing media.

It consists of two different sensors; namely, dielectric volumetric water content sensor and thermal sensor (thermistor). Using an oscillator running at 70 MHz, it can measure the dielectric permittivity of soil to indirectly determine the VWC. The measurable apparent dielectric permittivity (ε_a) is in the range of 1 (air) and 80 (water) and the accuracy is ±3% of the actual VWC of soil if the VWC of a soil is calculated using the Topp equation (Topp et al. 1980).

$$VWC = 4.3\times10^{-6}\varepsilon_a^{3} - 5.5\times10^{-4}\varepsilon_a^{2} + 2.92\times10^{-2}\varepsilon_a - 5.3\times10^{-2} \quad [3.1]$$

A thermistor in thermal contact with the sensor prongs provides the soil temperature in the range of -40 to 50°C with the accuracy of ±1°C and 0.1°C resolution.

3.6 Matric Suction Device (MPS-1 Hoskin Scientific probes)

The MPS-1 is a tool that can be used to estimate the water potential of soil and other porous materials (Figure 3.8). It has a low power requirement which makes it an ideal sensor for permanent burial in the soil and continuous reading with a data-logger or periodic reading with a handheld reader. The dimensions of the sensor are 75 mm × 32 mm × 15 mm. The MPS-1 measures the dielectric permittivity of a solid matrix – porous ceramic discs – to determine its water potential. The porous ceramic disc is highly dependent on the amount of water that is present in the pore spaces of the ceramic. Hence, the accuracy of the MPS-1 is dependent on the accurate measurement of water potential. The range of matric suction that can be measured using MPS-1 is in the range of 10 to 500 kPa with the accuracy of ±5 kPa from 10 to 50 kPa and ±20% of the reading from 50 to 500 kPa. Resolution is 1 kPa from 10 to 100 kPa and 4 kPa from 50 to 500 kPa.

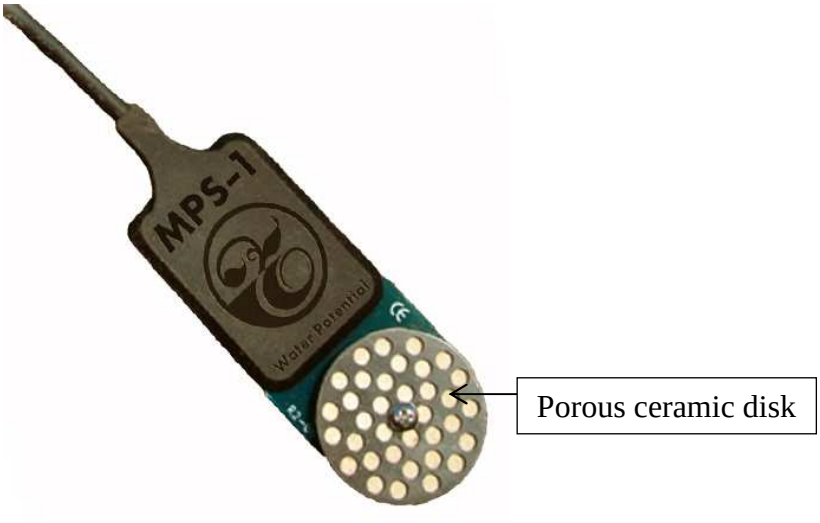

Figure 3.8: MPS-1 Dielectric Water potential sensor

3.7 Data Acquisition System (Em50 Hoskin)

Figure 3.9 shows the Em50 data acquisition system that was used in the present research program. This system has five sensor ports and one computer port (com-port). The dimension of the data acquisition system is 127 mm × 203 mm × 51 mm, configured by plugging a laptop or handheld into the com port. The ECH20 utility software included in the EM50 package provides a setup where windows can be used to specify how often the sensors (5TM and MPS-1) can be recorded.

Figure 3.9: EM-50 Data Logger

3.8 *PIV* Technology

Several images of the modified OUBCE soil surface were taken using a high definition (HD) camera with specifications of 720p auto focus HD video (Figure 3.10). The images taken over a long period of time as the soil surface was settling due to the desaturation in the tank associated with the *ARS*. The HD camera has dimensions of 48.8 mm by 109 mm and is connected to a USB port of a laptop on which Dorgem software was installed. This software has the provision to specify how often images can be taken and saved in a specified folder on the laptop. The images from the HD camera can be uploaded onto java-based software called JPIV. The property setting of JPIV was modified in the interrogation window in order to allow for an external plug-in called "image J-3D surface plot" to run successfully in the program. This plug-in provided an added advantage to JPIV software in its analysis of surface deformation, which is the primary objective of this research project. The software used a reference dimension (in this case, the dimensions of UOBCE inputted in pixels) to determine the change in surface deformation by comparing between pixel changes in the photo file. The summary of the results is represented on a contour graph plan. The "perspective" and "scale" functions allow the calibrated photos to be visualized in 3D-projection in the form of contours. More details

of how the collected information is converted into deformation data are summarized in Chapter 6 Section 6.7.

Figure 3.10: High Definition (HD) camera (source: Microsoft Life Cam manual)

3.9 Tempe Cell

The Tempe cell is a device commonly used to determine the soil water characteristic curve (*SWCC*) for soils in the suction range of 0 to 500 kPa. The Tempe cell is used to measure the *SWCC* typically for a higher suction range (i.e., 0 – 1500 kPa). The Tempe cell is a smaller unit and only facilitates to measure the *SWCC* of an individual specimen.

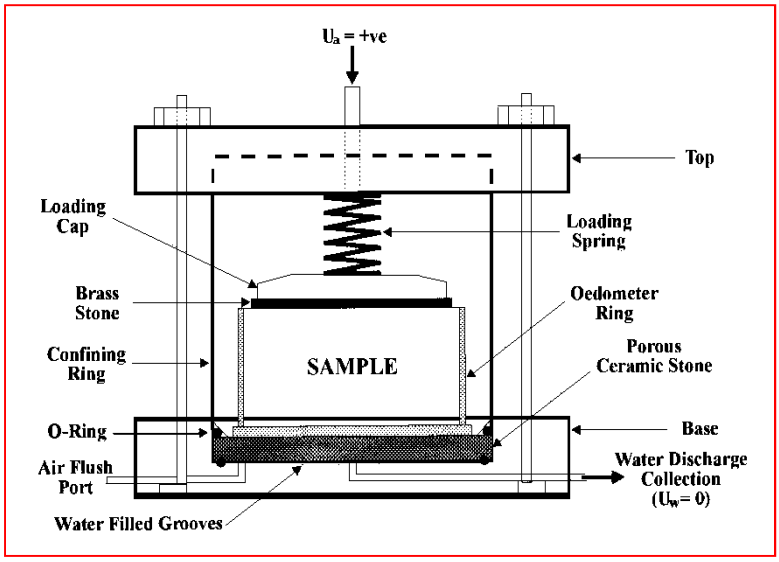

Figure 3.11: Schematic of a Tempe cell used in the research

Figure 3.11 shows the Tempe cell set up used for measuring the *SWCC*. A saturated soil specimen is placed on the saturated porous ceramic stone or disk in the pressure chamber. The air pressure in the chamber is raised to a prescribed value above atmospheric pressure (i.e., above zero gauge pressure). The pore-water pressure connection at the bottom of the cell is open to atmosphere (i.e., pore-water pressure, u_w = 0). The matric suction of the soil is equal to the gauge air pressure in the chamber since the pore-water pressure is maintained at atmospheric conditions. At equilibrium conditions, the soil specimen(s) has a water content that corresponds to a specific matric suction value applied. The mass of the soil specimen(s) is determined after the equilibration. Approximately, 1 or 2 days of time is required to achieve equilibration conditions for the tested loam. The equilibration time is dependent on the type of soil, thickness of soil specimen, applied suction and the coefficient of permeability of the soil specimen and the high-air entry disk.

Several values of matric suction that are increasing from low to high values are applied to obtain the *SWCC* relationship. Typically, 6 to 8 data points are collected such that the key features of the *SWCC* (i.e., the air-entry value and the different zones of unsaturation) are determined. The gravimetric water content of the soil specimen(s) is determined at the

end of the test (i.e., highest suction range tested). The information related to the other data points of the *SWCC* are determined from back calculations based on the volume-mass properties of the soil. The *SWCC* is plotted as the variation of water content, *w* or volumetric water content, θ, or degree of saturation, *S*, with respect to suction.

3.10 Pressure Plate Apparatus

The pressure plate is another device used to determine the Soil Water Characteristic Curve (*SWCC*). The pressure plate equipment is designed to apply matric suction to soil specimen utilizing the axis translation technique. Figure 3.12 shows a schematic of pressure plate equipment.

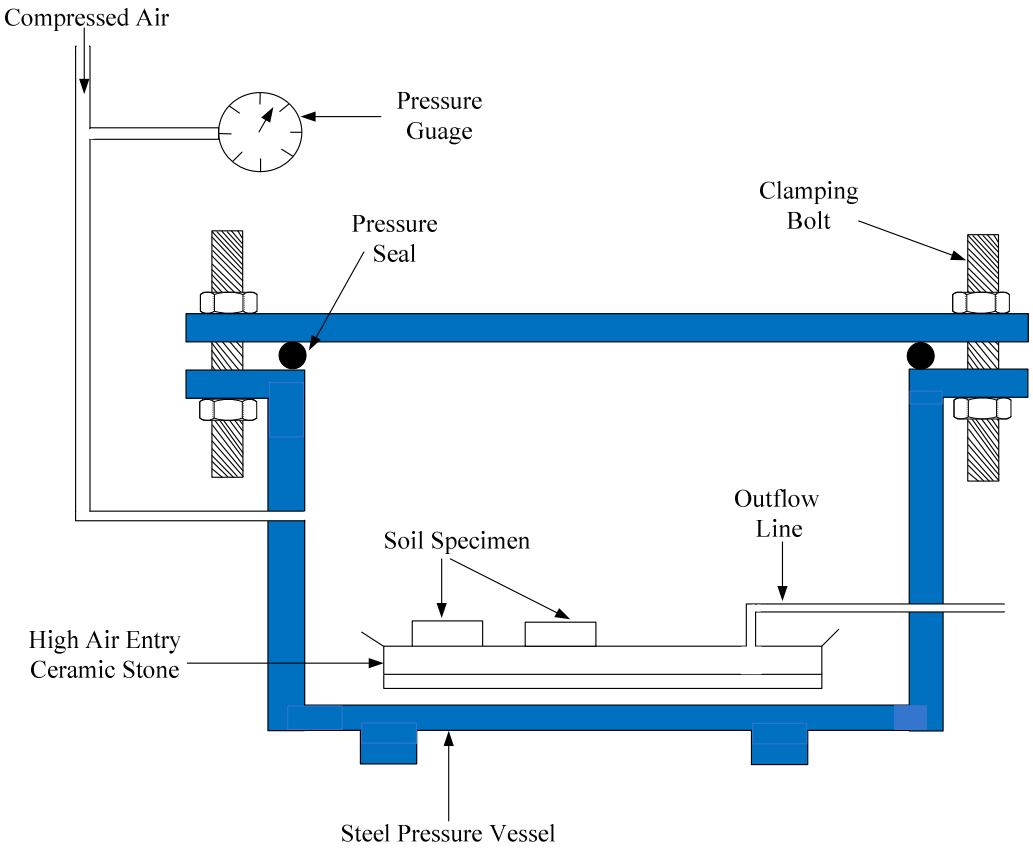

Figure 3.12: Schematic of pressure plate equipment used in the research

The pressure plate is larger and suitable to measure *SWCC* for several soil specimens simultaneously. It is important to provide a surcharge load onto each specimen to ensure proper contact and seating onto the high air entry stone. Poor seating problems will result in an over-estimation of the equilibrium water content for soil specimens. The mass of the soil specimens is determined after the equilibration. Approximately, 1 or 2 days of time is required to achieve equilibration conditions for the tested loam. Equilibration condition is assumed when no water is discharged from the pressure plate. The equilibration time is dependent on the type of soil, thickness of soil specimen, applied suction and the coefficient of permeability of the soil specimen and the high-air entry disk. The pressure plate is used to measure the *SWCC* typically for a higher suction range up to 1500 kPa. The gravimetric water content of each soil specimen(s) is determined at the end of the test (i.e., up to the highest suction range tested). The information associated to the other data points of the *SWCC* are determined from back calculations based on the volume-mass properties of the soil. The *SWCC* is plotted as the variation of gravimetric water content, w or volumetric water content, θ, or degree of saturation, S, with respect to suction.

3.11 Summary

Experimental program details and the methodology used for some of the key tests are briefly summarized in this chapter. Some succinct details of the various devices that were used for gathering the required data are presented. The modifications introduced to the UOBCE are highlighted. The artificial rooting system (*ARS*) used for generating the suction in the OUBCE is presented. In addition, the technique used for measuring the *SWCC* using the Tempe cell and Pressure plate was provided. Finally, the *PIV* technology that was used for determining the surface soil settlement due to the *ARS* is summarized.

CHAPTER 4

EXPERIMENTAL TESTING PROGRAM AND RESULTS

4.1 General

This chapter presents various test programs and results of the research. Details of these test programs are presented in three parts, i.e., test program I, II and III. In test program I, soil properties are determined using the specific gravity, sieve analysis, hydrometer, standard proctor test, direct shear test and Atterberg limits. Test program II presents details of measurement of matric suction, volumetric water contents, water head and volume of water in addition to the methodology used for collecting data from *PIV* photo images. The technique used to determine the suction modulus (modulus of elasticity, *H*) is also presented. Test program III summarizes the three different methods followed for the measurement of the soil-water characteristic curve (*SWCC*).

4.2 Test program I

The soil sample required for use in the research was obtained from a pit near the train yards/Sand-ford Fleming, Ottawa, Ontario, Canada. The following tests were carried out in the geotechnical laboratory of the University of Ottawa using the collected soil sample after preparation as part of test program I: (i) Specific gravity, (ii) Organic content, (iii) Sieve and hydrometer analysis, (iv) Standard Proctor test, (v) Direct shear tests, and (vi) Atterberg limits.

The loam soil collected had 75 % Sand and 15 % silt. As per the Unified Soil Classification System (USCS), the soil can be classified as CL-ML. The plasticity index, I_p is 6.3 %, and the specific gravity, G_s is 2.65. Figure 4.1 shows the grain size distribution curve along with other soil properties for the Ottawa loam soil.

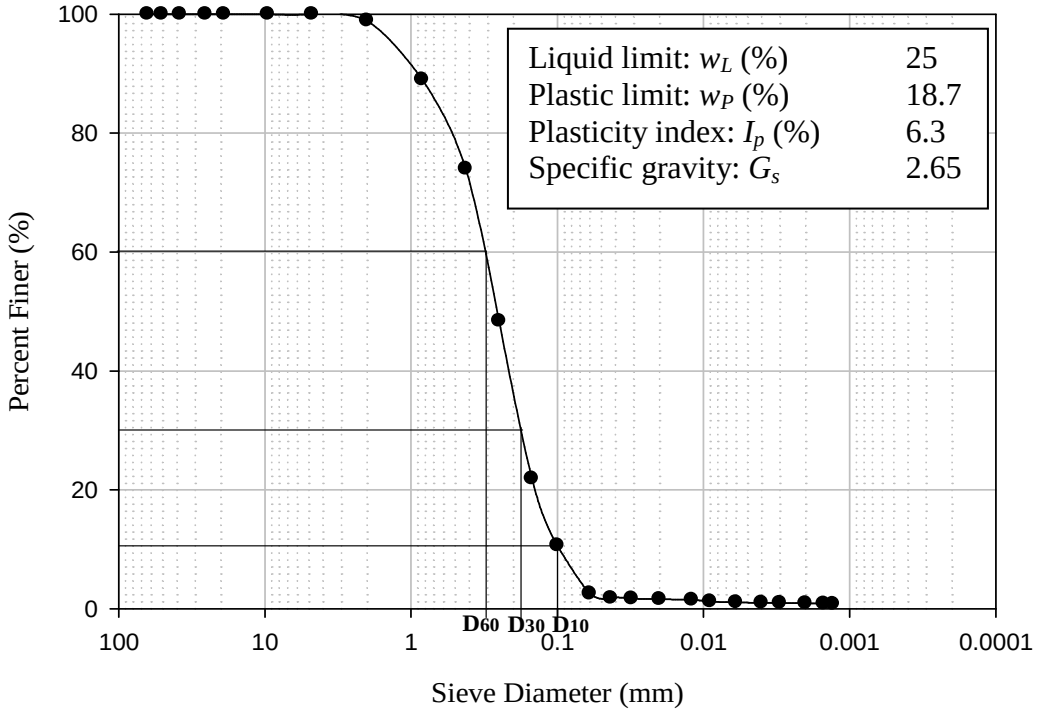

Figure 4.1: Grain size distribution of the sandy loam soil

The air-dried soil was gently broken to separate the soil lumps using a rubber mallet into individual particles and was then passed through a 4.75 mm sieve. The prepared loam soil was mixed with different water contents for conducting the compaction tests in several plastic bags. These plastic bags were stored in a humidity controlled environment for 24 hrs prior to conducting the standard proctor tests in order to achieve constant moisture content in the soil sample. Figure 4.2 shows the standard proctor test results. The optimum dry density was 16.7 kN/m^3, and optimum moisture content was 18 %.

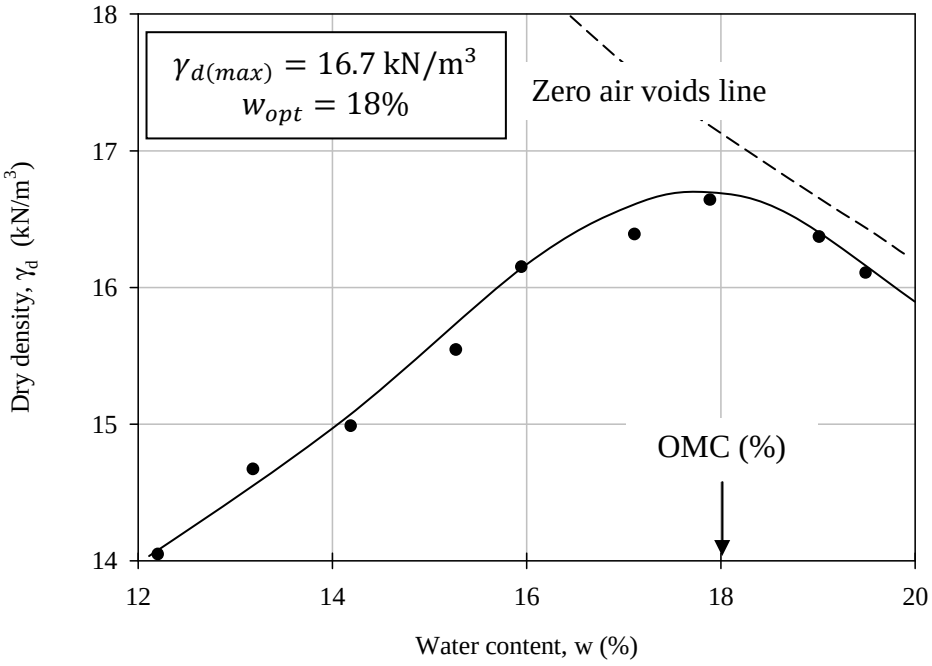

Figure 4.2: Compaction test results showing zero-air voids curve

Other tests such as the coefficient of permeability, organic content and direct shear tests were conducted and the results are summarized in Table 4.1.

Table 4.1: Summary of soil properties of the tested sandy loam

Hydraulic conductivity k (m/s)	5×10^{-5}
Organic content (%)	5
Dry unit weight (dense condition) (kN/m^3)	17.40
Dry unit weight (loose condition) (kN/m^3)	15.4
Uniformity coefficient (C_U)	3.3
Coefficient of curvature (Cc)	0.98
Optimum water content (%)	18
Internal frictional angle ϕ(°)	36.5
Effective cohesion c' (kPa)	1.3

4.3 Test program II

The test was performed in the modified UOBCE after the artificial rooting system (*ARS*) achieved equilibrium conditions with respect to matric suction values. Details of the modified UOBCE were summarized in Chapter 3. Several data and other information such as: (i) Photo images of the soil surface by *PIV* technology; (ii) MPS-1 for matric suction between 10 kPa to 500 kPa (iii) 5TM probes for volumetric water content (iv) Tensiometers for matric suction between 1 kPa up to 90 kPa (v) Piezometers for positive pore water pressures and (vi) Total volume of water extracted from soil, were recorded during the test program. Figure 4.3 shows a schematic of the sectional view with all the instrumentation used in the research program.

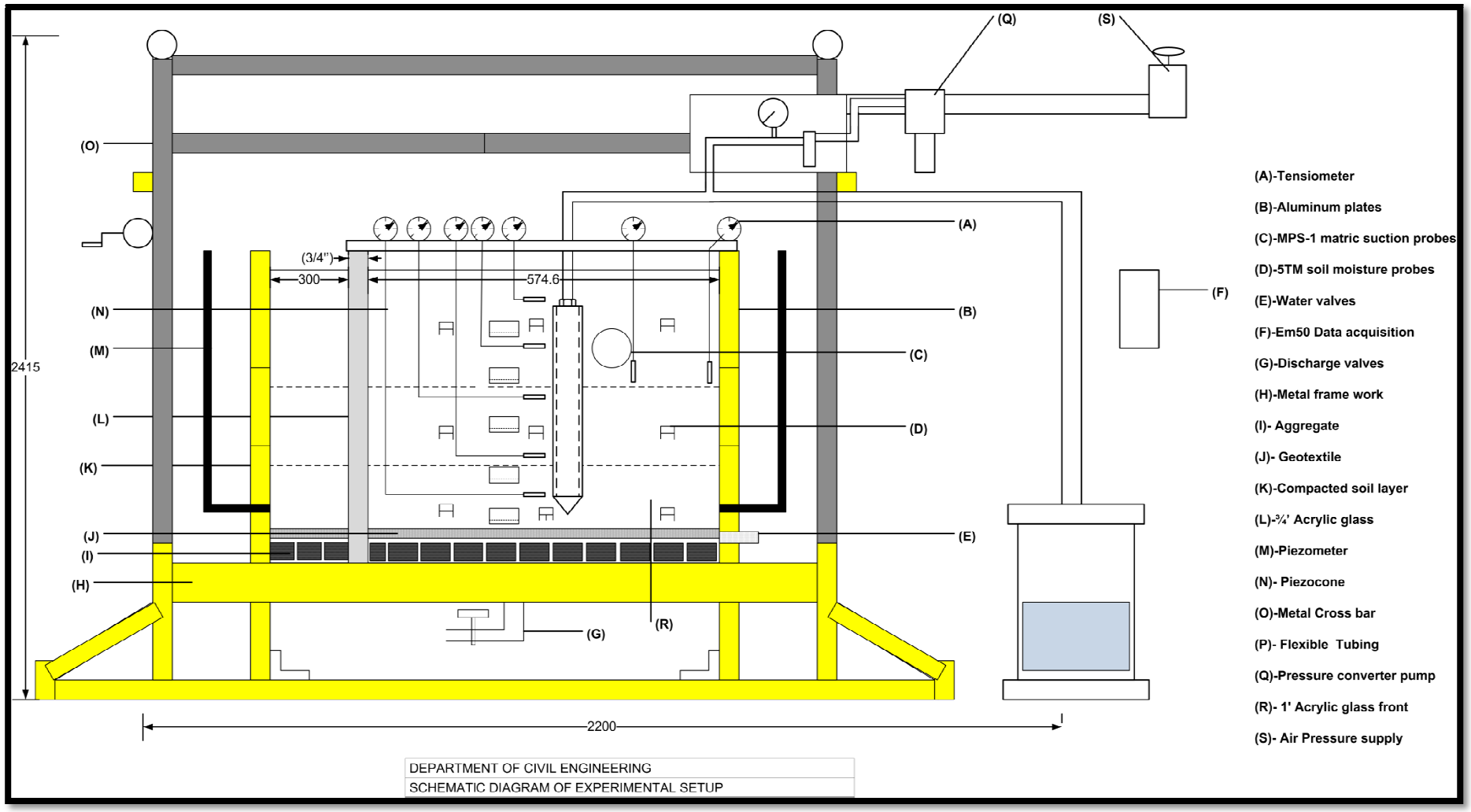

Figure 4.3: Schematic of Experimental program –II set-up

4.3.1 Presentation of Test Results

The Decagon EM50 data acquisition measured the volumetric water content at nine different locations of the test tank. The tank was divided into three regions and are labelled as A, B, and C respectively, as shown in Figure 4.4 below to observe the flow of water in the soil towards the *ARS*. Table 4.2 shows the volumetric water content values in the region B of the tank.

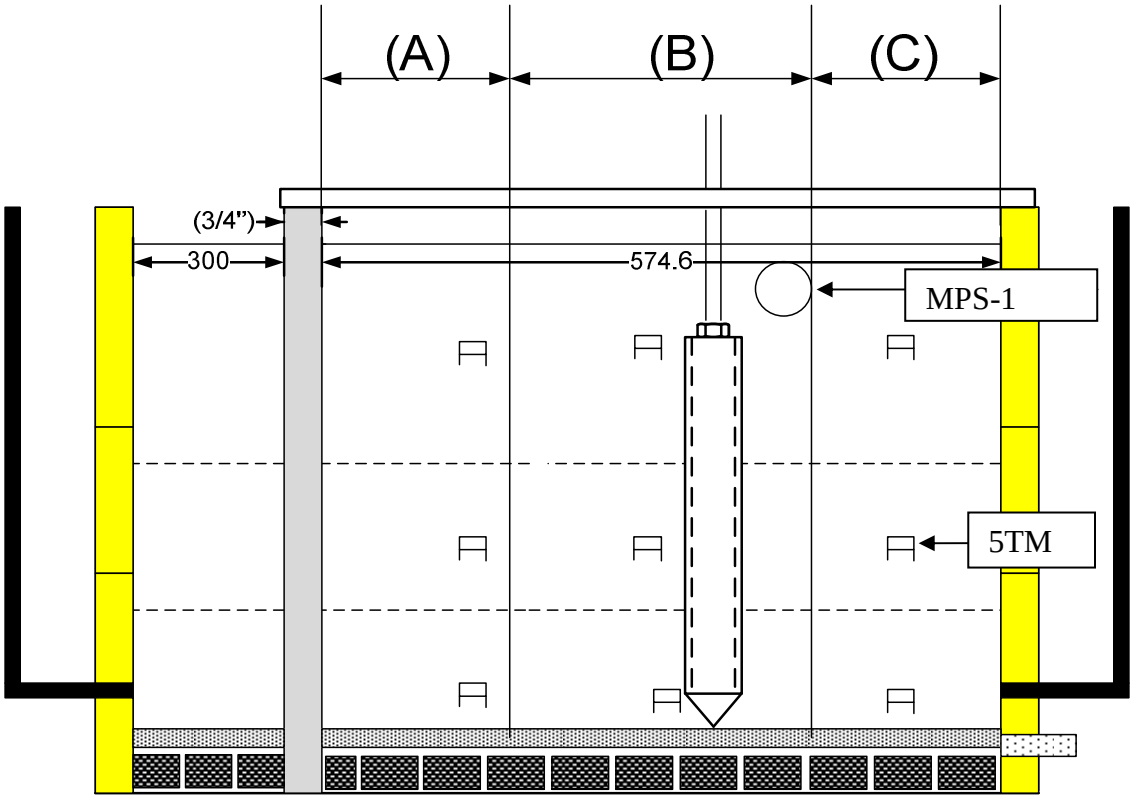

Figure 4.4: Arrangements of 5TM decagon probes, in sections A, B and C

Table 4.2: Volumetric water content at equilibrium for 5 kPa and 50 kPa applied suction

ARS Suction(kPa)	VWC- (A) m^3/m^3	VWC- (B) m^3/m^3	VWC- (C) m^3/m^3	Elevation (mm)	Equilibrium (days)
5	0.427	0.417	0.415	50	28
5	0.430	0.428	0.437	200	28
5	0.430	0.432	0.437	350	28

50	0.196	0.136	0.201	50	5
50	0.211	0.197	0.219	200	5
50	0.225	0.232	0.230	350	5

The MPS-1 results were not significant for the test duration because they can only measure matric suction accurately between 10 kPa and 500 kPa (Decagon MPS-1 specification manual). The average matric suction distribution in the experimental program was typically below 10 kPa around *ARS*.

The volume of water removed due to the application of different suction values by the *ARS* was plotted in Figure 4.5. The volume of water collected in the graduated cylinder increased as suction on the *ARS* was increased. The time required for achieving equilibrium conditions is shorter at higher *ARS* suction values, compared to lower *ARS* suction values.

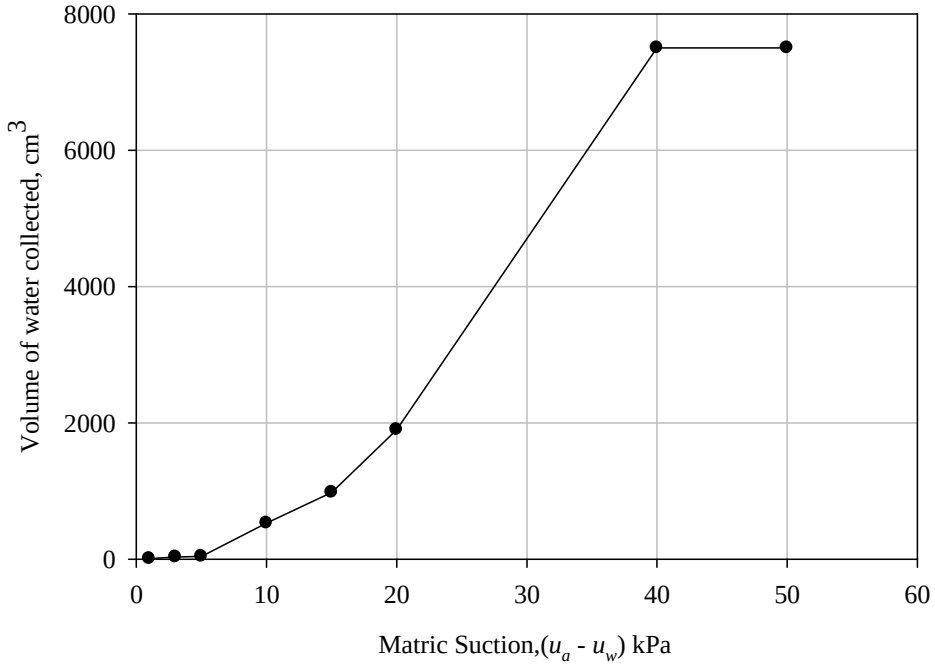

Figure 4.5: Volume in cm^3 of water collected at various suction values applied by the *ARS* suction

Figure 4.6 shows the difference in the water head after equilibrium condition had been achieved. The water head was 478 mm at 5 kPa of *ARS* suction. At 50 kPa of *ARS* suction, the water head was 110 mm.

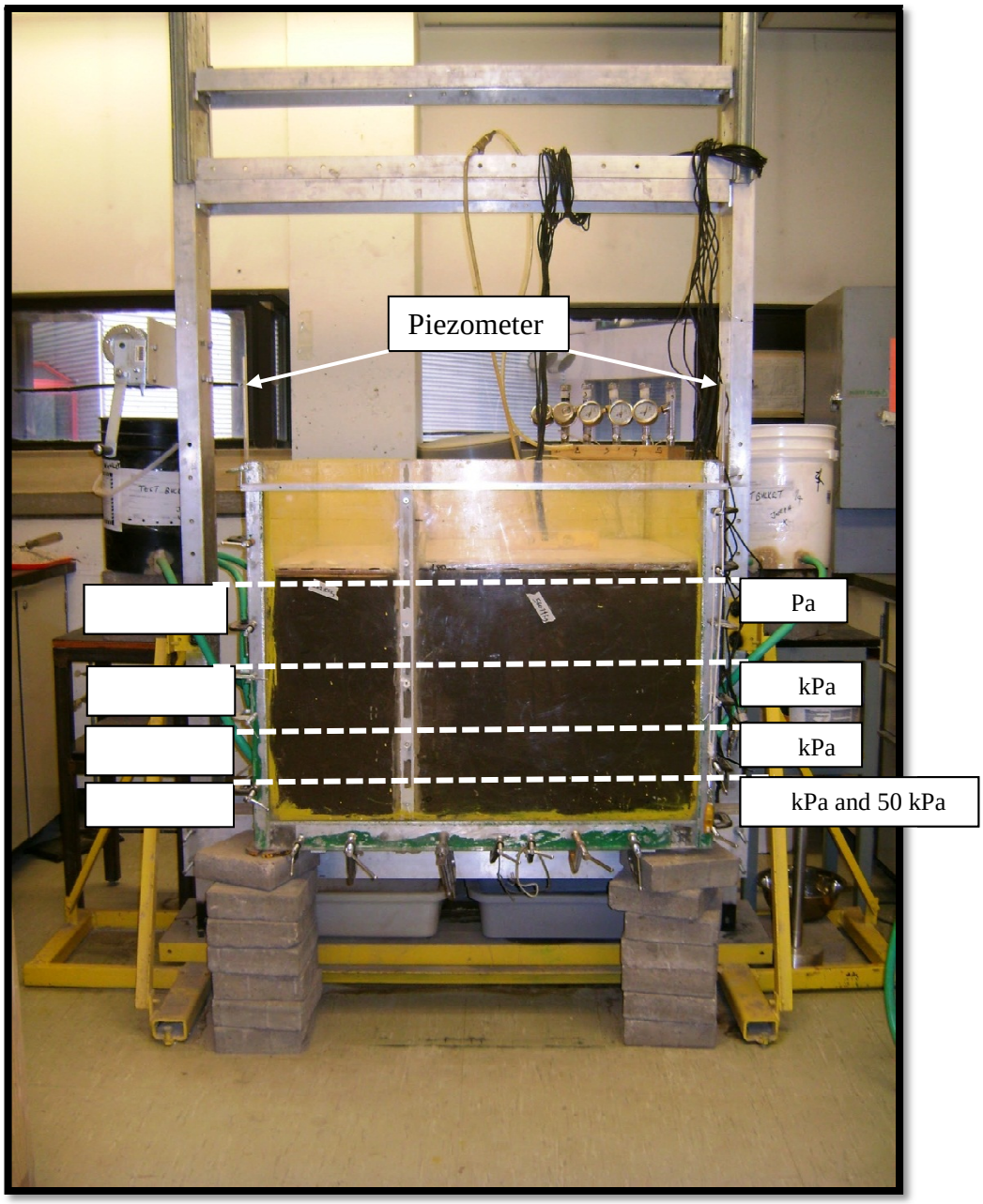

Figure 4.6: Variation of water head with respect to *ARS* suction at equilibrium

Figure 4.7 shows the schematic arrangements of Tensiometers used during the experiment. The Tensiometers were used to determine the negative pore water pressure (i.e., matric suction) distributed within the soil after equilibrium conditions were achieved. Table 4.3, presents the readings for (T-1 to T-8), which were collected after equilibrium was attained. The results show that higher matric suction in the soil occurs at high *ARS* suction (i.e. at 50 kPa) while lower matric suction occurs at lower *ARS* suction (i.e. 5 kPa).

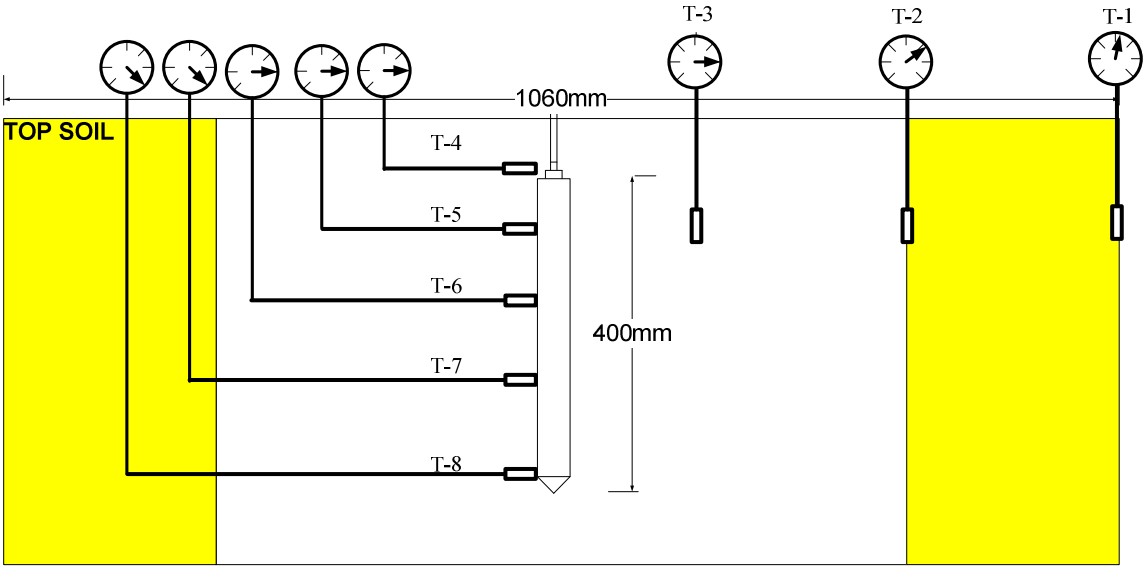

Figure 4.7: Schematic of Tensiometer arrangements in Tank B

Table 4.3: Tensiometers readings after equilibrium

ARS (kPa)	T-1 (kPa)	T-2 (kPa)	T-3 (kPa)	T-4 (kPa)	T-5 (kPa)	T-6 (kPa)	T-7 (kPa)	T-8 (kPa)
5	0	0	0	0	0	0	0	1
50	16	10	9	7	7	7	4	3

4.4 Suction Modulus (Modulus of elasticity, *H*)

Using the HD camera, Figure 4.8 illustrates the top view of the soil surface with pins segmenting the surface into smaller zones. The accuracy of *PIV* measured deformation depends on the resolution of pixels captured by the HD camera and analysed by the *PIV*

technology. The figure also shows the top soil surface deformed from the edges and more deformation towards the vicinity of the *ARS*. After deformation (Y), several soil contours were obtained for different *ARS* suction applied (i.e. 5 kPa to 50 kPa). The volume change (δV) was detected by measuring the differences in surface contours obtained from *PIV* output files.

$$\delta V = (V_1 - V_2) \quad [4.1]$$

where; (V_1) = initial surface contour, used for elevation in soil volume at saturated condition

(V_2) = final surface contour, used for elevation in soil volume after equilibrium (unsaturated condition)

The volumetric strain, $\varepsilon = (\delta V / V_1)$ [4.2]

For each volume change scenario (i.e. between 5 kPa and 50 kPa) the matric suction, $(u_a - u_w)$ was recorded from the eight (8) Tensiometers used and averaged to obtain $(u_a - u_w)_{ave}$. This accounts for all the matric suction recorded from Tensiometers (T-1 to T-8). The modulus H is the slope between $(u_a - u_w)_{ave}$ versus volumetric strain, ε. The Figure 4.9 presents the suction modulus measured during the laboratory tests.

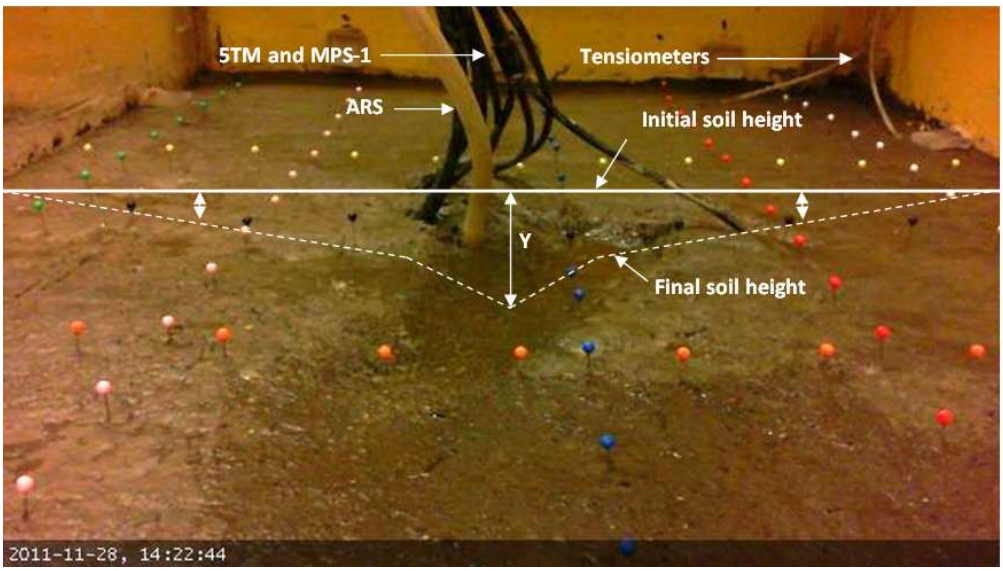

Figure 4.8: HD capture of soil deformation

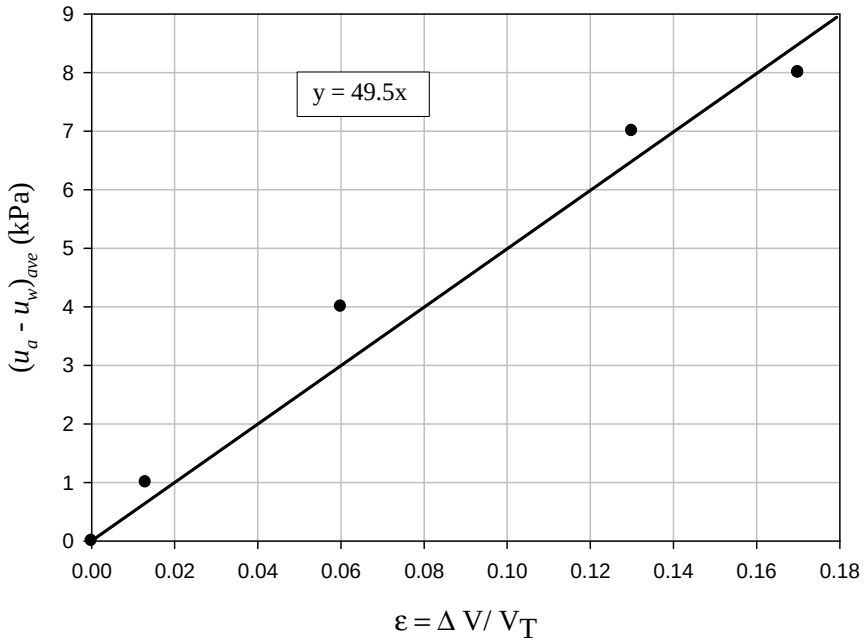

Figure 4.9: Suction modulus (*H*)

4.5 Test program III - Soil Water Characteristic Curve (*SWCC*)

The soil water characteristic curve (*SWCC*) is the relationship between soil water suction and the water content of the soil. When estimating *SWCC* using *ARS* and 5TM probes, different scenarios of *ARS* suction are applied until equilibrium is achieved. However, when equilibrium condition is achieved, the average volumetric water contents (i.e. 5TM's) correlates with each *ARS* suction scenarios. The average volumetric water content can be converted to gravimetric water content using;

$$\theta = w \times \frac{\rho_{soil}}{\rho_{water}} \qquad [4.3]$$

where, w = gravimetric water content

θ = volumetric water content

ρ_{soil} = density of soil

ρ_{water} = density of water

The void ratio (e) was back calculated from the void ratio at saturated condition and after equilibrium (50 kPa *ARS* suction). The data collected will be used with the relationship ($Se = wG_s$) to determine the *SWCC*. The estimated data obtained using 5TM and Tensiometers was denoted as (an "x") and called "UOBCE *SWCC*" demonstrated comparable results with the measured Tempe cell data denoted as (a circle) and Pressure plate denoted as (an inverted triangle) shown in Figure 4.10. The three *SWCC* test scenarios had a common boundary zone and air entry value of 4 kPa. The boundary zone was consistent between the three tests ranging between 5 kPa and 100 kPa. The residual zone of the *SWCC* measured for the loam soil was obtained using the pressure plate equipment. There was a notable correlation between the *SWCC*'s determined using the three different techniques discussed in Chapter 3.

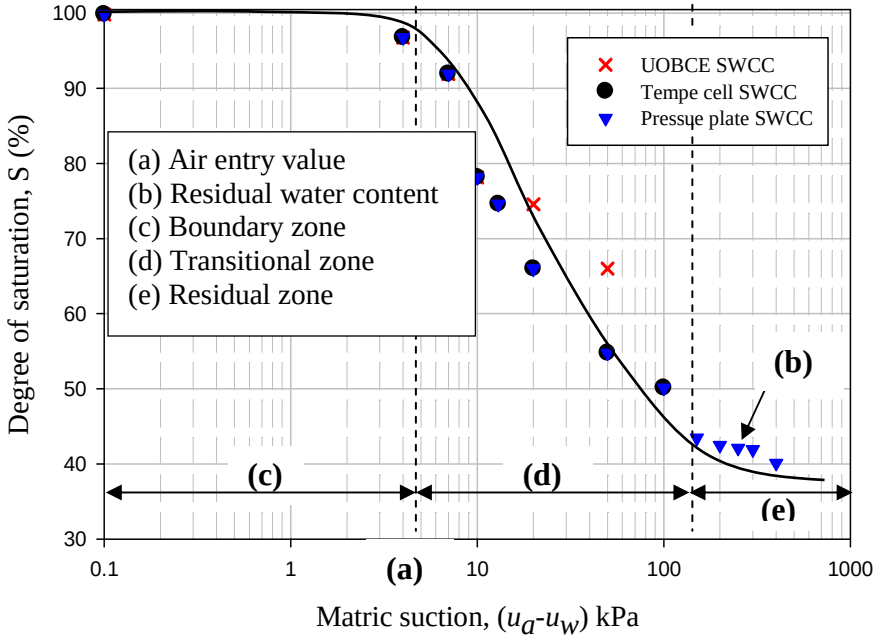

Figure 4.10: *SWCC* curve for Ottawa loam soil

4.6 Summary

This chapter summarizes the properties of the loam soil used for the test during the experimental program. The experiment was divided into three main tests and these were discussed in detail in this Chapter. Test program I presented the geotechnical engineering tests used to determine the soils properties. Test program II showed the results from the 5TM, MPS-1, Tensiometers and water head obtained using the modified UOBCE. The Modulus of elasticity (*H*) was also presented in test program II. Test program III presents the results of three different methods used to determine the *SWCC* in Chapter 6.

CHAPTER 5

NUMERICAL MODELING STUDIES

5.1 Introduction

Numerical modeling studies were undertaken using two different finite element softwares, SEEP/W and SIGMA/W (Geo-Slope Int. Ltd.) to simulate the settlements associated with the artificial rooting system (*ARS*). SEEP/W can be used to model both saturated and unsaturated flow and to analyze seepage as a function of time. In other words, SEEP/W facilitates to accommodate different processes such as the infiltration associated with the precipitation. On the other hand, SIGMA/W can be used as a tool to analyze stress versus deformation behavior in soils. In this thesis, both SEEP/W and SIGMA/W were utilized combined in order to investigate the hydro-mechanical response of the unsaturated soil resulting from the artificial roots. In other words, the initial saturation condition and the resultant pore-water pressure distribution in the soil due to the *ARS* was simulated using the SEEP/W. The subsequent displacements in the soil were then estimated using the SIGMA/W. The estimated pore water pressure change, which was obtained from solving the hydraulic process, was used to analyse the mechanical response and determine the strain in soil from which the deformation behaviour is determined. In this chapter, the key details related to the modeling of the experiment results are described.

5.2 Modeling the *ARS* using SEEP/W

The initial saturation condition and the variation of pore-water pressure distribution profiles with time caused by the *ARS* was simulated using the SEEP/W. Figure 5.1 shows the 2D experimental plan and geometry used for the axisymmetric numerical analysis in the SEEP/W.

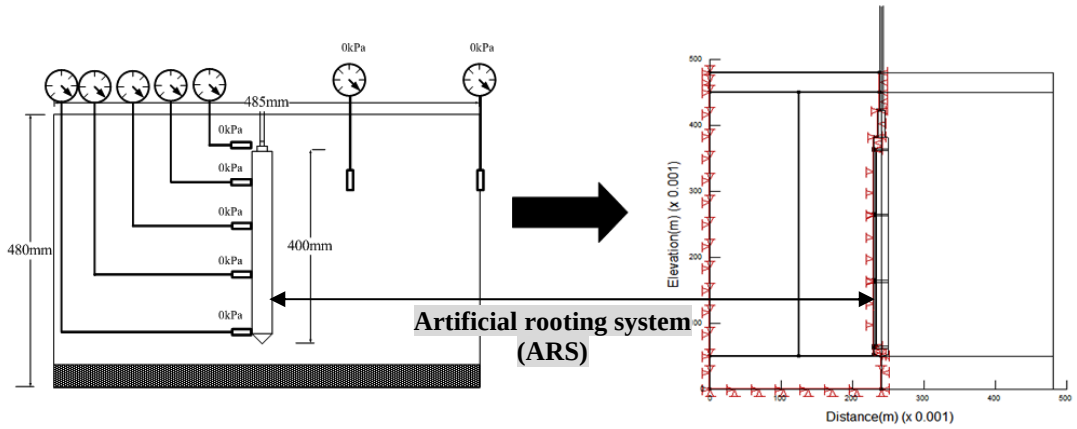

(a) (b)

Figure 5.1 (a) 2D experimental plan and (b) geometry used for the axisymmetric numerical analysis in the SEEP/W.

The general governing differential equation for 2D seepage can be written as Eq. 5.1.

$$\frac{\delta}{\delta x}\left(k_x \frac{\delta H}{\delta x}\right) + \frac{\delta}{\delta y}\left(k_y \frac{\delta H}{\delta y}\right) + Q = \left(\frac{\theta}{t}\right) \quad [5.1]$$

where, H = total head, k_x = hydraulic conductivity in the x-direction, k_y = hydraulic conductivity in the y-direction, Q = applied boundary flux, θ = volumetric water content, and t = time.

In SEEP/W, it is assumed that the net normal stress, $(\sigma - u_a)$ remains constant and the change in volumetric water content is induced only by the changes in the matric suction. Hence, if the pore-air pressure, u_a remains (i.e. atmospheric pressure) constant the volumetric water content is a function only of pore-water pressure, u_w (Eq. 5.2).

$$\partial\theta = m_w \partial u_w \quad [5.2]$$

where m_w = slope of the storage curve

Substituting Total head (H) – elevation head (y) into Eq. 5.2 yields

$$\partial\theta = m_w \gamma_w \partial(H - y) \quad [5.3]$$

Since the elevation is constant (i.e. $\partial y = 0$) the governing differential equation used in SEEP/W can be rewritten as Eq. 5.4 with.

$$\frac{\delta}{\delta x}\left(k_x \frac{\delta H}{\delta x}\right) + \frac{\delta}{\delta y}\left(k_y \frac{\delta H}{\delta y}\right) + Q = m_w \gamma_w \frac{\partial (H)}{\partial t} \quad [5.4]$$

The initial saturation condition was defined by drawing a water table at the elevation of 0.48 m from the bottom. The negative pore-water pressures (i.e. targeted matric suction values; Table 5.1) in the *ARS* were simulated by assigning constant negative pressure head (I think it should be pressure head, p not head, H) along the surface of the *ARS* as a boundary condition. The boundary condition of *zero unit flux* was assigned to the nodes along the tank to simulate no movement of water through the tank. SEEP/W allows the users to specify the duration of the transient analysis. Using this feature, the periods for the equilibrium conditions for each matric suction value were specified in the SEEP/W based on the experiment results (Table 5.2).

Table 5.1 : Negative head in meters converted to Suction in kPa

Negative pressure head (m)	Suction (kPa)
0.5	5
1	10
2	20
4	40
5	50

Table 5.2: Experimental time used to achieve equilibrium input as transient time steps

Applied suction in *ARS* (kPa)	Time to achieve equilibrium (time step) (days)
5	28
10	22
20	9
40	5
50	5

In this analysis, the soil was assumed to be homogenous and isotropic. The hydraulic conductivity function (i.e. variation of hydraulic conductivity with respect to suction) was determined using the hydraulic conductivity for saturated condition k_{sat} (= 5×10^{-5} m/sec) and the Soil-Water Characteristic Curve (*SWCC*). The k_{sat} was determined using the falling head permeability test in the laboratory. Figure 5.2 shows the *SWCC*s obtained from the tank and two different laboratory tests using Tempe cell and pressure plate apparatus. Relatively high hydraulic conductivity value (i.e. 1 m/sec) was assigned to the *ARS* regardless of suction value. The example of pore-water pressure distribution in the soil after applying a negative pore-water pressure into the *ARS* is shown in Figure 5.3.

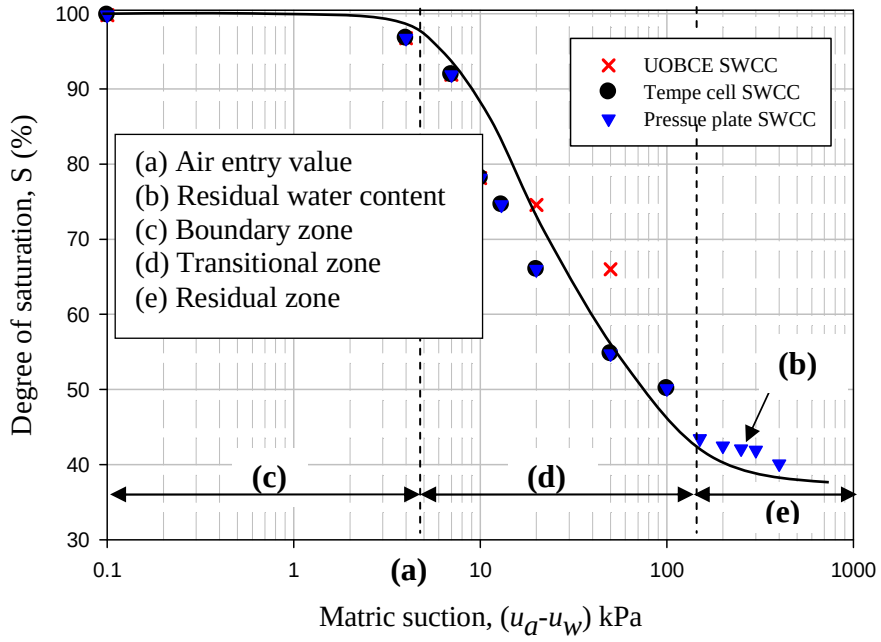

Figure 5.2: Soil-Water Characteristic Curve for the soil used in the experimental program.

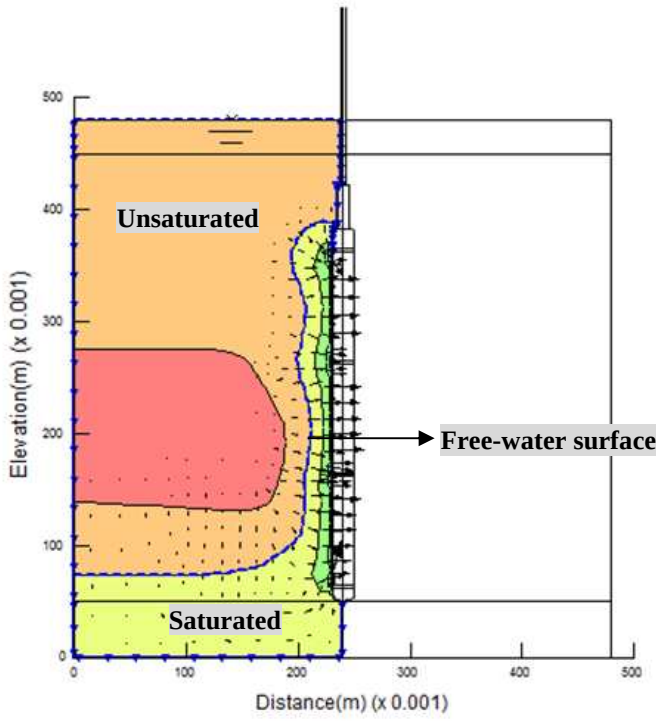

Figure 5.3: Pore-water pressure distribution in the soil obtained from the SEEP/W.

5.3 Modeling the settlement associated with the *ARS* using SIGMA/W

The displacements in the soil induced by the *ARS* were estimated using SIGMA/W. SEEP/W. When the *ARS* discharged water from the voids in the soil the effective stress increases due to the decrease in the pore-water pressure. In this case, the displacements in the soil associated with the *ARS* are caused by the increment of effective stress without any external loads or pressures. This implies that the displacements in the soil are governed by linear elastic theory since the change in the effective stress due to the *ARS* is relatively small.

Figure 5.4 shows the finite element meshes and boundary conditions established using the SIGMA/W. The dimension of soil mass in the model is 0.48 m by 0.25 m. The soil mass was discretized into quads and triangular global finite element meshes. A local finite element mesh of 0.0075 m was placed on the top soil at 0.1 m and along the *ARS* at

0.1 m. Figure 5.4 summarizes the properties of the soil and the *ARS* used in the SIGMA/W.

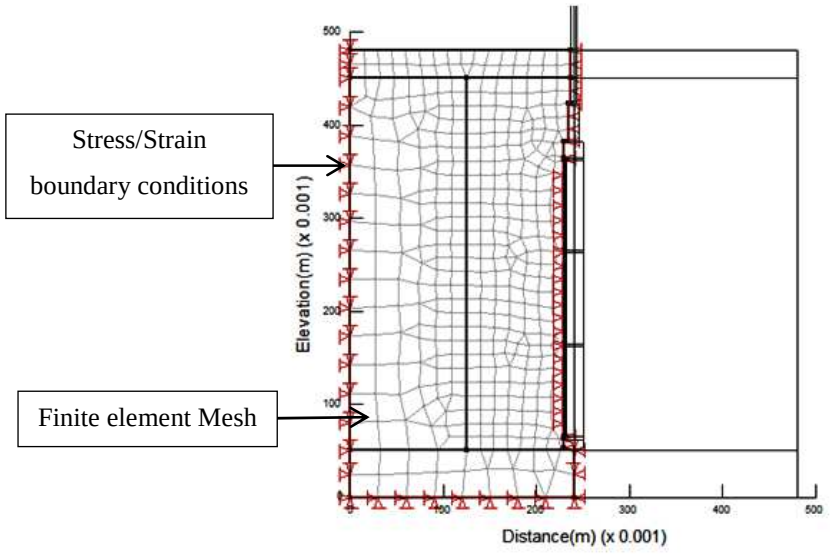

Figure 5.4: Finite element meshes and boundary conditions used in the SIGMA/W.

Table 5.3: Soil parameters for the deformation and seepage coupling analysis

Analysis	Parameters	
Soil	H (kPa)	49,485 (see section 4.5)
	G_s	2.65
	ν	0.3
	k_{sat}	5×10^{-5} m/sec
ARS	E (kPa)	10,000,000
	G_s	90
	ν	0.3
	k_{sat}	1 m/sec

The suction modulus, H [= $E/(1\text{-}2\nu)$] was determined based on the volume changes measured directly from the soil in the tank using *PIV* software (see Chapter 4 for more details).

5.4 Summary

The coupled finite element analysis (*FEA*) was carried out using SEEP/W and SIGMA/W, a software product of GEO-SLOPE (Krahn, 2007) assuming a linear elastic model. The volume change analysis was estimated using an axisymmetric perspective of the experimental program. The preliminary studies showed that there is a relationship that exists between the experimentally measured deformation and the SEEP/W simulated deformation. Moreover, the measured pore-water pressure readings and SEEP/W simulated pore-water distribution contours followed similar trends. The time duration for equilibrium and the transient time steps are also consistent because the SEEP/W allows the users to specify the duration of the transient analysis. In the next Chapter, comparisons between the measured and the estimated displacements will be presented.

CHAPTER 6

ANALYSIS OF RESULTS

6.1 Introduction

The principal objective of the research study is to predict the settlement behavior associated with tree roots suction. Present engineering practices with respect to alleviating potential settlement problems of a foundation or structure as a result of tree roots suction are based on rules of thumb. Different distances are recommended for planting trees based on their type from the foundation to avoid future problems anticipated with the tree roots suction. In this thesis, a theoretical framework has been proposed using the mechanics of unsaturated soils to predict the settlement behaviour associated with the suction changes caused by the tree roots. The equipment design details, methodology of generating suction using an artificial root system (*ARS*) in the test tank were discussed in Chapter 3. The laboratory test program and the test results were summarized in Chapter 4. Finite element modeling results of estimation of the settlement associated with the *ARS* are presented in Chapter 5. The numerical modeling deformations (settlements) in soil by simulated tree roots have been compared to measured data in the test tank in the laboratory. Research studies presented in the thesis show that there is a good comparison between the measured settlements from the laboratory studies and the predicted settlement using the finite element analysis. To the best of the knowledge of the author, there is no information in the geotechnical engineering literature with respect to laboratory investigations using an *ARS* that aims to investigate settlement behaviour and provide comparisons with modelling results. The theoretical framework, laboratory studies along with the modelling results and comparisons form the novelty of the research presented through this thesis.

6.2 Water movement

Water moves through the soil in saturated and unsaturated conditions in all directions from a region of higher potential (higher total hydraulic head) to a point of lower potential (i.e., low hydraulic head). Figure 6.1 shows typical movement of water in soil caused by the suction pull exerted by the *ARS*.

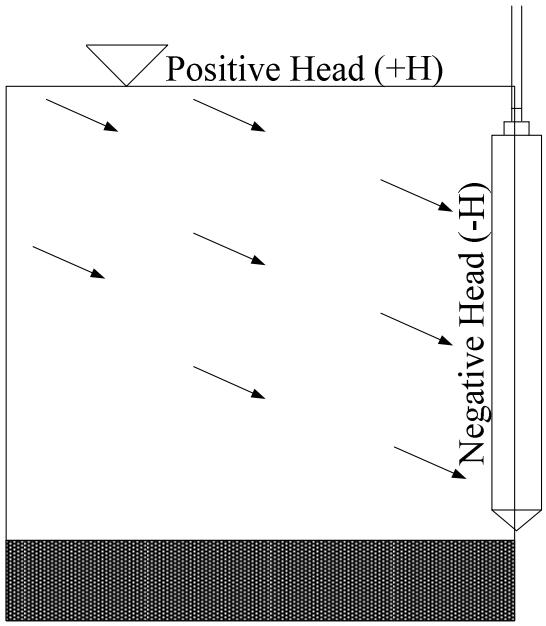

Figure 6.1: Assumed flow path resulting from head difference

The water flow under saturated and unsaturated conditions was simulated using the finite element SEEP/W programme [Chapter 5]. Total head boundary conditions were applied to the soil's surface in the SEEP/W simulation. Zero unit flux (q) boundary values were applied to the edges of soil tank's surface. This confines the analysis within the tank boundaries. The suction applied by the *ARS* was designated in the SEEP/W program and was applied using a negative pressure head. The flow vectors determined by SEEP/W at equilibrium Figure 6.2 agree with the water movement direction during transient analysis of the laboratory simulation.

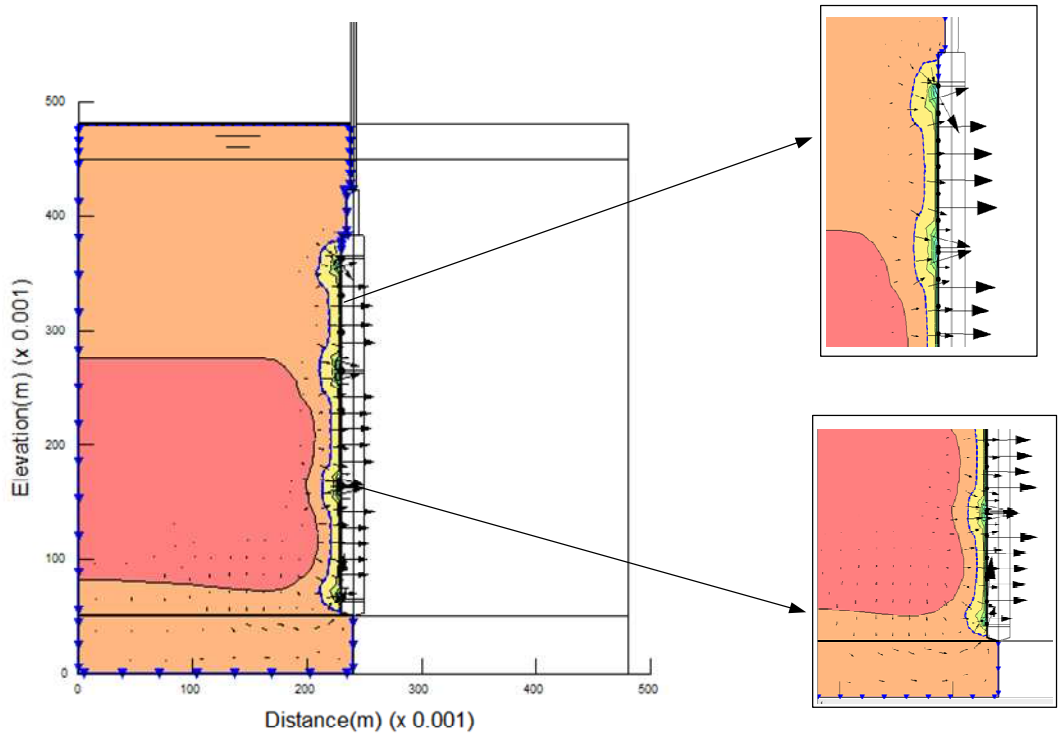

Figure 6.2: Movement of water towards *ARS*

6.3 Volumetric Water Content

The volumetric water content was measured throughout the experimental phase using nine different units of 5TM probes. The data was collected utilizing the EM50 acquisition system. The initial and final equilibrium water contents were determined for the *ARS* suction range between 1 kPa and 50 kPa. The tests were all conducted at room temperature and the results of these tests are presented in Figure 6.3. The average volumetric water content values obtained from the nine 5TM probes at equilibrium conditions was plotted as a curve with the corresponding suction values applied on the *ARS*.

The volumetric water content decreased as suction from the *ARS* increases. However, volumetric water content values were approximately the same for values of suction

between 40 kPa and 50 kPa. These results suggest that residual volumetric water content for the loam soil was achieved at 40 kPa. These results are consistent with the results of the *SWCC* measured in the laboratory using the *SWCC*[Chapter 4, Section 4.5].

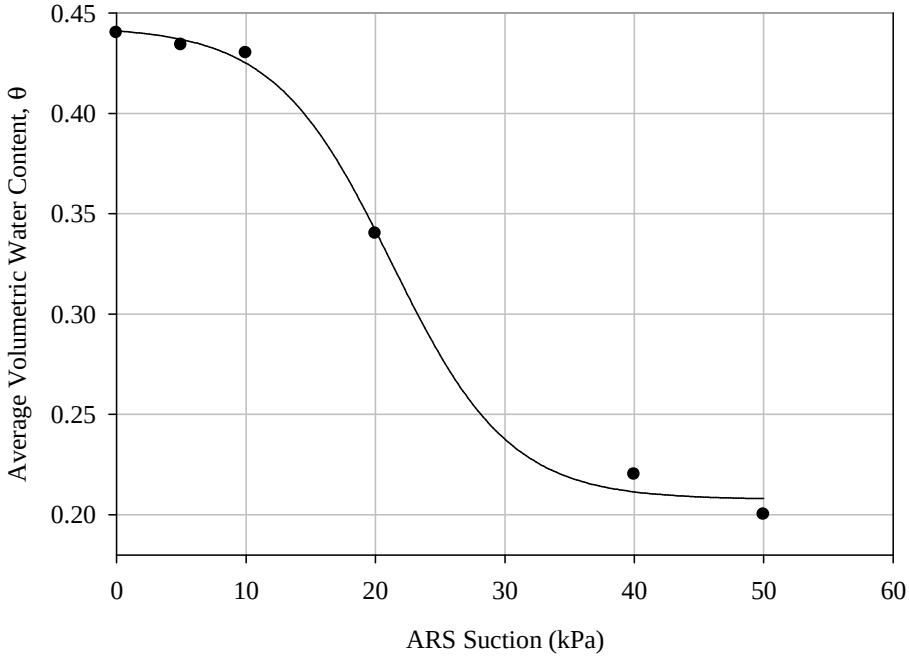

Figure 6.3: 5TM average volumetric water content versus matric suction

The 5TM probes located on section (A) and (C) of the perimeter of tank "B" showed lower volumetric water content values compared to the 5TM probes located at section (B) close to the *ARS* Figure 6.4. This may be attributed to loss of water close to the tank perimeter towards the source of suction pull (*ARS*).

The time required for the volumetric water content to reach equilibrium conditions depends on the suction applied by the *ARS*. The higher the *ARS* suction applied the lower is the time required for equilibrium.

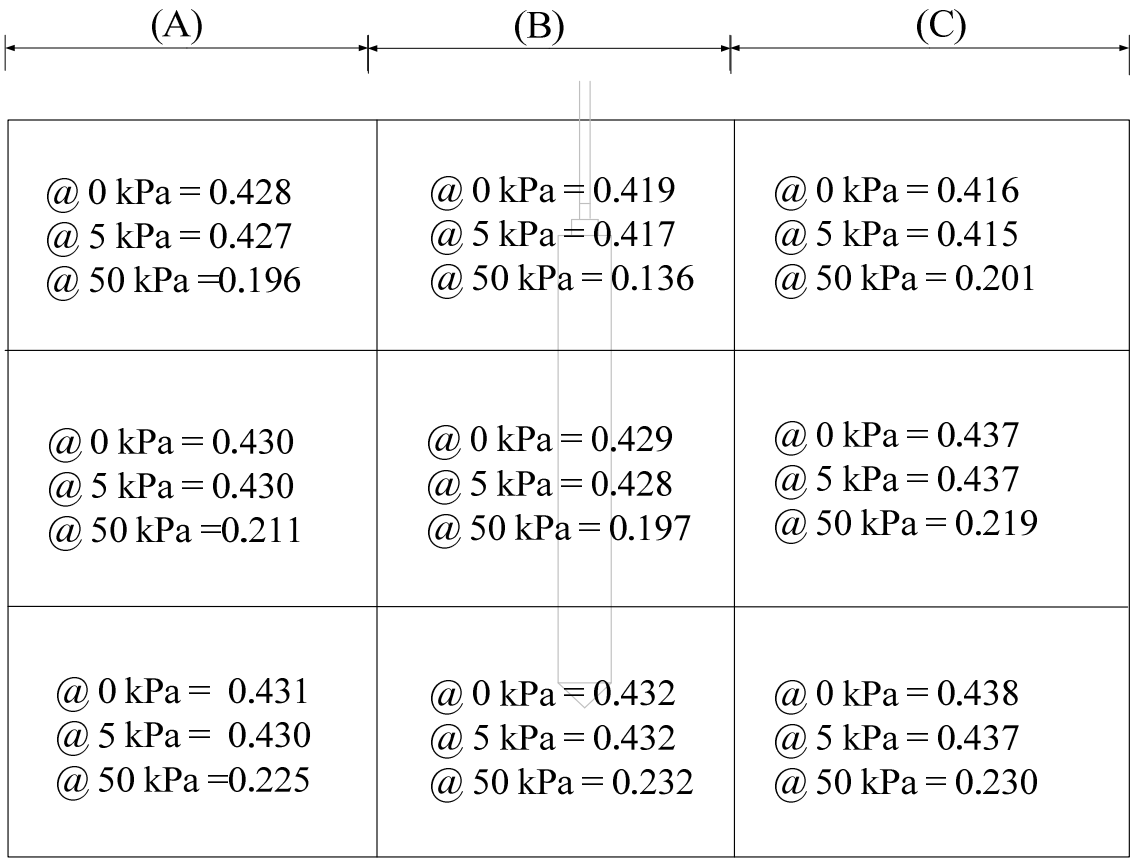

Figure 6.4: Tank B showing nine units of 5TM results after 5 kPa and 50 kPa (*ARS*) equilibrium

6.4 Equilibrium Time

The time required to achieve equilibrium conditions in the sandy loam soil depends on a number of factors, which include: (i) the value suction applied on the *ARS;* (ii) the volumetric water content of the soil; and (iii) the coefficient of permeability of the soil. When the volume of water drawn by the *ARS* remains constant in the collection cylinder over a period of time (typically 24 hours), it is assumed to have attained equilibrium condition. For example, at 40 kPa and 50 kPa suction applied to *ARS*, the soil-water volume of 7500 cm^3 was collected over duration of five days. On the sixth day, while still

keeping the *ARS* running, the volume of 7500 cm^3 remained unchanged suggesting an equilibration condition has been achieved.

An incremental time sequence was required in SEEP/W for performing the transient analyses. The accuracy of the results depends upon the equilibrium time, which was measured experimentally for precise comparisons. As observed in Figure 6.5, longer days are required to reach equilibrium conditions for lower suction. At 40 kPa and 50 kPa of *ARS* suction, a similar duration of five days was required to achieve equilibrium conditions. Experimental work was terminated when the volume in the collection cylinder remained constant for more than 24 hours.

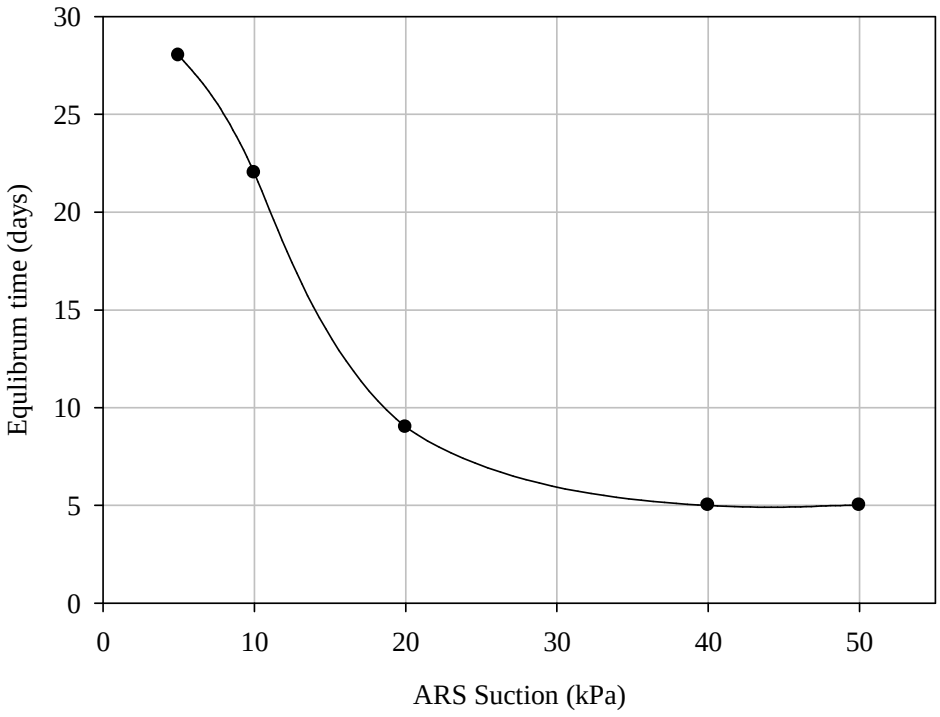

Figure 6.5: Variation of equilibrium time (days) with the suction applied on the *ARS* (kPa)

6.5 Negative Pore Water Pressure (Matric Suction)

Several Tensiometers as shown in Figure 6.6 were used to determine the distribution of matric suction within the soil at equilibrium conditions in the present study. The Tensiometers used are represented as T-1, T-2, T-3, T-4, T-5, T-6, T-7, and T-8. The Tensiometers (T-1, T-2 and T-3) were located along a profile at approximately 100 mm apart from each other. Tensiometers (T-4 to T-8) were arranged approximately 90 mm intervals from each other and aligned with the *ARS*.

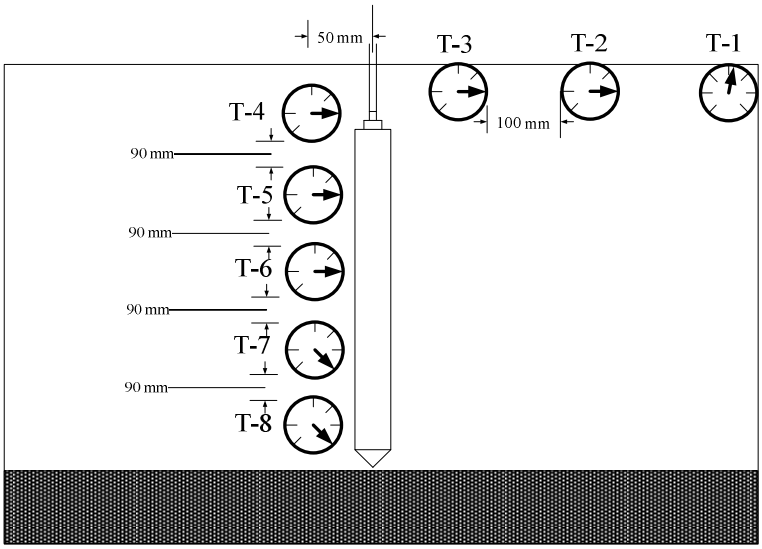

Figure 6.6: Arrangement of Tensiometers

The Tensiometer (T-1) responded with (1 kPa) matric suction reading at equilibrium conditions near the corner of the tank when suction a suction value of 5 kPa was applied to the *ARS*. A water head difference of 2 mm was observed from its initial water table level at equilibrium condition. The soil in the tank appeared saturated; however, at the four corners of the tank the soil appeared to be relatively dry and experienced a small volume change. Tensiometers (i.e., T-2 to T-8) recorded zero matric suction suggesting the soil is in a state of saturated condition.

The next stage of test was conducted by saturating the soil in the tank again (achieving similar initial conditions) prior to the application of the next suction value (i.e., 10 kPa). This procedure was repeated for different suction values. When suction values of 40 kPa and 50 kPa were applied to *ARS*, T-1 recorded the highest suction value (16 kPa) as compared to other Tensiometers (T-2 = 10 kPa, T-3 = 9 kPa). Tensiometers T-4, T-5 and T-6 recorded 7 kPa and the other two Tensiometers T-7 and T-8 recorded 4 kPa and 3 kPa, respectively. The experimental work was terminated at 50 kPa because no further change in matric suction occurred in T-1 to T-8. The volumetric water contents (5TMs), MPS-1, and *PIV* deformation also were recorded at all suction values at equilibrium conditions.

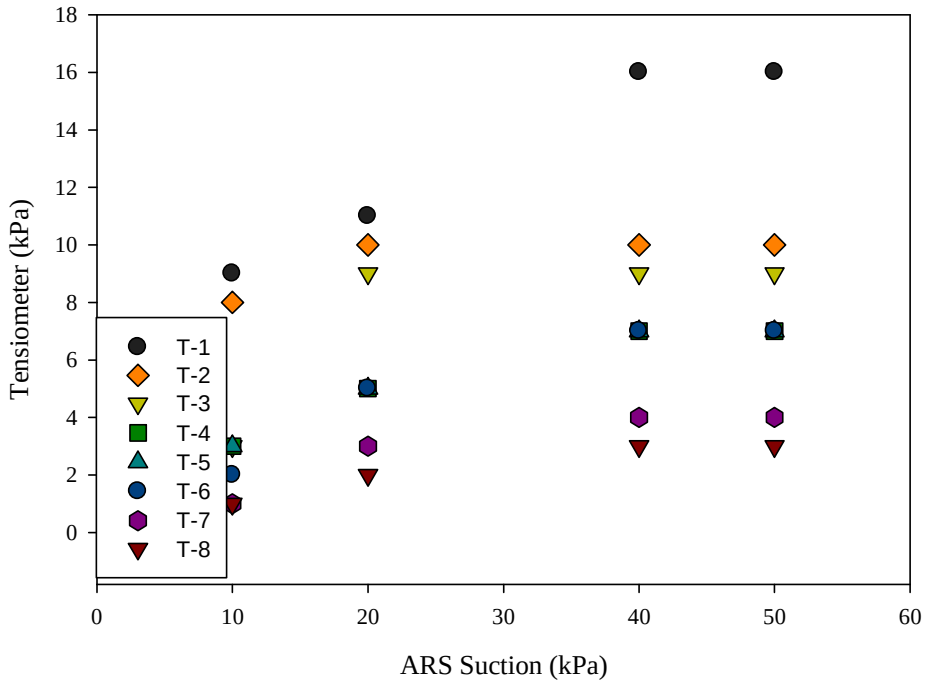

Figure 6.7: Response of matric suction values by different Tensiometers for various suction values applied to the *ARS*

Figure 6.7 summarizes the measured matric suction data using several Tensiometers for the different suction values applied to the *ARS*. These values presented were all recorded after achieving equilibrium conditions in the test tank. Tensiometers did not show any response when suction values of 1 kPa and 4 kPa were applied to the *ARS*. This is because the air-entry value of the soil is approximately 5 kPa (which is higher than the applied suction to the *ARS*) and the corresponding suction in the vicinity of the *ARS* and the soil in the tank is low or negligible and has not contributed to any desaturation.

The coefficient of permeability function is a key tool required in finite element modelling. In the present study, the equation proposed by van Genuchten (1980) was used in the prediction of the permeability function. The saturated coefficient of permeability and the *SWCC* are the required for using the van Genuchten (1980) equation. The saturated coefficient of permeability of the soil was determined from the falling head test in the present study (i.e., 5×10^{-5} m/s). The average value of residual water content after achieving equilibrium conditions for 40 kPa (*ARS*) using 5TM was (0.21 m^3/m^3). In addition to the *SWCC* and the saturated coefficient of permeability, the residual water content is another parameter required in the finite element modeling.

Figure 6.8 shows the location of Tensiometers T-4 to T-8 readings and the matric suction readings after achieving equilibrium conditions for different values of suction applied to the *ARS*. The Tensiometers close to the *ARS* had no response recording zero matric suction by applying 5 kPa suction, which indicates the soil in the tank was in a state of saturated condition. The graph gradually shifts to the right with an increase in *ARS* suction values to 10 kPa, 20 kPa, 40 kPa and 50 kPa values. In general, the Tensiometers recorded the matric suction values that were decreasing with depth towards the water table. This indicates a decreasing water head present in the soil after each test was completed.

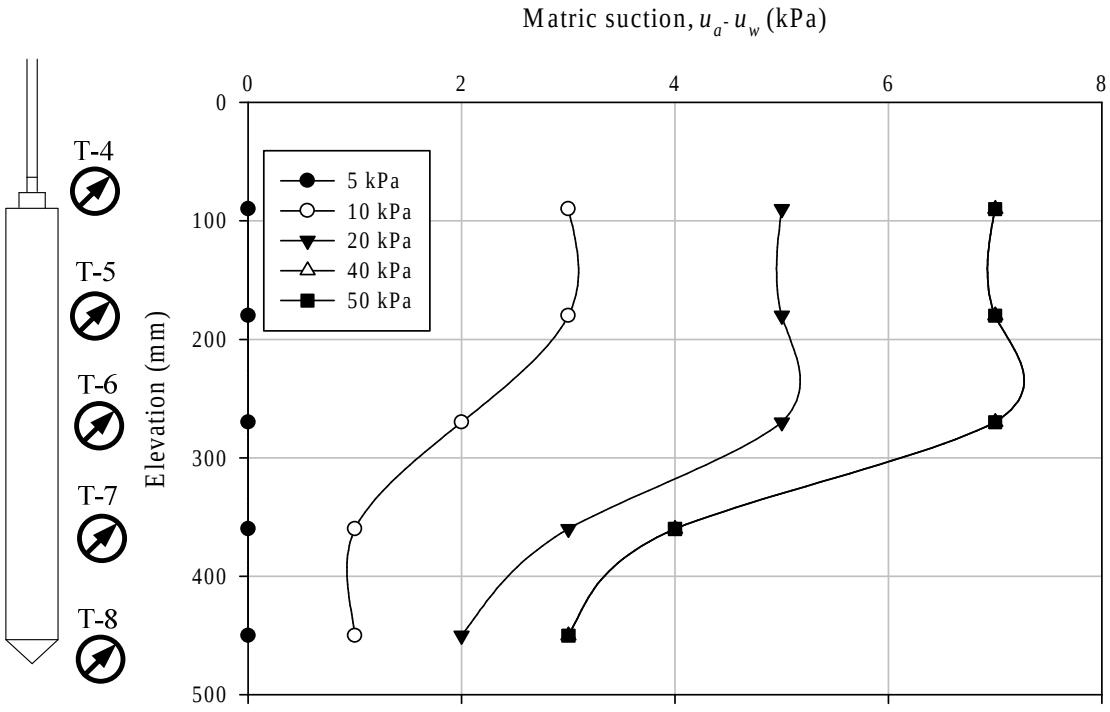

Figure 6.8: Tensiometer (kPa) versus Elevation (mm)

The graphical comparison of the above figure was obtained in SEEP/W by selecting nodes within the same depth (suction profile) of the *ARS*. Because the nodes are in quads and triangles approximate nodes would be on a straight line. Figure 6.9 shows the nodal points selected for the matric suction distribution at the end of the (5 kPa) SEEP/W transient analysis. The equilibrium time and the duration of the transient analysis have a uniform time, which was obtained from the laboratory.

Tensiometer T-1, T-2 and T-3 arranged on the soil surface were represented with nodes along the *x*-axis. Tensiometers T-4, T-5, T-6, T-7 and T-8 arranged with the soil profile depth (elevation) were represented with nodes 50 mm from the *ARS*. The nodes selected to represent Tensiometer T-1 to T-3 were arranged on the top soil and share common depths but variant distances to the *ARS*.

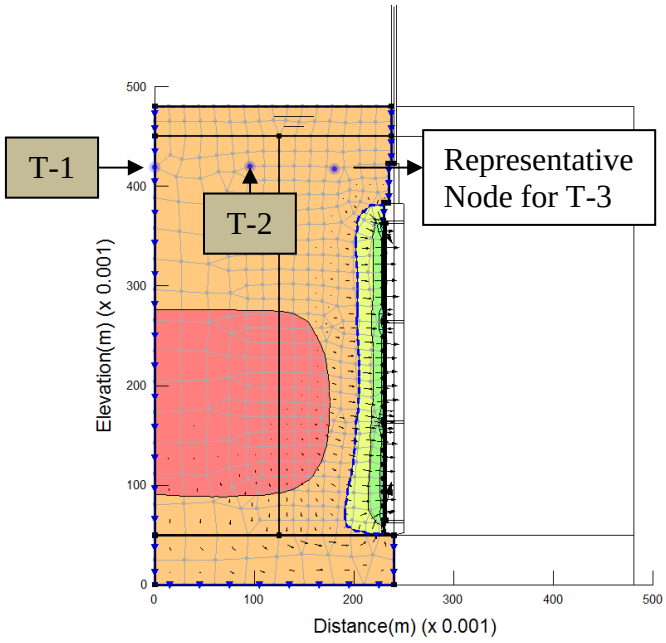

Figure 6.9: Nodes selected to represent (T-1, T-2 and T-3)

The SEEP/W results represented in the graph were obtained after (5 kPa) of *ARS* suction had achieved equilibrum. From Figure 6.10, it can be noted that before equilibrum was achieved the soil around the vicinity of Tensiometer (T-3) was tending gradually towards negative pore water pressure. This indicates loss of water moving through the *ARS*. Tensiometer (T-1) on the tank edge and Tensiometer (T-2) remained constant, without influence from the applied suction pull of the *ARS*.

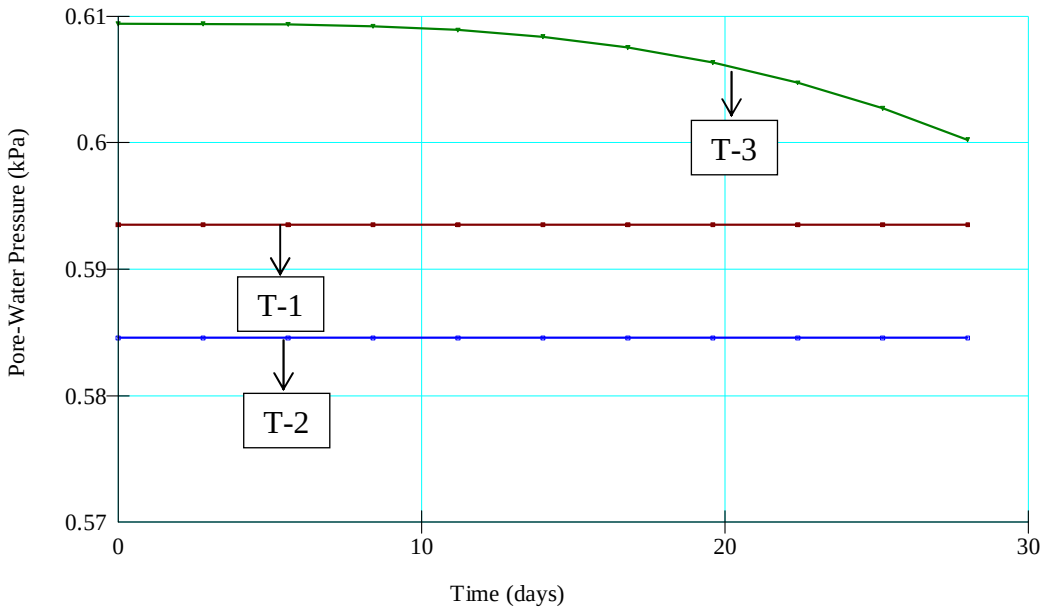

Figure 6.10: Distribution of Pore water pressure with Time (5 kPa *ARS*)

During the experimental phase, Tensiometer (T-1) recorded (1 kPa), and Tensiometers (T-2 and T-3) both complied with the numerical analysis as they remained in a saturated state with no response on the Tensiometers. A number of factors such as boundary conditions around the soil-tank interface could give rise to matric suction. The movement of water towards the *ARS* generating matric suction around the soil-tank boundries that could allow the Tensiometer (T-1) to respond. This is because bottom saturation was closed after the piezometer height was slightly above soil.

Tensiometer T-4, T-5, T-6, T-7 and T-8 in SEEP/W, illustrated in Figure 6.11, shows elevation Y (m) and the representative nodes in saturated condition.

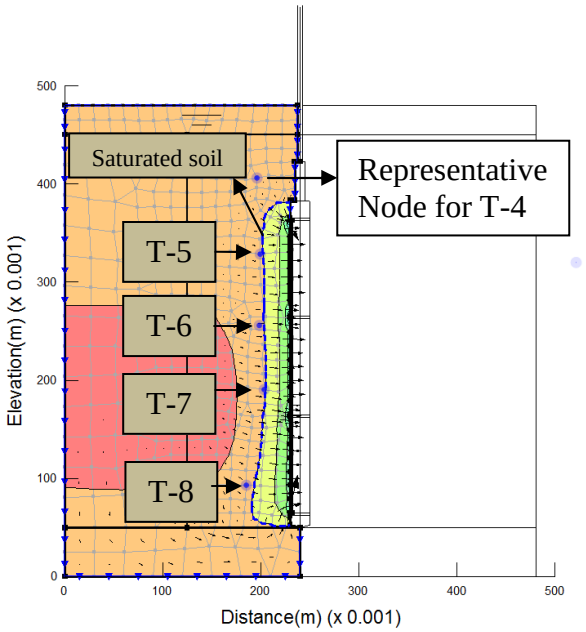

Figure 6.11: Location of nodes used for T-4 to T-8 for (5 kPa *ARS*)

Figure 6.12 illustrates zero matric suction distributed on the entire soil close to the *ARS*, indicating the soil was in a saturated condition. These results suggest that the SEEP/W results are consistent with the matric readings of the Tensiometers (T-4 to T-8).

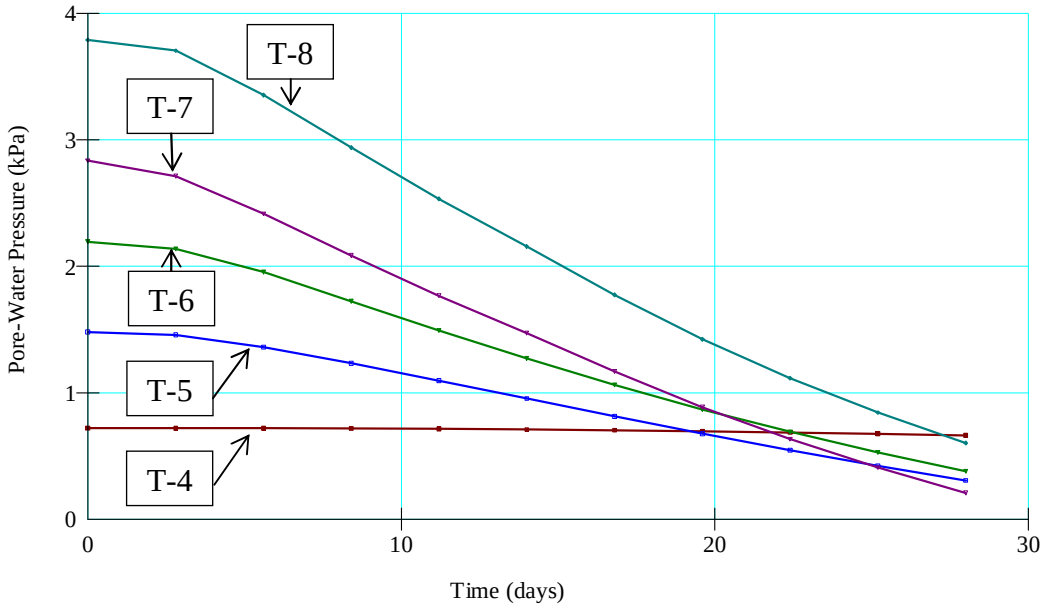

Figure 6.12: Distribution of pore water pressure with time (5 kPa *ARS*)

At 50 kPa of *ARS* suction, the nodes selected were approximately located where the Tensiometers (T-1 to T-8) were located during the experimental phase. Tensiometers (T-1, T-2 and T-3) are presented by nodes along the *x* axis with common depths, as shown in Figure 6.13.

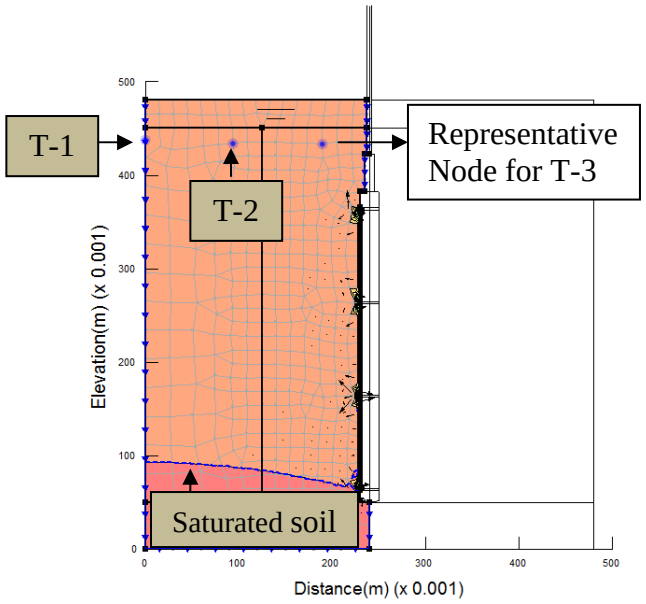

Figure 6.13: Nodes selected to represent (T-1, T-2 and T-3)

Figure 6.14 represents the variation fo the pore water pressure with time for the representative nodes, denoting T-1 to T-3.

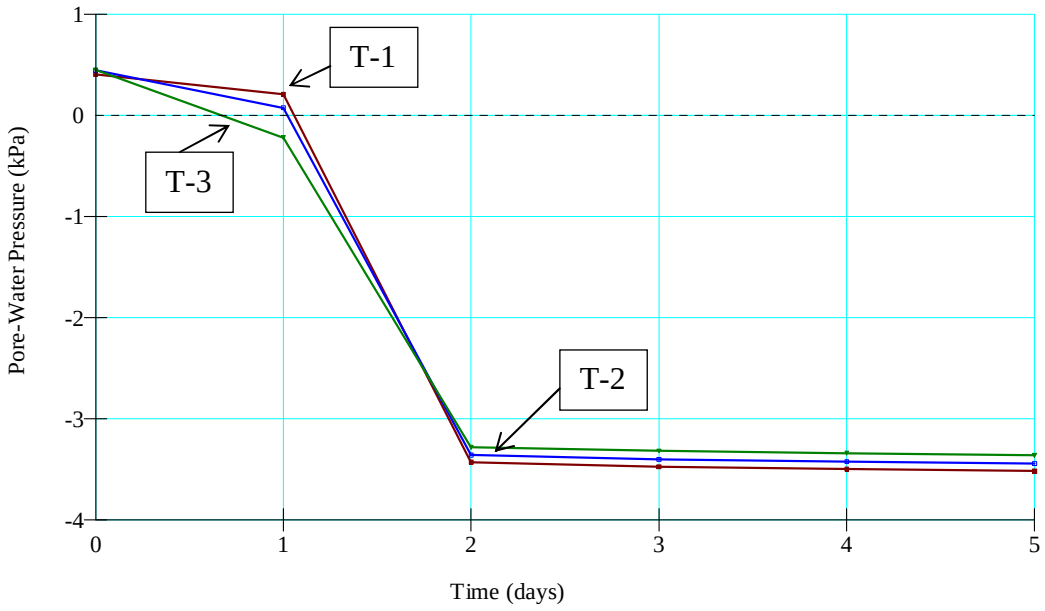

Figure 6.14: Distribution of Pore water pressures with Time (50 kPa *ARS*)

The graph illustrates that the soils within the vicinity of Tensiometer (T-3) responded earlier, as compared to (T-1 and T-2). The Tensiometers gradually sloped towards negative pore water pressure within the first 24 hrs, after which a rapid drop in the slope was observed. This behavior indicates that there was a significant transition on the second day. The effect of these changes to surface deformation will be further discussed in section 6.8. The Tensiometers aligned along the *ARS* in the elevation Y (m) are presented in Figure 6.15.

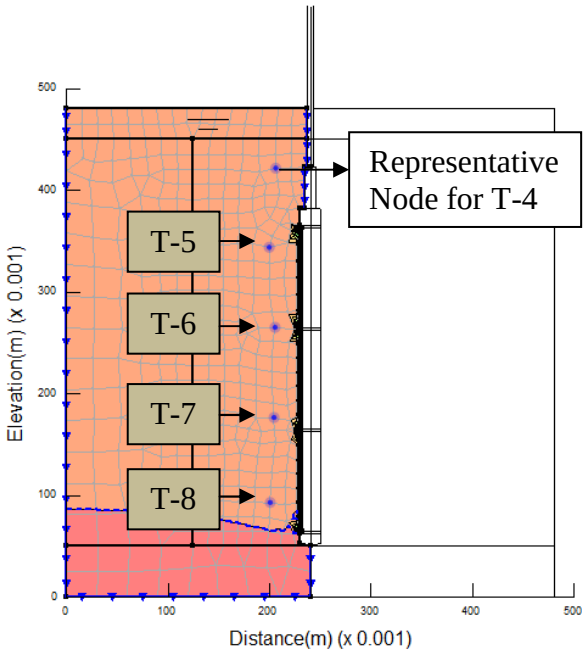

Figure 6.15: Location of nodes used for T-4 to T-8 for (50 kPa *ARS*)

As illustrated in Figure 6.16, observation showed that soil in the vicinity of Tensiometers T-4, T-5 and T-6 remained unsaturated within the first few hours of the first test day. Tensiometers (T-7 and T-8) experienced a slow but gradual slope, tending towards the negative pore water pressure. This indicates that on the first day the water table was high enough to keep (T-7 and T-8) in a saturated condition. On the second day, the Tensiometers (T-4 to T-6) experienced higher matric suction values, while the soil around Tensiometers (T-7 and T-8) desaturated rapidly. On the third day, the soil was in an unsaturated state, with Tensiometer (T-4) measuring a matric suction slightly above (3 kPa). Tensiometers (T-5 and T-6) recorded approximately 2 kPa, while Tensiometer T-7 and T-8 recorded (1.5 kPa and 0.3 kPa), respectively. There were no significant changes in the Tensiometer readings after the third day. The matric suction remained constant until the fifth day, suggesting equilibrium condition. These results indicate that most soils deformation occurred within three days of the total test duration in the laboratory.

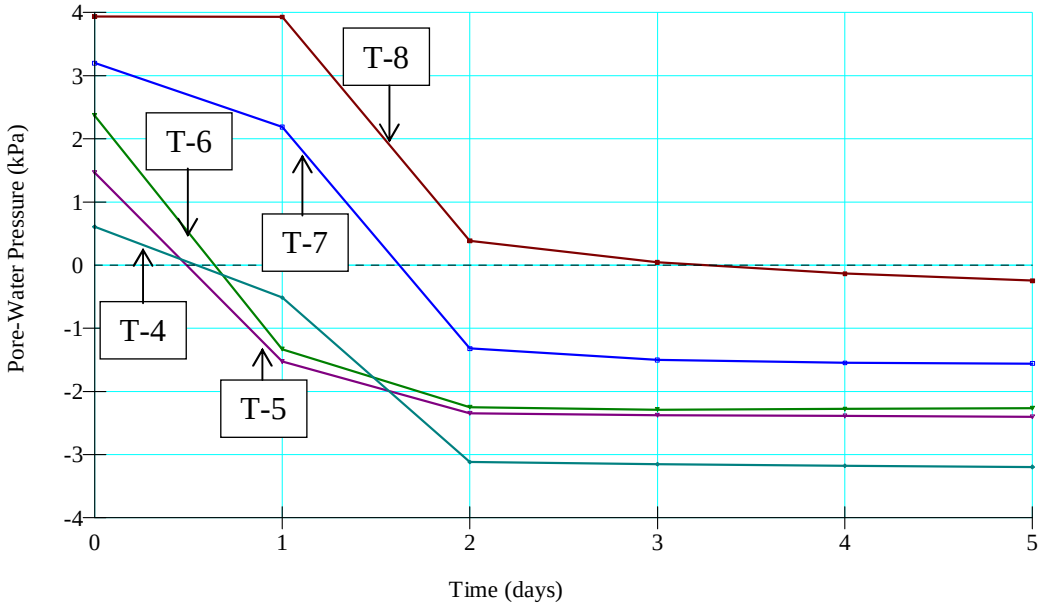

Figure 6.16: Pore water pressure (kPa) with Time (days) for 50 kPa *ARS*

The results obtained for 50 kPa of *ARS* suction were as follows: 7 kPa for T-4 to T-6, 4 kPa for T-7 and 3 kPa for T-8. However, while removing the soil from Tank B, it was observed that the porous ceramic tip of the Tensiometer had drifted from its original location during assembly towards the *ARS*. Figure 6.17 presents the observed final positions as compared to the initial position of Tensiometers porous tips during soil removal from tank B. It was observed that the porous tips had drifted towards the *ARS* caused by the *ARS* suction pull applied during each step.

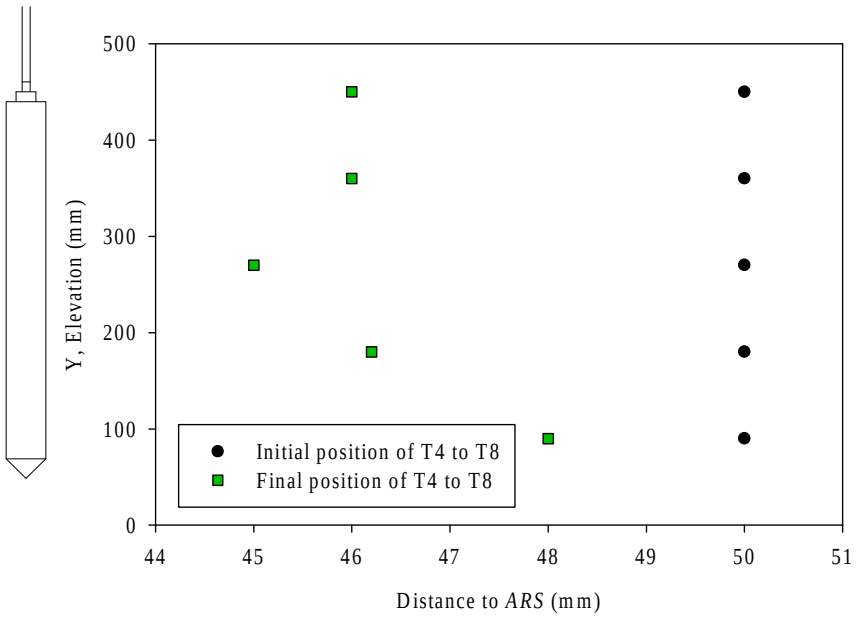

Figure 6.17: Position of Tensiometer (T-4 to T-8)

The final positions obtained from T4 to T8 were used in the SEEP/W in order to simulate the matric suction results. Figure 6.18 presents a magnified view of the numerical SEEP/W model after 50 kPa of suction had achieved equilibrium. Soils close to the *ARS* experienced an increase of matric suction because it was closer to the source of suction pull generated by the *ARS*. In addition, the scale in Figure 6.18 indicates different matric suction boundaries which increase towards the *ARS*. The different levels of suction are differentiated using different colours.

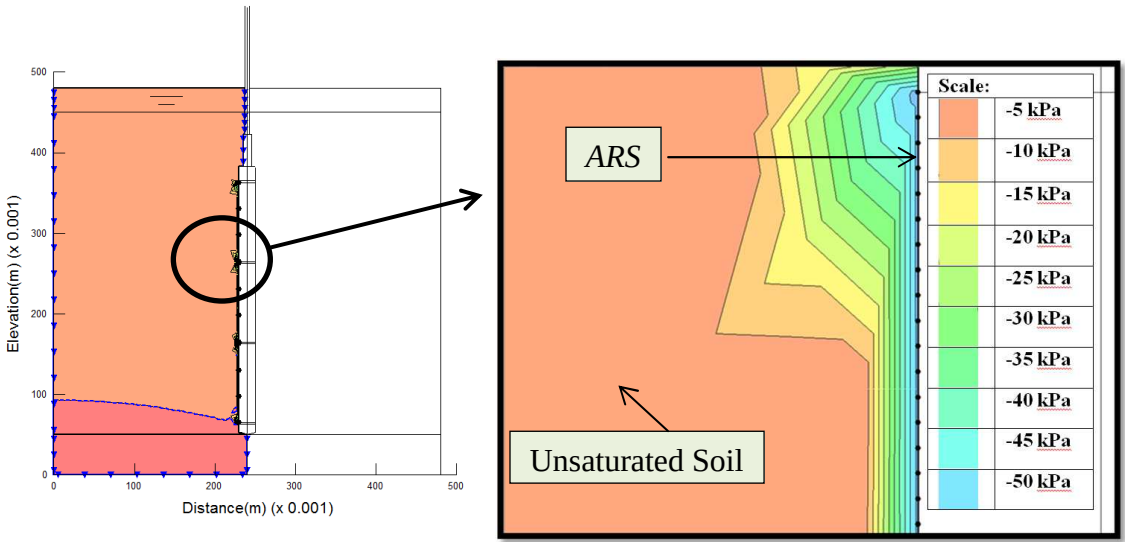

Figure 6.18: Distribution of matric suction around *ARS* in SEEP/W

Figure 6.19 presents the results obtained after 50 kPa of *ARS* suction was applied to the final positions of T-4 to T-8, which were used in the SEEP/W analysis. The *ARS* suction of the (50 kPa) significantly desaturated the soil around the vicinity of (T-4 to T-8) over a duration of 5 days. The Tensiometers (T-4 and T-5) measured matric suctions of approximately (11 kPa) after 24 hrs. Tensiometer (T-6) measured (10 kPa) while Tensiometers (T-7 and T-8) measured approximately (5 kPa). The numerical results show that the Tensiometers closer to the water table have lower matric suction values. The change from a fully saturated soil to an unsaturated soil occurred within the first 24 hrs on application of 50 kPa *ARS* suction. Residual conditons were achevied on the second day and continued until the fifth day.

The SEEP/W results justify the observed drift of the Tensiometer's tips. The change in soil volume caused by the suction could lead to the repositioning of the Tensiometer's ceramic tip. The suction pull from the surface of the *ARS* could cause minor movement of the porous tips, resulting in a shift towards the source of suction. The Tensiometers (T-1, T-2 and T-3) all remained different from the representative nodes on SEEP/W indicating no match on boundry soils away from the *ARS*.

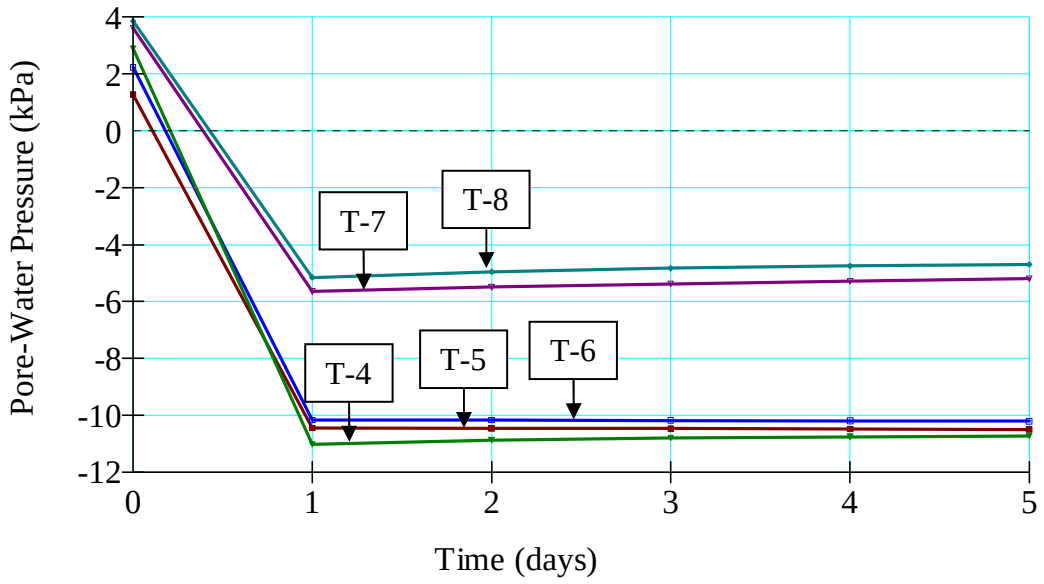

Figure 6.19: Pore water pressure (kPa) with Time (days) for 50 kPa

6.6 Zone of influence of suction

The zone of influence of suction was defined using the matric suction distribution contours in the soil after achieving equilibrium conditions. The zone of influence of suction lies within the envelope where maximum and minimum matric suction is measured. For example, Figure 6.20 shows equilibrium occurring after 5 kPa *ARS* suction was reached. The Tensiometer at the corner of the tank measured 1 kPa of suction, while other Tensiometers tending towards the *ARS* remained at zero. The reason for these results can be attributed to the soil water migrating towards the *ARS* leaving the boundaries dry. Figure 6.21 shows suction distribution at 50 kPa after equilibrium was reached. The zone of influence of suction lies within the modified UOBCE tank, where the maximum and the minimum matric suction was measured. The primary limitation associated with the laboratory testing was associated to the suction applied using the *ARS* during the experimental study. The complex nature, structure and behaviour of actual tree roots were not simulated in the present study. However, the methodology can be

expanded upon with a focus on understanding soil deformation around the vicinity of tree roots using the *ARS*. There were notable similarities between the experimental and simulated results of the soil surface deformation and the matric suction distributed within the vicinity of the *ARS*. The research methodology presented in this thesis can be used for providing reasonable predictions of settlements associated tree root suctions.

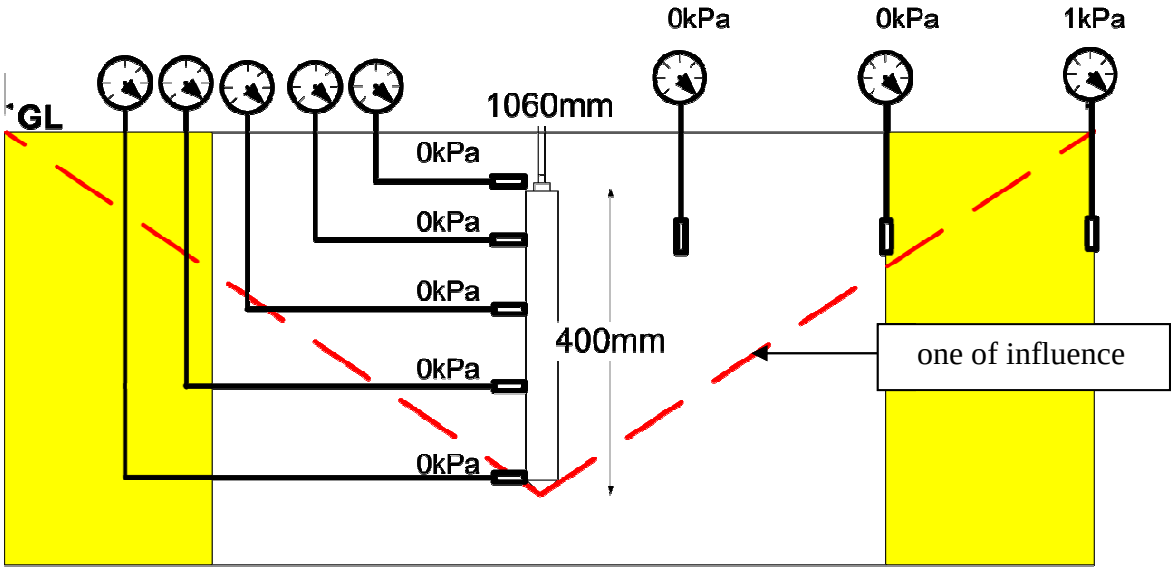

Figure 6.20: 5 kPa- Influence zone using negative pore water pressures

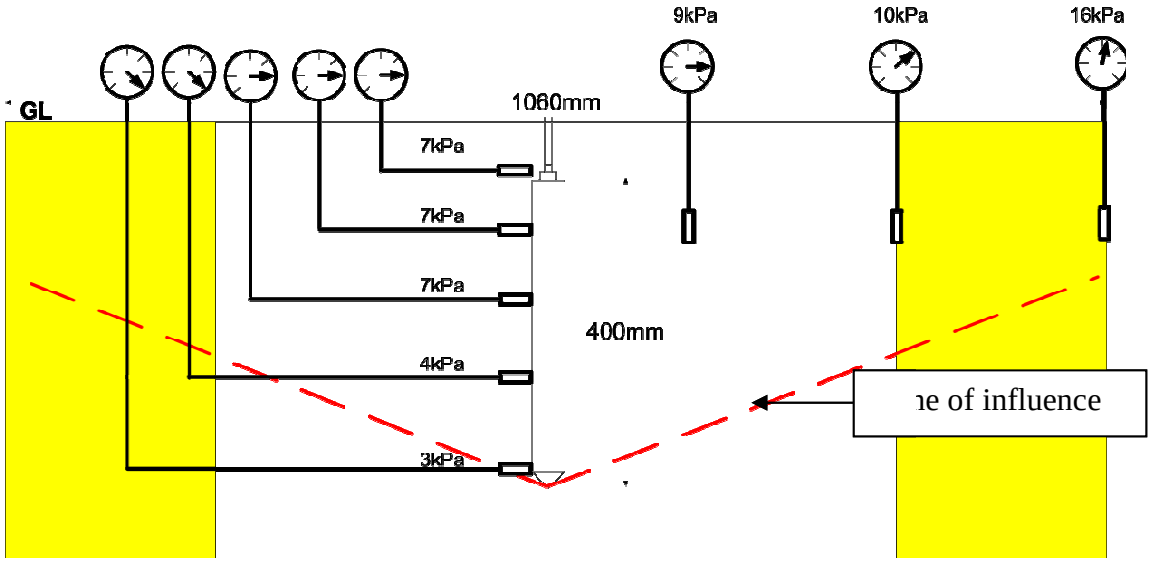

Figure 6.21: 50 kPa-Influence zone using negative pore water pressures

6.7 Soil Surface Deformation

SIGMA/W was used together with the SEEP/W program in order to perform a coupled FEM analysis. SIGMA/W calculates the deformations resulting from changes in pore water pressures while SEEP/W calculates transient pore water pressure changes that control these deformations.

The SIGMA/W deformation model uses the modulus of elasticity in a linear elastic model as its key parameter. The suction modulus, defined as the deformation related to matric suction, was measured using average matric suction, $(u_a - u_w)_{ave}$ as stress and volumetric strain, $\varepsilon = \delta V / V_1$ (refer to Chapter 4, Figure 4.9). The *PIV* measured volume change was determined using changes in the pixel of the surface of the soil. The suction

modulus from Chapter 4 (49.5 kPa) was used as Modulus, *E* input parameter in the SIGMA/W program to model the soil settlement.

Figure 6.22 shows the surface settlement of various applications of suction from the *ARS* using SIGMA/W. The shift of soil particles (change in volume) increases as excess moisture was removed from the soil by *ARS* suction.

Section 6.5 discussed negative pore water pressures in the experimental and numerical modelling phase. The behaviour of negative pore water pressure (i.e., matric suction) before equilibrium time was observed in the SEEP/W analysis. Matric suction is one of the two independent stress state variables for unsaturated soils (Fredlund and Morgenstern, 1977). The graphical representation of matric suction from SEEP/W enables proper understanding of the soil volume changes. For example, after application of 50 kPa of *ARS* suction, Tensiometers (T-1, T-2 and T-3) gradually increased in matric suction. This indicates that soil deformation (volume change) was pronounced around the vicinity of Tensiometers (T-1, T-2 and T-3). Since matric suction lasted two days before reaching residual pore pressures, the boundary conditions selected in the SIGMA/W model was fixed in both *x* and *y* directions. This prevents movement on the *x* and *y* axis during the model analysis, subsequently avoiding any additional deformation.

As shown in Figure 6.23, the *PIV* has measured soil settlements (deformations) caused by various suctions applied by the *ARS*. The deformation measured using the *PIV* application detects the changes in photo pixels separated by time. There is an increase in soil settlement as suction increases on the *ARS*. The soil settlement was identical for suction ranging between 40 kPa and 50 kPa.

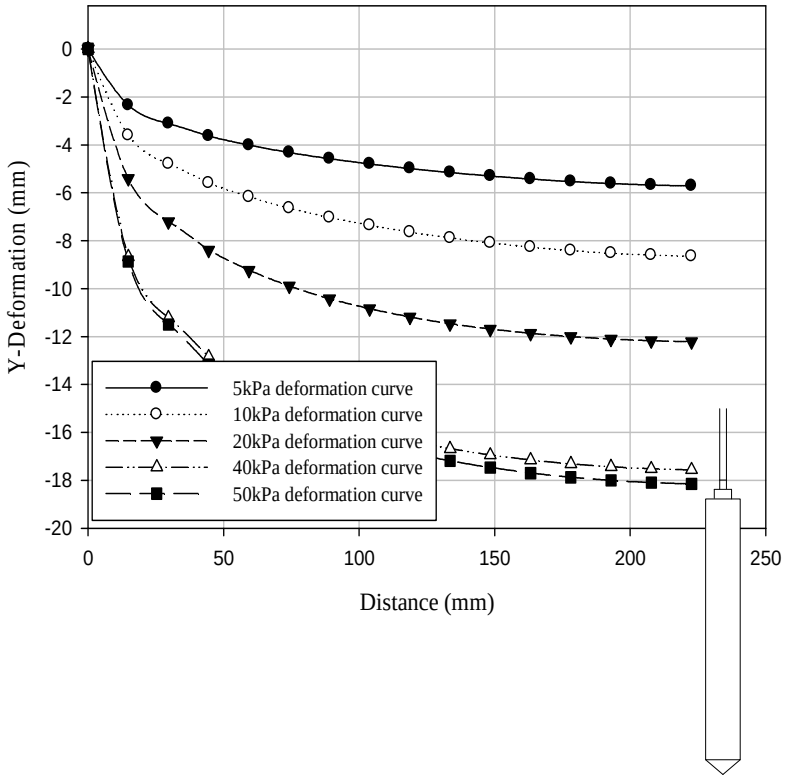

Figure 6.22: SIGMA/W Y (mm) settlement with distance (mm) from *ARS*

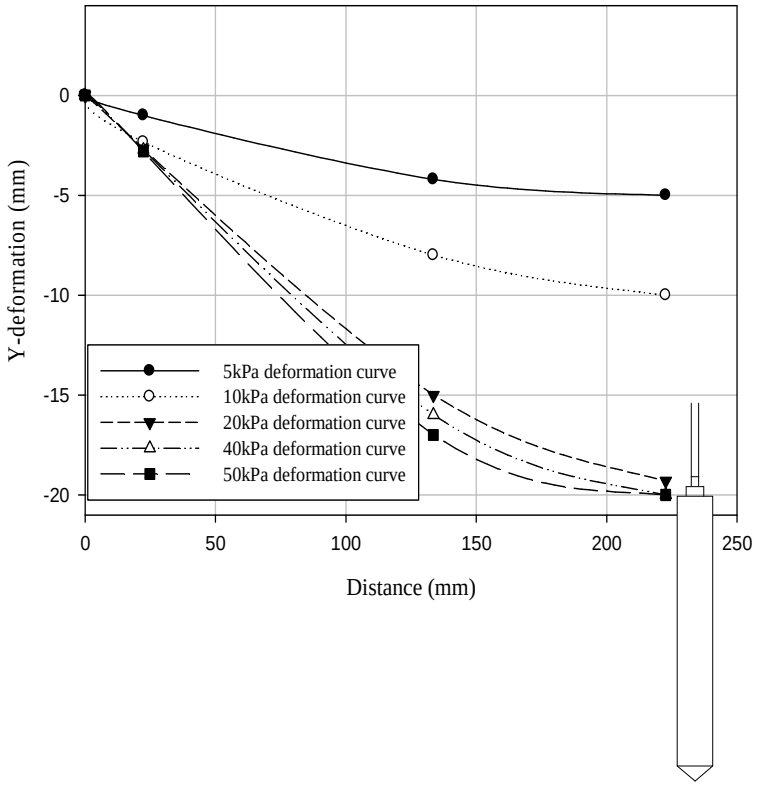

Figure 6.23: *PIV*- Y (mm) settlement with distance from *ARS*

Figure 6.24 compares the *PIV* measured deformation with SIGMA/W after 5 kPa suction applied by the *ARS*. The deformation shows a maximum deformation of 5.8 mm close to the *ARS*. In the laboratory, the *PIV* technology also measured maximum deformation of 5.0 mm close to the *ARS*. In both cases, there was no sign of deformation on the tank edges and deformation increased towards the location of the *ARS*. The maximum deformation at the *ARS* vicinity presented for *PIV* technology was 20 mm and 18 mm for SIGMA/W. These results suggest that modelling method can be reliably used in the estimation the soil deformation associated with the tree roots suction.

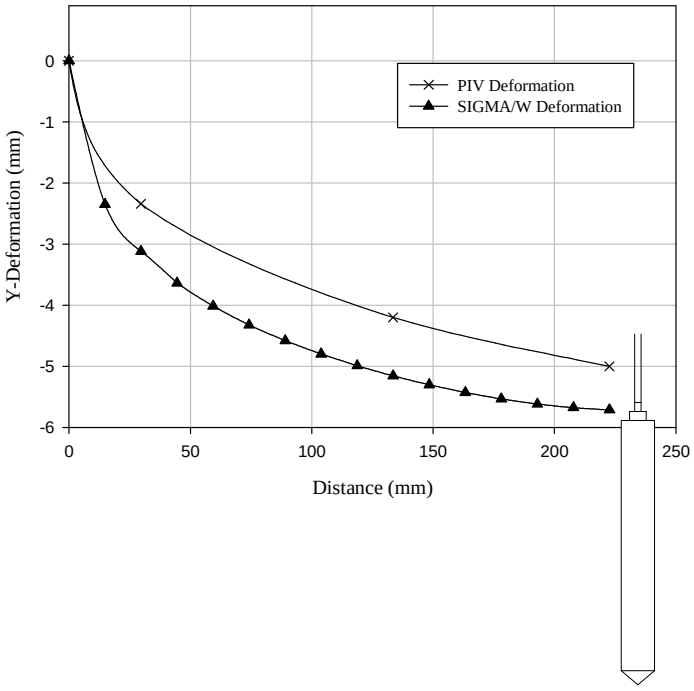

Figure 6.24: *PIV* and SIGMA/W deformation caused by 5 kPa applied suction by the *ARS*

Figure 6.25 provides comparison between surface deformation from the *PIV* technique and the SIGMA/W analysis at 50 kPa of suction from the *ARS*. Soil deformation did not occur close to the tank boundaries in both *PIV* technology and SIGMA/W.

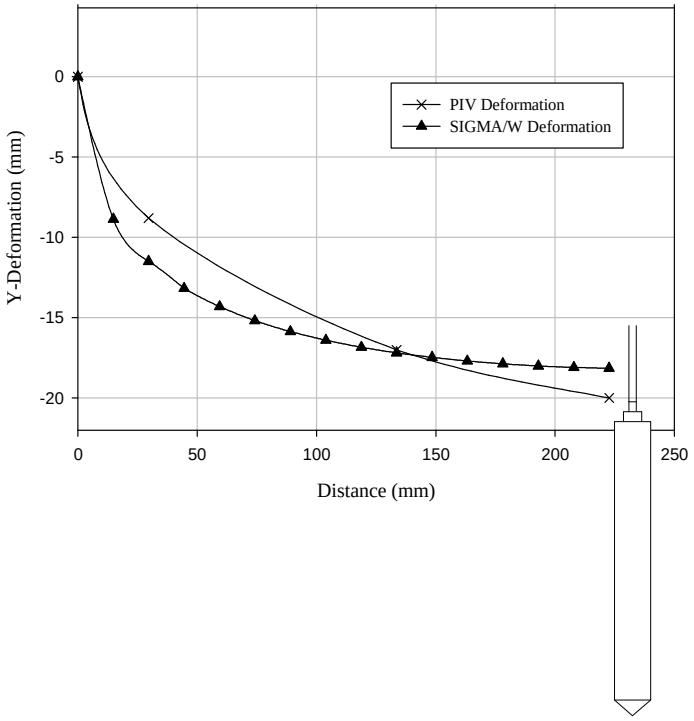

Figure 6.25: *PIV* and SIGMA/W deformation caused by 50 kPa applied suction by the *ARS*

The *PIV* technology accuracy depends upon the specifications of the camera and positioning used to collect time pixel changes. The limitation of the *PIV* technology was its inability to determine more than a line on the soil surface profile.

6.8 Analysis of Volume change in Sandy Loam Soil

The constitutive surface of the soil structure can be used as a tool to identify volume change within a soil mass. The relationship can be established by combining the results of deformation (volume change) with the Soil Water Characteristic Curve (*SWCC*), as

summarized in [Chapter 4]. An important component of this relationship gives the shape of the constitutive surface with void ratio as presented in Figure 6.26.

If the soil suction and net normal stress applied to the soil structure were increased from stress conditions at point A to a stress condition similar to point B, there would be soil suction to cause the void ratio to decrease.

This chapter presents the change in matric suction caused by the *ARS* with time. The matric suction increased due to reducing void ratio and water content withdrawn by the *ARS*. For example, after equilibrium for 50 kPa *ARS* suction, there was sufficient matric suction acting in the loam soil because more water had been withdrawn by the *ARS*. The soil comes into equilibrium under applied stress gradient (soil particles) and two phases that flow under applied stress gradient (i.e., air and water) (Fredlund and Rahardjo, 1993).

The methodology presented in this chapter can be used to estimate the anticipated volume change associated with tree roots using the Geo-slope software. The methodology presented in consistent with the mechanics of unsaturated soil mechanics.

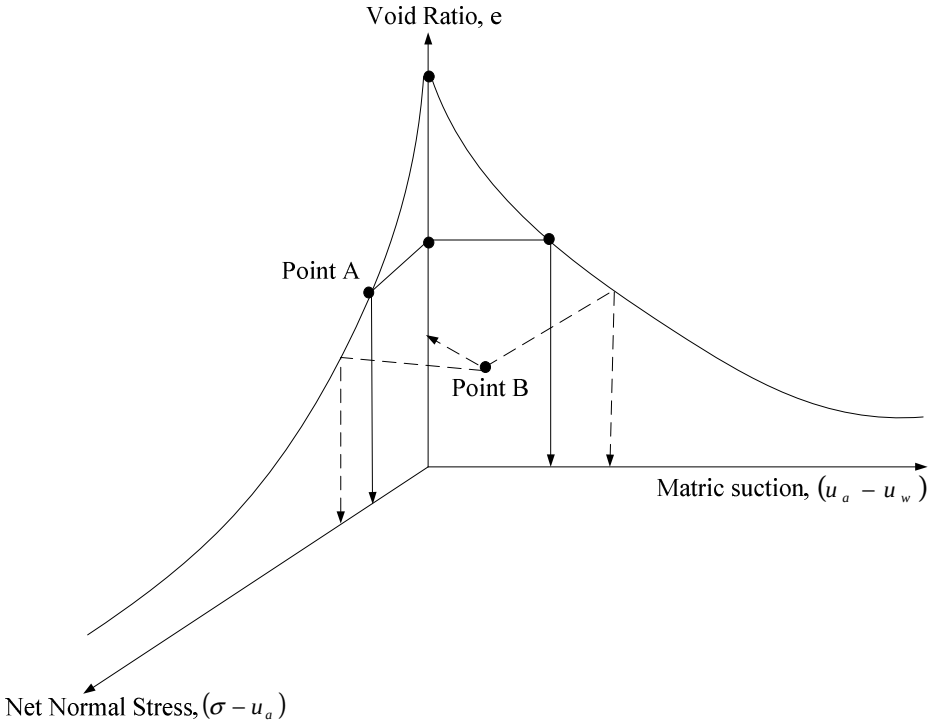

Figure 6.26: Soil structure constitutive surface in arithmetic scale (Reference: Fredlund and Rahardjo, 1993)

6.9 Summary

In this study, the matric suction, volumetric water contents and volume change (deformation) values were all reliably measured in the modified UOBCE using different instrumentation. Two different scenarios are presented in this chapter which include *ARS* suction 5 kPa and 50 kPa. The results for 5 kPa *ARS* suction obtained from the SEEP/W and Tensiometers T-1 to T-8 present reasonable matric suction results. The SIGMA/W and *PIV* technology used to determine soil deformation also presented corresponding results. At 50 kPa *ARS* suction, the SEEP/W and Tensiometers T-4 to T-8 showed good matric suction agreements. The SIGMA/W and *PIV* technology also presented similar consistent results for soil deformation. The analysis results showed that decreasing volume change (settlement) influenced by *ARS* suction pull decreases with the decrease

in degree of saturation, matric suction and void ratio. The results presented in this study are encouraging; suggesting that the parameters obtained from the laboratory could be used in finite modeling method to successfully simulate soil deformation and distribution of matric suction with reasonable accuracy.

The study can be used to analyze the stability of shallow foundations, retaining wall, roads and walk ways subgrade as well as buried pipes around the vicinity of tree(s) roots.

CHAPTER 7

CONCLUSIONS

The conclusions of the research study conducted are summarized in the Chapter. In addition, the practical applications of this research undertaken are detailed succinctly.

7.1 Proposed Methodology

i. The Artificial Rooting System (*ARS*) designed for conducting the research presented in this thesis was found to be satisfactory to simulate tree root action. Only a single root was simulated in the present research; however, this technique can be extended to simulate complex behaviour of the complex tree roots system.

ii. The *PIV* technique was found to be reliable tool to measure the soil surface deformation behaviour associated with the changes in the soil suction.

iii. The peristaltic pump used to simulate suction values in the *ARS* was not functioning satisfactorily when the tests were continued over a long period of time. This disadvantage of peristaltic pump was overcome by using vacuum generator (i.e. convert air-pressure to vacuum)

7.2 GEO-SLOPE Software

The numerical analyses results in this research showed that the two finite element softwares, SEEP/W and SIGMA/W can be effectively used to model the coupled seepage and stress behaviour. SEEP/W successfully simulated the operation of the *ARS* and the resultant positive and negative pore-water pressure distribution profiles in the soils. SIGMA/W estimated the deformation behaviour of the soil based on the pore-water pressure distribution profile obtained by SEEP/W. There was good comparison between the measured displacements (using *PIV* technique) and those estimated from the

numerical analysis. It was also found that the suction modulus, *H* is a key parameter in estimating the tree related settlements in soils instead of the elastic modulus, *E*.

7.3 Applications of the Research

The present research can be applicable to engineering practice in various ways as follow.

i. This research work can be implemented in the building code by recommending ideal positions of trees to prevent possible tree-roots related damages to shallow foundations.

ii. The proposed empirical model can be further improved by determining modulus of elasticity *H* reliably using more controlled tests and also considering various parameters that influence it.

iii. The proposed experiment methodology and analysis technique can be combined with *SWCC* to reliably estimate the tree-soil deformations considering wetting and drying cycles or based on the climate data.

REFERENCES

Ali, N. & Rees, S.W. 2006. “Simulating water uptake by tree roots: An initial assessment”, Geotechnical Special Publication, pp. 2245.

Ali, N. & Rees, S.W. 2008. “Preliminary analysis of tree-induced suctions on slope stability”, Unsaturated Soils: Advances in Geo-Engineering - Proceedings of the 1st European Conference on Unsaturated Soils, E-UNSAT 2008, pp. 811.

Ali, N., Farshchi, I., Mu'azu, M.A. & Rees, S.W. 2012, “Soil-root interaction and effects on slope stability analysis”, Electronic Journal of Geotechnical Engineering, vol. 17 C, pp. 319-328.

Ali, N.B. & Abdullahi, M.M. 2010. “Simulation of vegetative induced deformation in an unsaturated soil”, American Journal of Environmental Sciences, vol. 6, no. 2, pp. 130-136.

ASTM, D2216. (1994A), “Laboratory determination of water (moisture) content of soil and rock by mass”, In annual book of ASTM Standards, American Society of Testing Material, Philadelphia, PA, 4.08, 177-180.

ASTM, D2974. (1993) “Standard test method for moisture, ash and organic matter of peat and organic soils”, In annual book of ASTM Standards, American Society of Testing Material, Philadelphia, PA, 4.08, 400-402.

ASTM, D422. (1994b), “Standard test method for particle size analysis of soils”, In annual book of ASTM Standards, American Society of Testing Material, Philadelphia, PA, 4.08, 10-16.

ASTM, D698. (1994c), “Test method of laboratory compaction characteristics of soils using standard effort”, In annual book of ASTM Standards, American Society of Testing Material, Philadelphia, PA, 4.08, 69-76.

ASTM, D854. (1994d), “Standard test method for specific gravity of soils”, In annual book of ASTM Standards, American Society of Testing Material, Philadelphia, PA, 4.08, 80-83.

Bar-tal, A., Bar-yosef, B. and Chen, Y. 1991, “Validation of a model of the transport of zinc to an artificial root.” Journal of Soil Science, 42: 399-411.

Belmans, C., Wesseling, J.G. & Feddes, R.A. 1983, “Simulation model of the water balance of a cropped soil: SWATRE”, Journal of Hydrology, vol. 63, no. 3-4, pp. 271-286.

Blight, G.E. 2003, “The vadose zone soil-water balance and transpiration rates of vegetation”, Geotechnique, vol. 53, no. 1, pp. 55-64.

Bozozuk, M. and Burn, K.N. 1960, “Vertical ground movements near elm trees,” Géotechnique, 10: 19-32.

Briggs, L.J and Lapham. 1900, “An artificial root for inducing capillarity movement of soil moisture.” Special articles, Bull. 19, Division of soils, U.S. Dept. of Agri.: 566-570.

Cameron, D.A. 2001, “The extent of soil desiccation near trees in a semi-arid environment”, Geotechnical and Geological Engineering, vol. 19, no. 3-4, pp. 357-370.

Cameron, D.A., Jaksa, M.B., Potter, W., and O’ Malley, A. 2006, “Influence of trees on expansive soils in southern Australia.” Taylor and Francis Group, chapter 21: 295-314.

Canada Mortage and Housing Corporation (CHMC). 2005, “Understanding and dealing with interactions between trees, sensitive clay soils and foundations.” About your house fact sheets, vol. 8; p. 62226.

Crawford, C.B. & Bozozuk, M. 1990, “Thirty years of secondary consolidation in sensitive marine clay”, Canadian Geotechnical Journal, vol. 27, no. 3, pp. 315-319.

Crawford, C.B. 1968, "Quick clays of eastern Canada", Engineering Geology, vol. 2, no. 4, pp. 239-265.

Driscoll, R. 1983, “The influence of vegetation on the swelling and shrinking of clay soils in Britain.”, Geotechnique, vol. 33, no. 2, pp. 93-105.

Driscoll, R. 1984, “Review of British experience of expansive clay problems.”, National Conference Publication - Institution of Engineers, Australia, pp. 192.

Fatahi, B., Khabbaz, H. & Indraratna, B. 2009, “Parametric studies on bioengineering effects of tree root-based suction on ground behaviour”, Ecological Engineering, vol. 35, no. 10, pp. 1415-1426.

Fatahi, B., Khabbaz, H. & Indraratna, B. 2010, “Bioengineering ground improvement considering root water uptake model”, Ecological Engineering, vol. 36, no. 2, pp. 222-229.

Feddes, R.A. 1988, “Modelling and simulation in hydrologic systems related to agricultural development: State of the art”, Agricultural Water Management, vol. 13, no. 2-4, pp. 235-248.

Feddes, R.A., Kowalik, P., Kolinska-Malinka, K. & Zaradny, H. 1976, “Simulation of field water uptake by plants using a soil water dependent root extraction function”, Journal of Hydrology, vol. 31, no. 1-2, pp. 13-26.

Fredlund, D.G. 2000, “The 1999 R.M. Hardy Lecture: The implementation of unsaturated soil mechanics into geotechnical engineering”, Canadian Geotechnical Journal, vol. 37, no. 5, pp. 963-986.

Geo-Slope, “Seep/W for finite element seepage analysis”, User’s guide (version 5). Canada: Geo-Slope International; 2002, p. 549.

Goh, S.G., Rahardjo, H. & Leong, E.C. 2010, “Shear strength equations for unsaturated soil under drying and wetting”, Journal of Geotechnical and Geoenvironmental Engineering, vol. 136, no. 4, pp. 594-606.

Graf, F., Frei, M. & Böll, A. 2009, “Effects of vegetation on the angle of internal friction of a moraine”, Forest Snow and Landscape Research, vol. 82, no. 1, pp. 61-77.

Green, S.R., Kirkham, M.B. & Clothier, B.E. 2006, “Root uptake and transpiration: From measurements and models to sustainable irrigation”, Agricultural Water Management, vol. 86, no. 1-2, pp. 165-176.

Hettiaratchi, D.R.P. 1990, “Soil compaction and plant root growth”, Philosophical Transactions - Royal Society of London, B, vol. 329, no. 1255, pp. 343-355.

Holtz, W.G. 1983, “The influence of vegetation on the swelling and shrinking of clays in the United States of America.”, Geotechnique, vol. 33, no. 2, pp. 159-163.

Indraratna, B., Fatahi, B. & Khabbaz, H. 2006, “Numerical analysis of matric suction effects of tree roots”, Proceedings of the Institution of Civil Engineers: Geotechnical Engineering, vol. 159, no. 2, pp. 77-90.

Manuwa, S.I. 2009, “Performance evaluation of tillage tines operating under different depths in a sandy clay loam soil”, Soil and Tillage Research, vol. 103, no. 2, pp. 399-405.

Marinho, F.A.M. 2005, “Nature of soil-water characteristic curve for plastic soils”, Journal of Geotechnical and Geoenvironmental Engineering, vol. 131, no. 5, pp. 654-661.

Mathur, S. 1999, “Settlement of soil due to water uptake by plant roots”, International Journal for Numerical and Analytical Methods in Geomechanics, vol. 23, no. 12, pp. 1349-1357.

Mohamed, F.M.O 2006, “A semi-empirical approach for the interpretation of the bearing capacity of unsaturated soils ", Thesis University of Ottawa 2006.

Mohamed, F.M.O and Vanapalli, S.K. 2006, “Laboratory investigations for the measurement of the bearing capacity of an unsaturated coarse-grained soil,” In Proc. 59th Can. Geotech. Conf., Vancouver 2006.

Navarro, V., Candel, M., Yustres, Á., Alonso, J. & García, B. 2009, "Trees, lateral shrinkage and building damage", Engineering Geology, vol. 108, no. 3-4, pp. 189-198.

Navarro, V., Candel, M., Yustres, A., Sánchez, J. & Alonso, J. 2009, "Trees, soil moisture and foundation movements", Computers and Geotechnics, vol. 36, no. 5, pp. 810-818.

Oh, W.T., Vanapalli, S.K. & Puppala, A.J. 2009, "Semi-empirical model for the prediction of modulus of elasticity for unsaturated soils", Canadian Geotechnical Journal, vol. 46, no. 8, pp. 903-914.

Ohu, J.O., Raghavan, G.S.V., Prasher, S. & Mehuys, G. 1987, "Prediction of water retention characteristics from soil compaction data and organic matter content", Journal of Agricultural Engineering Research, vol. 38, no. 1, pp. 27-35.

Penner, E. & Burn, K.N. 1978, "Review of engineering behaviour of marine clays in eastern Canada." Canadian Geotechnical Journal, vol. 15, no. 2, pp. 269-282.

Prasad, R. 1988, "A linear root water uptake model", Journal of Hydrology, vol. 99, no. 3-4, pp. 297-306.

Quigley, R.M., Gwyn, Q.H.J., White, O.L., Rowe, R.K., Haynes, J.E. & Bohdanowicz, A. 1983, "Leda clay from deep boreholes at Hawkesbury, Ontario. Part 1: Geology and geotechnique.", Canadian Geotechnical Journal, vol. 20, no. 2, pp. 288-298.

Ravina, I. 1983, "The influence of vegetation on moisture and volume changes.", Geotechnique, vol. 33, no. 2, pp. 151-157.

Raymond, G.P., Gaskin, P.N. & Addo-Abedi, F.Y. 1979, "Repeated compressive loading of Leda clay." Can Geotech J, vol. 16, no. 1, pp. 1-10.

Sangrey, D.A & Paul M.J 1971, "Regional study of landsliding near Ottawa", Canadian Geotechnical Journal, vol. 8, no. 2, pp. 315-335.

Satriani, A., Loperte, A., Proto, M. & Bavusi, M. 2010, “Building damage caused by tree roots: Laboratory experiments of GPR and ERT surveys”, Advances in Geosciences, vol. 24, pp. 133-137.

Saxton, K.E., Rawls, W.J., Romberger, J.S. & Papendick, R.I. 1986, “Estimating generalized soil-water characteristics from texture.”, Soil Science Society of America Journal, vol. 50, no. 4, pp. 1031-1036.

Sillers, W.S. & Fredlund, D.G. 2001, “Statistical assessment of soil-water characteristic curve models for geotechnical engineering”, Canadian Geotechnical Journal, vol. 38, no. 6, pp. 1297-1313.

Silvestri, V., Tabib, C. & Behidj, F. 1994, “Observations and modelling of soil water content changes around trees”, Canadian Journal of Civil Engineering, vol. 21, no. 6, pp. 980-989.

SlavĬkovã, J. 1967, “Compensation of Root suction force within a single root system”, Biologia Plantarum, vol. 9, no. 1, pp. 20-27.

Smethurst, J.A., Clarke, D. & Powrie, W. 2006, “Seasonal changes in pore water pressure in a grass-covered cut slope in London Clay”, Geotechnique, vol. 56, no. 8, pp. 523-537.

Topp, G.C., J.L. David, and A.P. Annan 1980. Electromagnetic, Determination of Soil Water Content: Measurement in Coaxial Transmission Lines. Water Resources Research16:3. p. 574-582.

Van Bruggen, A.H.C., Semenov, A.M. & Zelenev, V.V. 2000, “Wavelike distributions of microbial populations along an artificial root moving through soil”, Microbial ecology, vol. 40, no. 3, pp. 250-259.

Vanapalli, S.K. & Oh, W.T. 2010, “Mechanics of unsaturated soils for the design of foundation structures”, International Conference on Engineering Mechanics, Structures, Engineering Geology, International Conference on Geography and Geology - Proceedings, pp. 363.

Vanapalli, S.K., Fredlund, D.G., Pufahl, D.E. & Clifton, A.W. 1996, "Model for the prediction of shear strength with respect to soil suction", Canadian Geotechnical Journal, vol. 33, no. 3, pp. 379-392.

Vu, H.Q. & Fredlund, D.G. 2006, "Challenges to modelling heave in expansive soils", Canadian Geotechnical Journal, vol. 43, no. 12, pp. 1249-1272.

Ward, W.H. (1953). "Soil movements and weather," In Proc. 3rd Int. Conf. Soil Mech., Zurich 1953, 2: 477-481.

White, D.J., Take, W.A. & Bolton, M.D. 2003, "Measuring soil deformation in geotechnical models using digital images and PIV analysis", 10th International Conference on Computer Methods and Advances in Geomechanics, Tucson, Arizona. Pp 997-1002 pub

White, D.J., Take, W.A. & Bolton, M.D. 2003, "Soil deformation measurement using particle image velocimetry (PIV) and photogrammetry", Geotechnique, vol. 53, no. 7, pp. 619-631

.

APPENDIX-A

First Preliminary test showing *ARS* and peristaltic pump

Second Preliminary test showing LVDT's used for surface deformation on Loam soil

APPENDIX-B

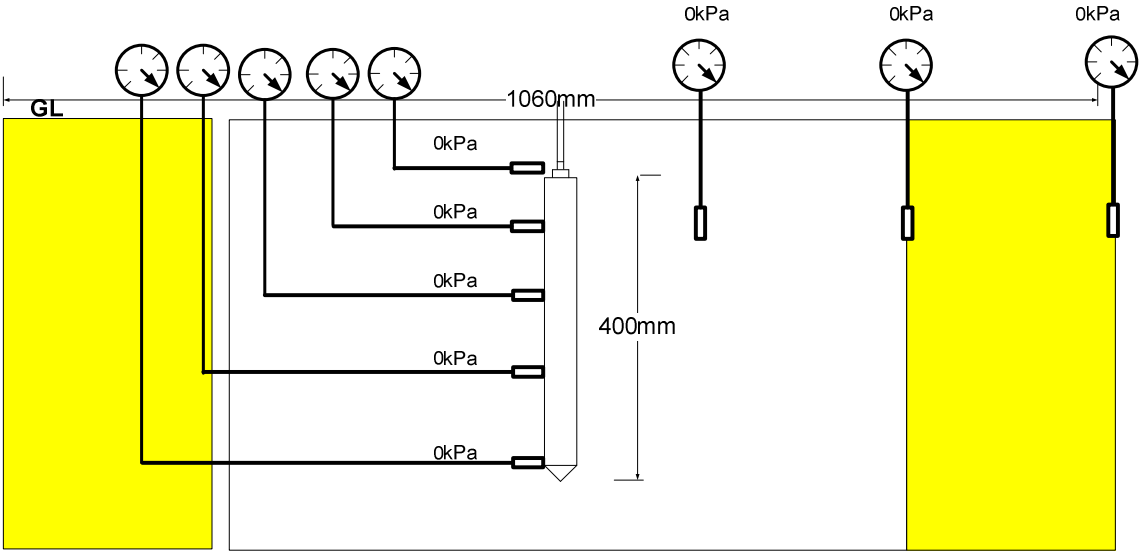

Shows Tensiometers readings along the ARS for 0kPa

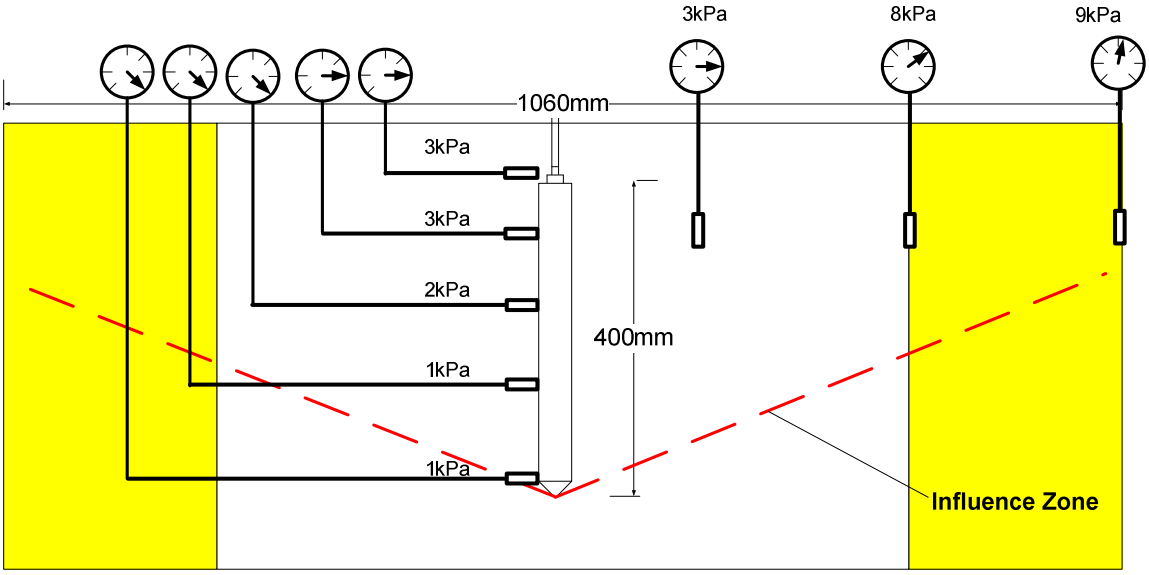

Shows Tensiometers readings along the ARS for 10kPa

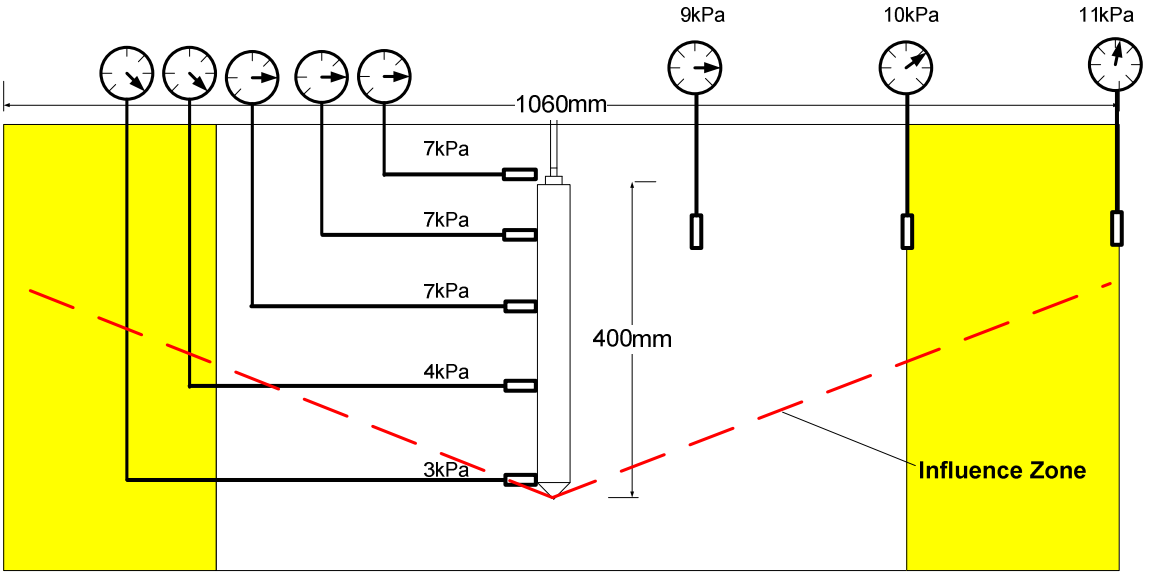

Shows Tensiometers readings along the ARS for 20kPa

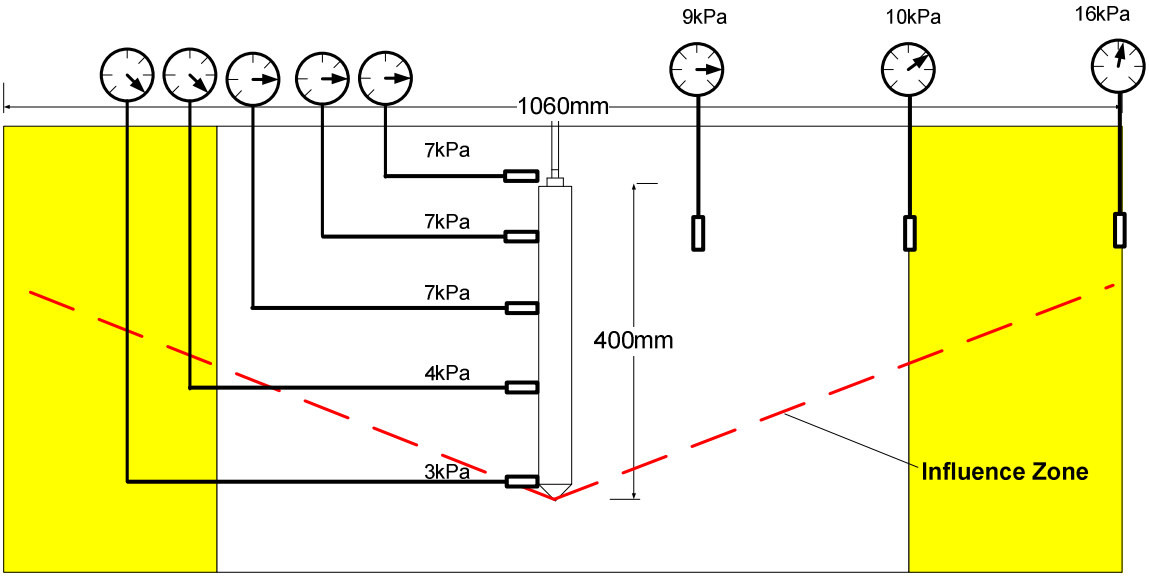

Shows Tensiometers readings along the ARS for 40kPa

APPENDIX-C

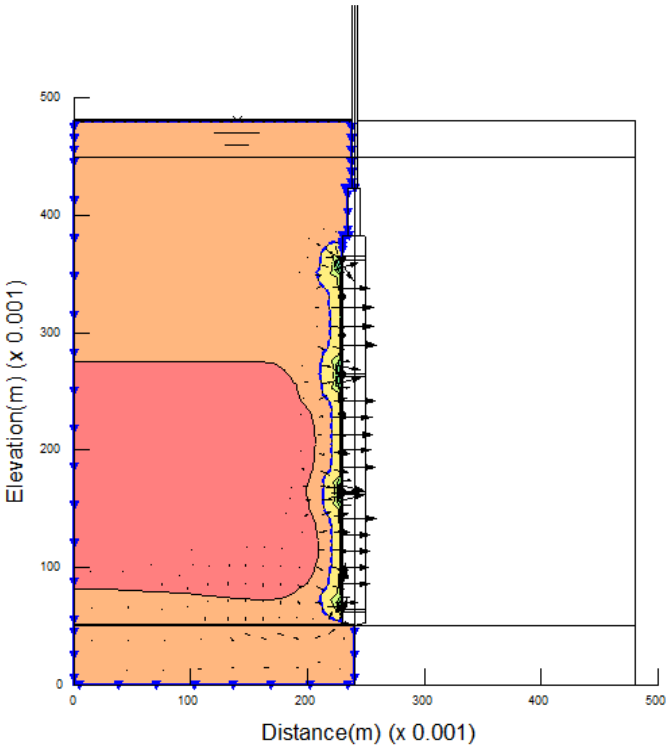

Shows pore water distribution after 22 days of 10kPa suction

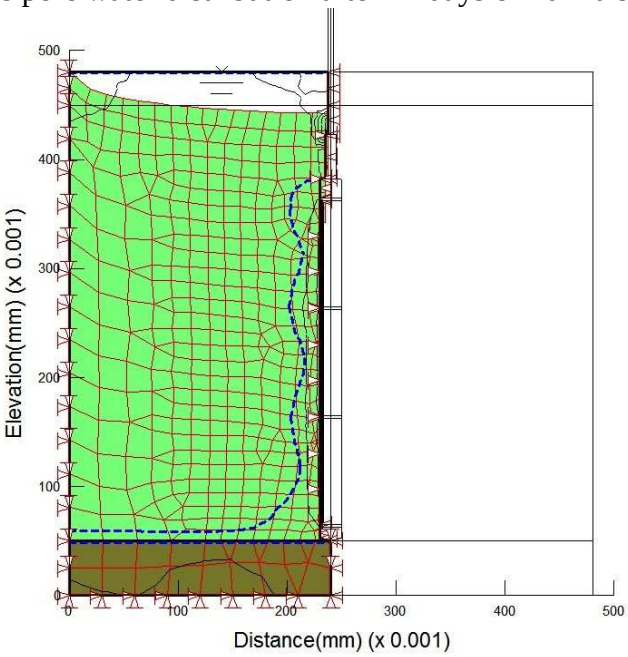

Shows deformation after 22 days of 10kPa suction

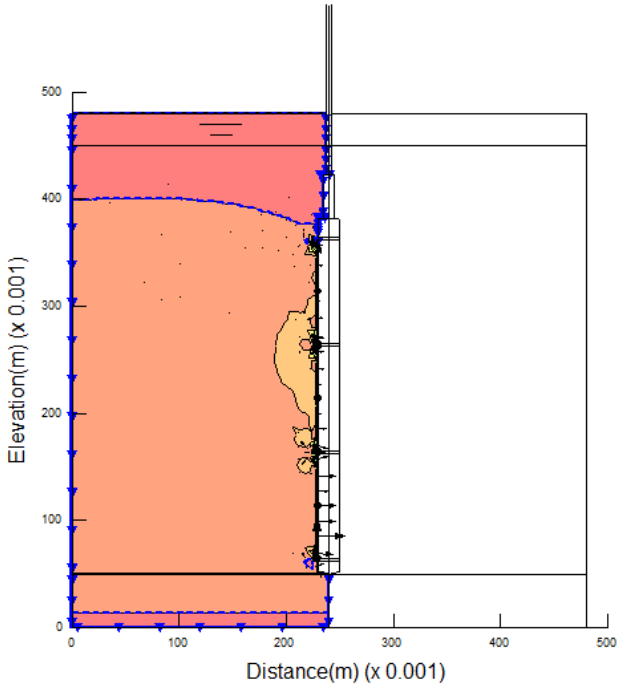

Shows pore water distribution after 9 days of 20kPa suction

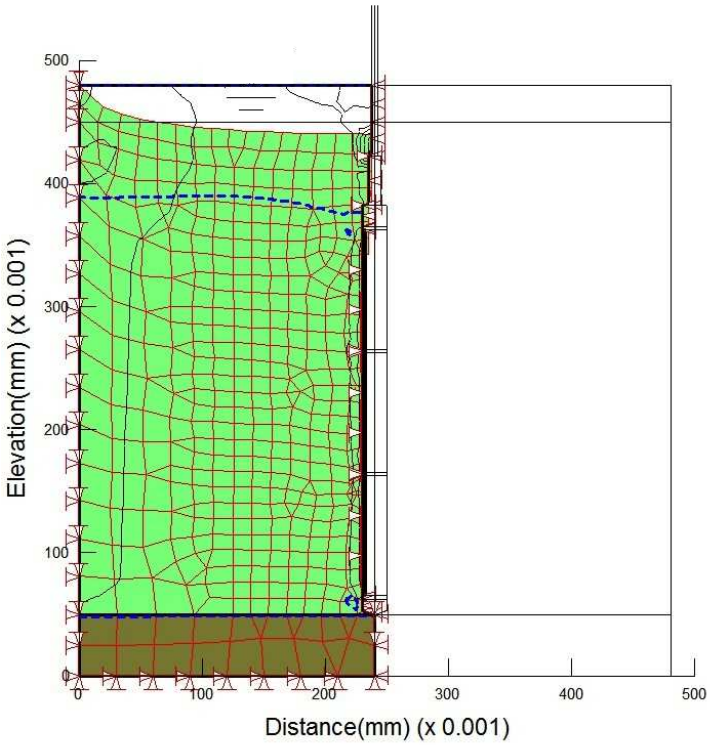

Shows deformation after 9 days of 20kPa suction

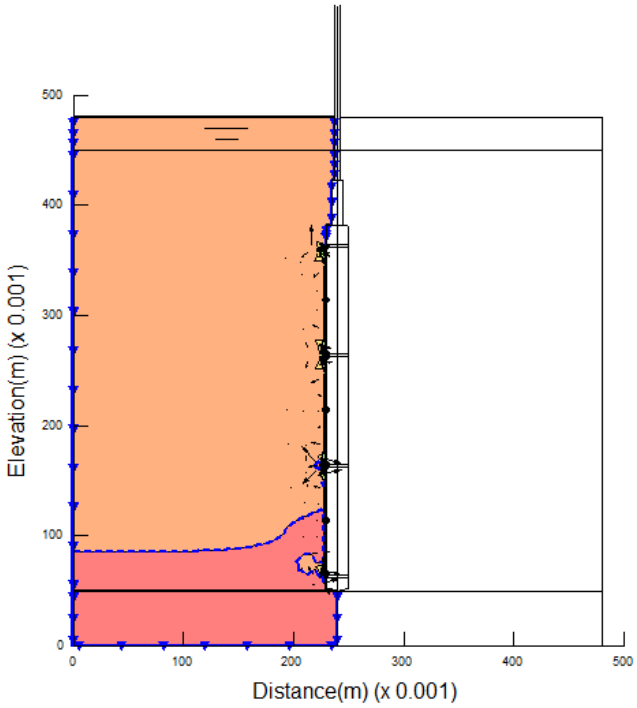

Shows pore water distribution after 5 days of 40kPa suction

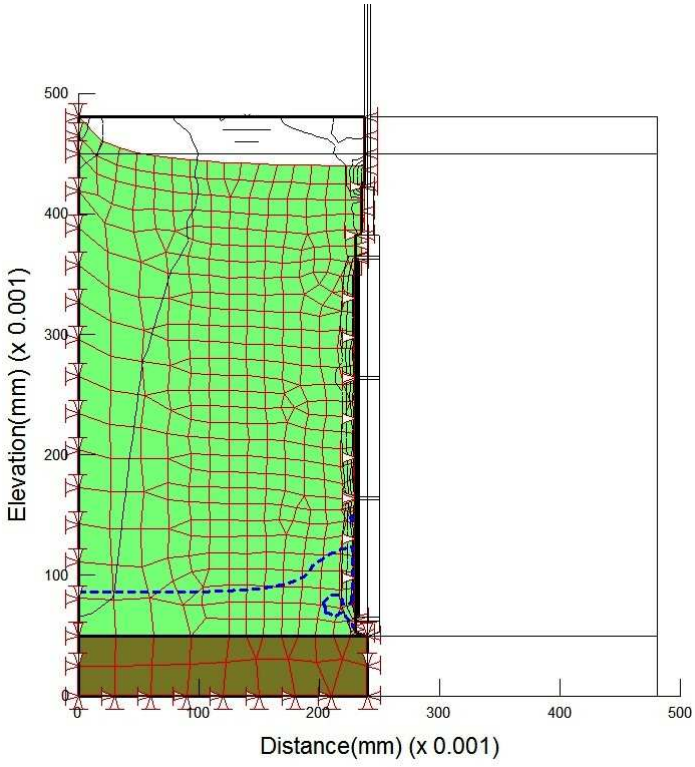

Shows deformation after 5 days of 40kPa suction

APPENDIX-D

Table1: Volumetric water content at 0 kPa to 40kPa Suction from ARS.

ARS Suction(kPa)	VWC- (A) m^3/m^3	VWC- (B) m^3/m^3	VWC- (C) m^3/m^3	Elevation (mm)	Equilibrium (days)
0	0.428	0.419	0.416	50	0
0	0.430	0.429	0.437	200	0
0	0.431	0.432	0.438	350	0
10	0.413	0.401	0.405	50	22
10	0.425	0.419	0.425	200	22
10	0.431	0.421	0.467	350	22
20	0.312	0.305	0.327	50	9
20	0.331	0.321	0.344	200	9
20	0.373	0.398	0.381	350	9
40	0.196	0.136	0.201	50	5
40	0.211	0.197	0.219	200	5
40	0.225	0.232	0.230	350	5

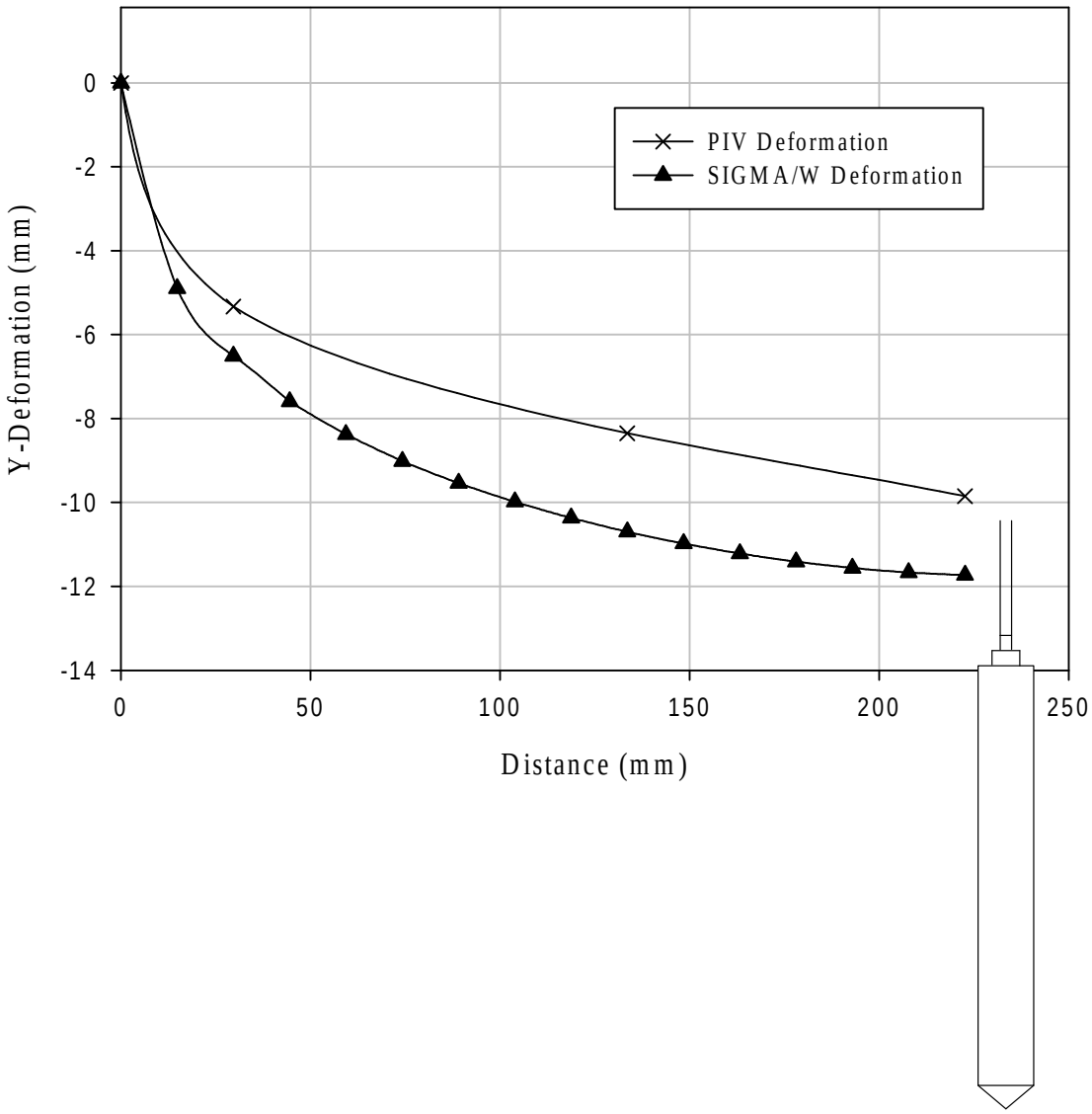

PIV and SIGMA/W deformation caused by 10kPa applied suction on *ARS*

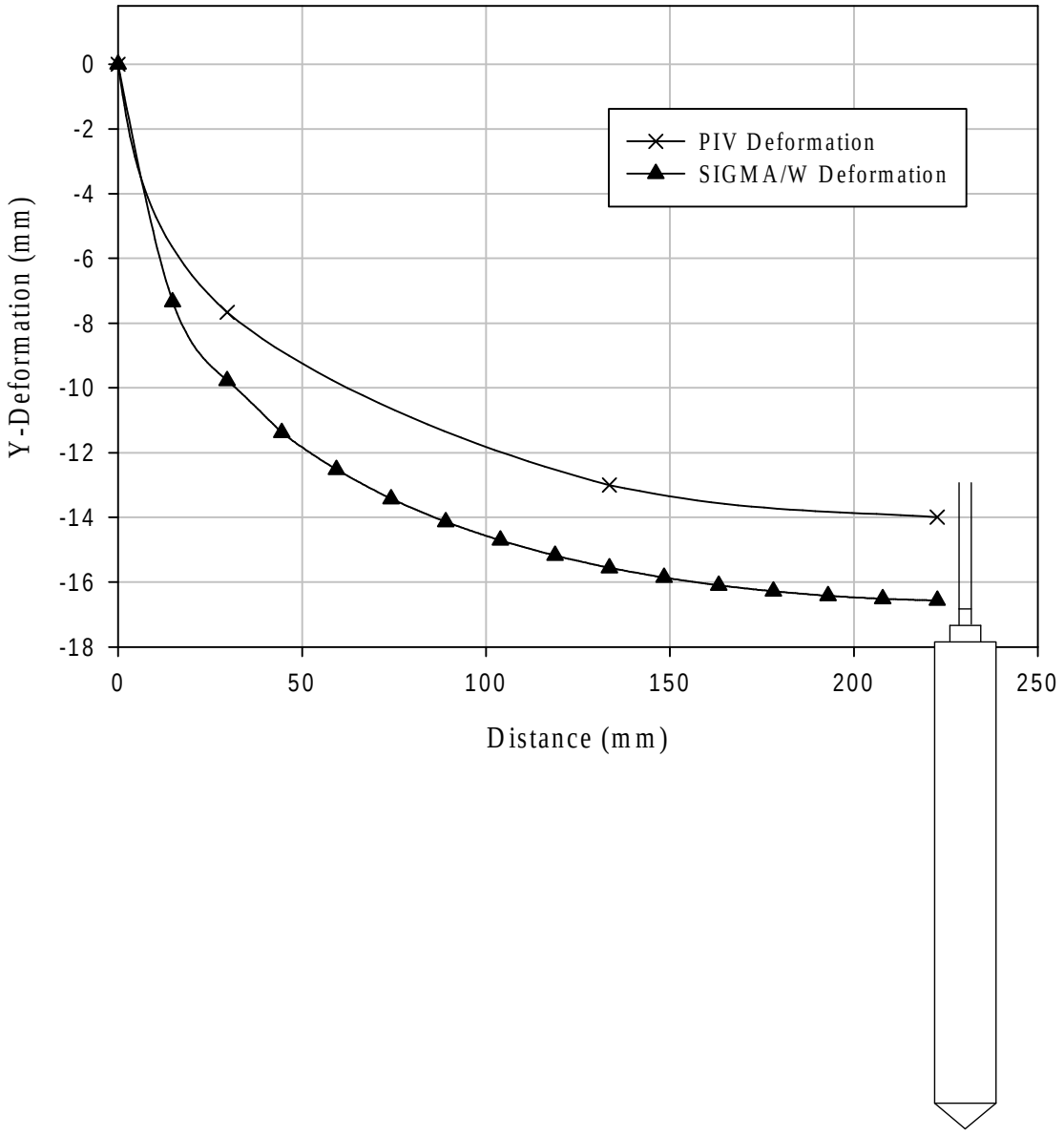

PIV and SIGMA/W deformation caused by 20kPa applied suction on *ARS*

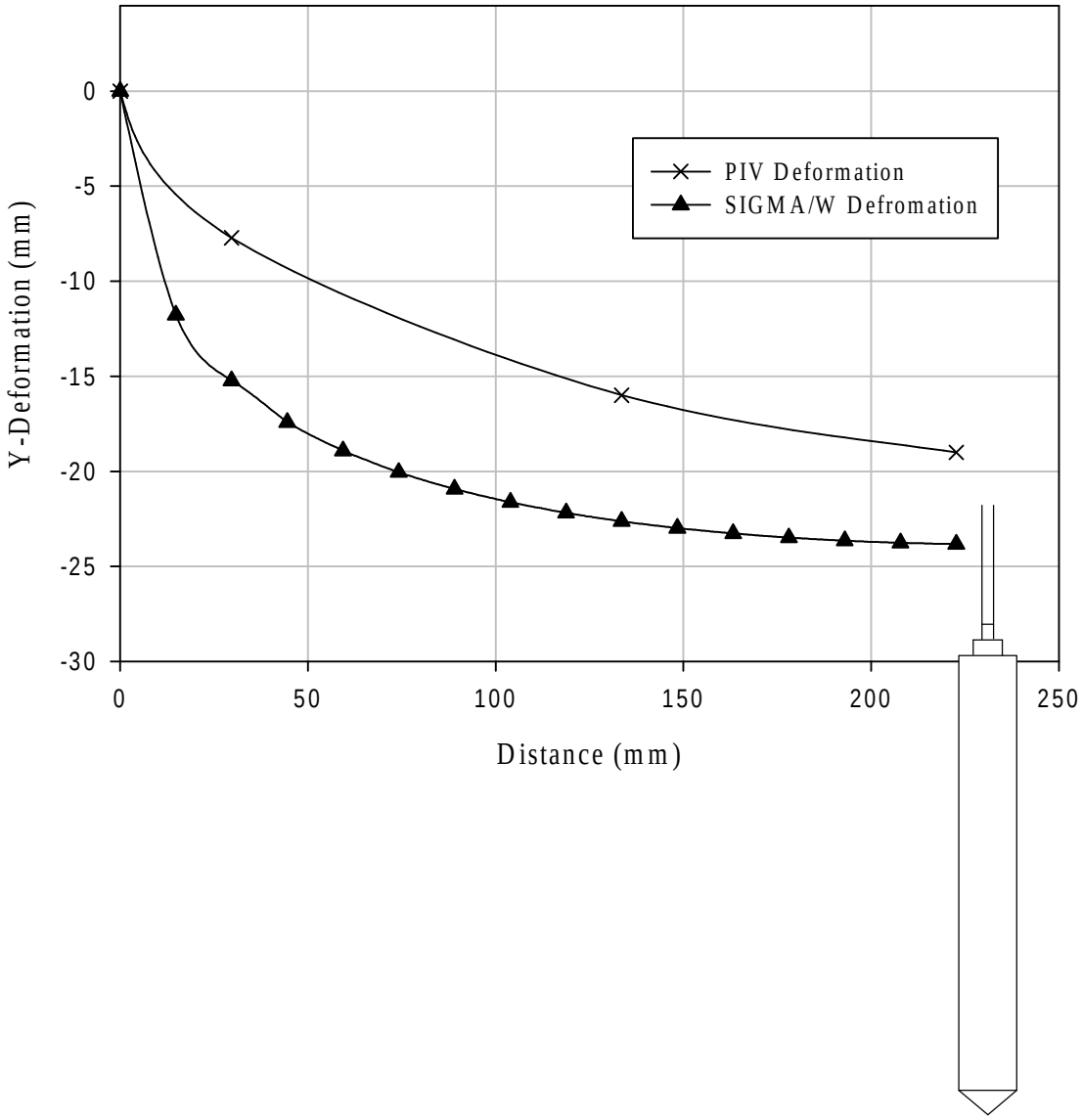

PIV and SIGMA/W deformation caused by 40kPa applied suction on *ARS*

City of Ottawa/Ville d`Ottawa
Forestry Services

Table 2: RECOMMENDED TREE SPECIES FOR THE OTTAWA AREA

Botanical Name/ Common Name	Arterial Road	Hard Surface	Residential street	School yard	Park	Sensitive marine clay soil	naturalization		Height (m)		
									Small (5-10)	Medium (10-15)	Large (15 +)
SPECIES NATIVE TO ONTARIO											
DECIDUOUS TREES											
Acer rub/ Red Maple			X	X	X		X			X	
Acer saccharinum/ Silver maple					X		X				X
Acer saccharum/ Sugar maple			X	X	X		X				X
Amelanchier spp./ Serviceberry	X	X	X		X	X	X		X		
Celtis occidentalis/ Hackberry	X	X	X	X	X		X			X	
Gleditsia triacanthos/ Honey locust	X	X	X	X	X		X			X	
Prunus pensylvanica/ Pin cherry					X		X			X	

Botanical Name/ Common Name	Arterial Road	Hard Surface	Residential street	School yard	Park	Sensitive marine clay soil	naturalization		Height (m)		
									Small (5-10)	Medium (10-15)	Large (15 +)
Populus grandidentata/ Large tooth aspen							X				X
Populus tremuloides/ Trembling aspen							X				X
Quercus alba/ White oak					X		X				X
Quercus macrocarpa/ Burr oak					X		X			X	
Quercus palustris/ Pin oak			X		X		X			X	
Quercus rubra/ Red oak	X	X	X		X		X				X
Tilia Americana/ Basswood					X		X				X
CONIFEROUS TREES											
Larix laricina/ Eastern larch					X		X				X
Picea glauca/ White spruce				X	X		X				X
Pinus banksiana/ Jack pine					X		X				X

Pinus strobus/ White pine				X	X		X				X
Tsuga Canadensis/ Canadian hemlock					X		X				X

Source: City of Ottawa Forestry Services